2020

A study into the effects of spray and jet characteristics on flash evaporation system

Farshid Fathinia
Edith Cowan University

Edith Cowan University

Copyright Warning

A Study into the Effects of Spray and Jet Characteristics on Flash Evaporation System

A Thesis with Publications presented in fulfilment of the requirement for the degree of
Doctor of Philosophy

Farshid Fathinia

(MESc)

School of Engineering
Edith Cowan University
Joondalup, WA 6027, Australia

Abstract

Low temperature flash evaporation desalination is a separation system that isolates liquids from other materials when seawater or any fluid undergoes evaporation. Extreme flash evaporation occurs when a low heated liquid is injected into the vacuum area, where the pressure is far below the saturated pressure of the liquid entering the area. This approach of flash evaporation is a key part of this type of system. It has a great potential to develop and improve the implementation of low thermal desalination plants but requires more specific study. Further analysis shows that previous investigations have not given a comprehensive insight into the atomization of sprays or jets in seawater flashing spray desalination. Alternatively, most of the earlier research focused at the macro scale whereby the general process of flashing and its performance was studied. Little or no information is available on the droplet characteristics in spray and jet flash evaporation due to the difficulty of experimental exploration.

In this research study, the effect of operating conditions such as initial temperature, inlet flow rate, superheat degree, nozzle diameter, and salinity of the saltwater on the temperature distribution and evaporation rate of flashing spray is explored and comparisons are made between the results of the present experiments and previous studies. In order to simplify the design of the flash chamber and estimating the evaporation rate, spray angle and droplet size (two important characteristics of spray nozzles) have been analysed using a high-speed camera. These experimental measurements are also compared with mathematical calculation of droplet sizes. In addition, some other experiments have been done to improve the performance of system by utilizing a multi-nozzle head in various arrangements. Investigation of difference between the jet and spray nozzles having single and multiple arrangements is also performed under various operational conditions

The result concluded that flow rate has a different effect on the evaporation rate depending on whether spray or jet flash evaporation is taking place. Increasing the flow rate in sprays leads to higher flash evaporation but lowers the evaporation rate in jets. The spray angle as one of the most important characteristics of the spray is also largely affected by the superheat degree regardless of nozzle type and empirical equation is suggested to correlate this parameter with inlet pressure, saturation

pressure. Furthermore, placing nozzles in the farthest distance of each other on the multi-nozzle head leads to maximum 28% performance improvement compared to the conventional single nozzle. At the end of research, it is found that the evaporation rate and gain output ratio of the system using spray nozzle in both single and multiple nozzles are higher than the jet nozzle. This research will contribute to better understanding and development of thermally driven desalination plants.

Keywords: Flash evaporation, Spray, Jet, Temperature distribution, Evaporation rate, Gain output ratio.

Declaration

I certify that this thesis does not, to the best of my knowledge and belief:

i. Incorporate without acknowledgement any material previously submitted for a degree or diploma in any institution of higher education;

ii. Contain any material previously published or written by another person except where due reference is made in the text; or Contain any defamatory material.

iii. I also grant permission for the Library at Edith Cowan University to make duplicate copies of my thesis as required.

Signed: Farshid Fathinia

Data: 15/02/2020

Acknowledgements

My gratitude goes to a number of people, without whom it would have not been possible for me to undertake this program during my three years at Edith Cowan University.

First of all, I would like to thank my principal supervisor, Associate Prof. Mehdi Khiadani and co-supervisor, Associate Prof. Yasir Al-Abdeli, for their encouragement and constant support over the last three years. They introduced me to the field of desalination and guided me throughout my PhD. The valuable suggestions, recommendations, and scholarly comments of anonymous reviewers and editors from the various international journals are gratefully acknowledged. These individuals and organisations have helped to improve the quality of the manuscript and to identify future research directions.

I am thankful to the technical and admin staff of the School of Engineering at ECU for their cooperation with regard to the project. The PhD research project is made possible by an Edith Cowan University School of Engineering Research Scholarship. Thanks are also due to my parent and wife, without whom nothing (or not much) would have been possible. All the support they have provided me over the past three years was the greatest gift anyone has ever given me. Finally, I would like to thank all my friends in Australia who have supported me over the last few years.

List of Journal Publications Arising from this Candidature

Published Journal Papers

- F. Fathinia, Y.M. Al-Abdeli, and M. Khiadani, *Evaporation rates and temperature distributions in fine droplet flash evaporation sprays.* International Journal of Thermal Sciences. Vol. 145, 2019: p. 106037. https://doi.org/10.1016/j.ijthermalsci.2019.106037
- F. Fathinia, M. Khiadani, and Y.M. Al-Abdeli, *Experimental and mathematical investigations of spray angle and droplet sizes of a flash evaporation desalination system.* Powder Technology. Vol. 355, 2019: p. 542-551. https://doi.org/10.1016/j.powtec.2019.07.081
- F. Fathinia, M. Khiadani, Y.M. Al-Abdeli, and A. Shafieian, *Performance improvement of spray flash evaporation desalination systems using multiple nozzle arrangement.* Applied Thermal Engineering. Vol. 163, 2019: p. 114385. https://doi.org/10.1016/j.applthermaleng.2019.114385

Journal Papers Under Review

- F. Fathinia, M. Khiadani, Y.M. Al-Abdeli, 2020. *A comparative study of jet and spray flash evaporation desalination systems*. Experimental Thermal and Fluid Science

Table of Contents

List of Tables

List of Figures

List of Symbols, Nomenclature

A	area (m^2)
C	specific heat capacity (J/kg˚C)/ concentration of salt (% mass)
d	nozzle diameter (mm)
C_D	drag coefficient
D	droplet diameter (m)
D_v	diffusion coefficient (m^2/s)
D_{32}	sauter mean diameter
D_d	droplet diameter (m)
E	Evaporation rate (%)
F	force (N)
g	gravity acceleration (N/kg)
h	enthalpy (J/kg)
h_{fg}	latent heat of vaporization (J/kg)
K	thermal conductivity (W/m.˚C)
K	coefficient
m	mass (kg)
M	molecular weight (kg/mol)
M_f	mass flow rate liquid (kg/s)
M_v	mass flow rate vapour(kg/s)
$\dot{m}$	mass flow rate (kg/s)
N	Gaussian function
N	number of droplets
NEF	Non-equilibrium fraction
NETD	Thermal loss (K or ˚C)
P	pressure (pa)
Q	flow rate (l/min)
r	nozzle diameter (m)/radial direction (m)
R	universal gas constant (J/mol.˚C)
Re	Reynolds number
R_d	droplet radius (m)
S	Salinity (kg/kg)
s	distance (m)/sample variances
t	time (s)
T	temperature (˚C)
u	velocity (m/s)
V	volume (m^3)
z	axial direction (m)
v	specific volume (m^3/kg)
ρ	density (kg/m^3)
λ	molecular mean free path, m
υ	kinetic viscosity (m^2/s)
α	spray angle (˚)
Ω	collision integral for mass diffusion
δ	collision diameter (m)
ϕ	correction factor
θ	dimensionless temperature

σ	surface tension (N/m)
φ	relative humidity
ε	error
ΔT	superheat degree (˚C)
π	constant (3.14)
v	vapour
d	droplet
actual	actual heat
L	liquid
in	inlet
out	outlet
exp	experimental
emp	empirical
equ	equilibrium
sat	saturation
s	systematic
vac	vacuum
r	random
B	buoyancy
∞	surrounding
g	gravity
a	drag

Chapter 1

Topical overview[1]

1.1 Introduction

Water is an essential part of mankind's life and it can be discovered in lakes, reservoirs, and groundwater. In recent decades, many systems and apparatuses have been constructed for the purpose of producing fresh water from these sources.

Increasing demand for fresh water due to rapid growth of population and agricultural use of water for irrigation are causing concern. The pollution of rivers and lakes by sewage is also a concern to researchers and scientists. As a result, they focused more on subject of freshwater scarcity. Some useful measures such as controlling water consumption, reclamation of groundwater, or reusing wastewater for industrial purposes have been implemented but more needs to be done [1].

Rivers, lakes, reservoirs, and groundwater make up about 1% of the earth's water, while 97% of the earth's water is in the sea [2]. This huge source of water has been subject of many classic studies in recent years to establish and develop the reliable and economical desalination technologies.

Desalination technologies involve separating fresh water from the nearly inexhaustible supply of seawater for different applications, and most of these techniques require a large amount of energy [3]. Using fossil fuels is a common solution for to the problem of obtaining energy for water purification. But looking at the statistics shows that both world energy consumption and CO_2 emissions from burning fossil fuels have been doubled from 1971 to 2010. Also, this amount has been increased 15% from 2010 to 2020 [4]. It is apparent that this upward trend will have a negative impact on the environment resulting in acid rain, ozone layer damage, and increasing greenhouse gases.

[1] This thesis is presented and organised as "Thesis with publication" format.

For this reason, several research projects have attempted to find ways to manage the consumption of fossil fuels in economically viable ways. It is important to know the quality of produced water and minimum environmental pollution are two critical issues which should be considered to reach desirable outcome. Fortunately, some promising solutions have been suggested and implemented. These include using renewable energy and waste heat energies as the main supply sources[5]. However, the main challenge faced by many researchers is the optimizing and enhancing the efficiency of these systems.

In the next section, desalination process and common types of this technology will be discussed.

1.2 Desalination technologies

Desalination is a generating freshwater from salty water. The process of desalination can be divided into two categories based on the energy consumption: Non-thermal and thermal. Figure 1.1 shows these classification of the desalination technologies [6].

Non-thermal desalination plants involve high electrical energies [7]. The membrane process as a principle technology of this category will be described briefly in the following section. In thermal desalination, distillation and crystallization methods could provide for half the world's desalination requirements which will be discussed after introducing membrane technologies.

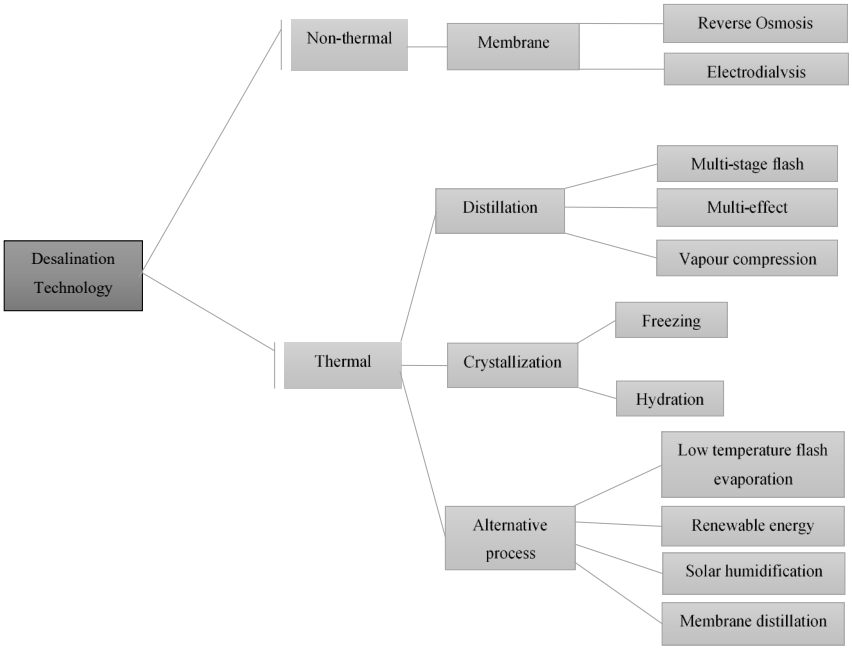

Figure 1.1 Classification of the desalination technologies

Flash evaporation in low temperature thermal desalination, which is a novel alternative process of thermal desalination that has recently attracted the attention of scientists, will be introduced in section 1.2.4.

1.2.1 Non-thermal membrane

The membrane process has two main commercial processes which are:

- Reverse osmosis
- Electrodialysis

The ability of membranes to isolate and separate water from salt has been applied in both of processes, however the methodologies are different.

In order to distinguish between these two groups, Figure 1.2 presents schematic of the membrane process. The figure shows that reverse osmosis is based on a pressure driven process and employ pressure to pass the saltwater through the membrane for the purpose of desalination. Electrodialysis, based on a voltage driven process and electrodes, play an important role in separating salt from water [5].

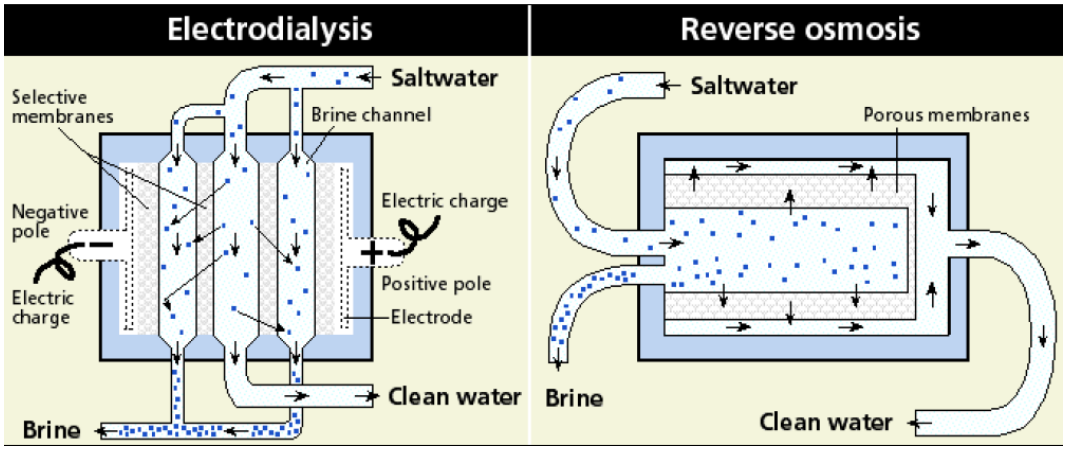

Figure 1.2 Schematic of membrane process [5]

1.2.2 Distillation

Distillation is an extremely common technology which most desalination processes rely on. During distillation, a liquid is heated up to evaporation point using the latent heat of droplets. It is then condensed in the form of fresh water. In this way, brine and compounds of working fluid will be isolated and the quality of the distilled water will be very high. A major disadvantage of this method is that it consumes high amount of energy. As a result, the method is not viable. The application of low cost and available energy would make this technology more viable [5]. The following processes are primary types of distillation:

- Multi-stage flash distillation
- Multiple effect distillation
- Vapour completion distillation

1.2.3 Crystallization

Crystallization desalination technology has two types which are freezing and hydration. The most common method of crystallization is freezing, which involves firstly freezing ice out of the seawater and then the salt adhering to the ice is replaced with pure water. Finally, to produce potable water, the process involves simultaneously melt the ice and recovering the heat of fusion [8]. There was considerable interest in this type of desalination in the 1960s who researchers studied and developed extensively but the complexity of separating the ice mixture and water is still introduced as a main drawback of this technology [9]. In addition, the high cost of energy requirement for the process is another limitation.

There are three types of freezing:

- Vacuum freezing
- Freezing with direct contact
- Freezing with indirect contact

1.2.4 Low temperature flash evaporation desalination

After collection and analysing the development of previous process, researchers proposed various techniques to control and manage the intensity of the energy. These techniques have been classified as alternative processes within the thermal branch which modified prior processes in regard to energy, cost, and availability. Low temperature flash evaporation has a low energy requirement. It is one of a number of promising methods that has been constructed in different ways with unit concept. In this section, this innovative rig will be described and in the following chapters will focus on the principle part of this system, i.e., flash evaporation.

Low temperature flash evaporation is a separation system that isolates liquid and its components when water undergoes evaporation. It has to be exposed in a depressurized area. In other words, low heated liquid flow starts to evaporate when it is injected into the vacuum zone, where the pressure is far below of its saturated pressure (corresponding to the inlet temperature). In this case, pressure acts on the surface of the liquid and becomes superheat. This could be interpreted as a reduction in the pressure of the surface area leading to a loss of intermolecular bonding between molecules and become unstable. Therefore, for the droplets to regain their equilibrium condition they turn to steam. The components of the liquid (i.e. salt, sulphur …) due to the extra energy required for breaking their bonds, remain stable without phase changing [10]. The vapour generated is condensed through the heat exchanger and distilled water is produced. Figure 1.3 indicates the schematic of a low temperature flash evaporation rig. The wasted hot steam could be used as a source of energy for heating the liquid [11].

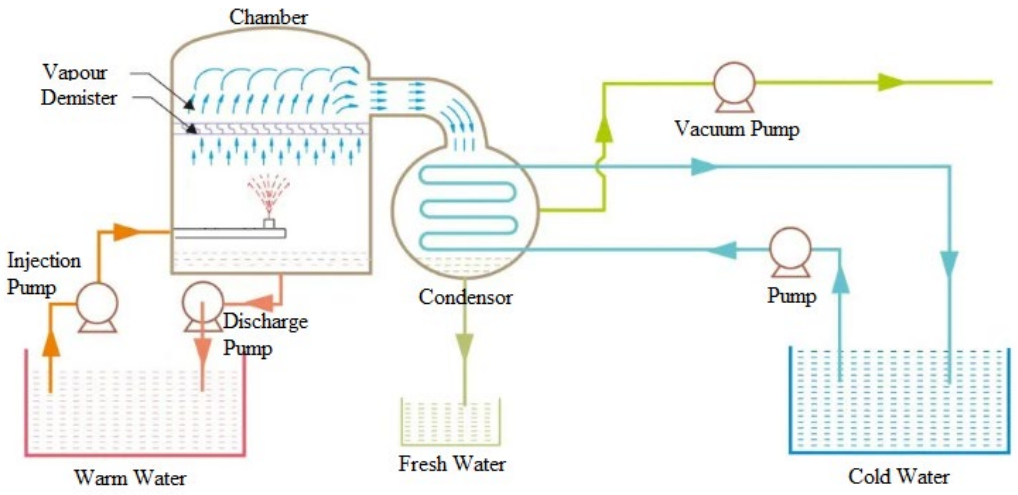

Figure 1.3 Schematic of low temperature flash evaporation rig

It is now well established from a variety of distillation systems that flash evaporation is a key part of this type of system that require more specific study in order to achieve optimal performance.

1.3 Flash evaporation

Flash evaporation is the process of rapid vaporizing of saturated liquid due to the sudden drop in the surrounding pressure of liquid in a drum. This pressure reduction leads to the considerable temperature decline and the release of the latent heat of droplets to change the phase of liquid. This phenomenon is commonly used for vapour production in water desalination systems and storage processes that require steam.

There are two basic approaches currently being adopted in research into flash evaporation. One is the pool evaporation approach and the other is spray and jet evaporation [6].

The next section will first consider existing research into the pool evaporation approach and will then discuss existing research into spray and jet evaporation.

1.3.1 Pool evaporation

In In pool evaporation, a specified amount of liquid is kept in a pressure controlled sealed chamber. The chamber is connected to a vacuum tank. By exposing the liquid to an environment which is lower than the liquid's saturation pressure, it becomes superheated. The excess heat of the fluid is released and is then converted to the latent heat of vaporization. This type of evaporation has a wide range of application in industries such as salt disposal [12], using a low pressure water spray for cooling [13], cooling grapes during wine production [14] and sea water desalination [15]. Based on the velocity type of liquid bulk in a chamber which is horizontal or not, pool evaporation is divided into two categories: static and circulatory flash evaporation.

The primary fundamental conception of static flash evaporation was investigated by Miyatake et al. [16] and Miyatake et al. [17]. In the first experiment, they carried out flash evaporation utilizing water as a working fluid with approximately superheat degrees range of 3K to 5K and a water temperature of 40˚c to 80˚c. After validating the experimental results, they proposed the flash evaporation rate with a new coefficient. In the second attempt to understand the issue, they considered a range of 2.5K to 5.5K for superheat degree with the same condition for a water temperature (40˚c to 80˚c). But the liquid level fluctuated and varied between 100mm and 200mm. They also demonstrated that there is not an ever upward trend between flowing down of liquid level for liquid temperature with larger values.

Fath [18] evaluated the non-equilibrium coefficient and correlated this coefficient to the rate of flash evaporation inside the chamber. He also performed a simulation to measure the performance of the system. Fath showed that increasing the superheat degree, flashing surface area and residence time of sea water led to reach thermodynamic equilibrium.

The study on static flash evaporation of NaCl-water was widely implemented by numerous scientists. [19] revealed that increasing the height of water film concentration weakened the liquid phase change and boiling heat transfer. This increasing height also decrease the performance of flash evaporation by considering the condition of initial water film concentration between 0 and 15, superheat ranged between 1.7K and 53.9K. They also compared their results with the result of same

experiment conducted using pure water and analysed all the factors that influenced the results.

In the next experiment, Zhang et al. [20], studied the steam-carrying effect in static flash with various speed of flashing. Their experimental setup of static flash evaporation is shown in Figure 2.1. Different orifice plates in the size of 5 mm to 80 mm were set up between the vacuum chamber and the flash. This produced various speeds. The mass ratio of the inlet liquid to the flash vapour was named the steam-carrying ratio and the results showed that the steam-carrying ratio will increase while speeding up the flash steam.

In a follow-up study, Zhang et al. [21] investigated the efficiency of energy conversion in the static flash evaporation of NaCl-water and defined energy conversion efficiency (ECE) as the total dropped energy from a mass of primary water film which varied between 0.023 and 0.991 in their experiment. They reported that the ECE was increased by enhancing the temperature of the water film and decreasing the flash speed, while increasing the initial concentration, superheat degree, and initial height lead to a decrease in the ECE.

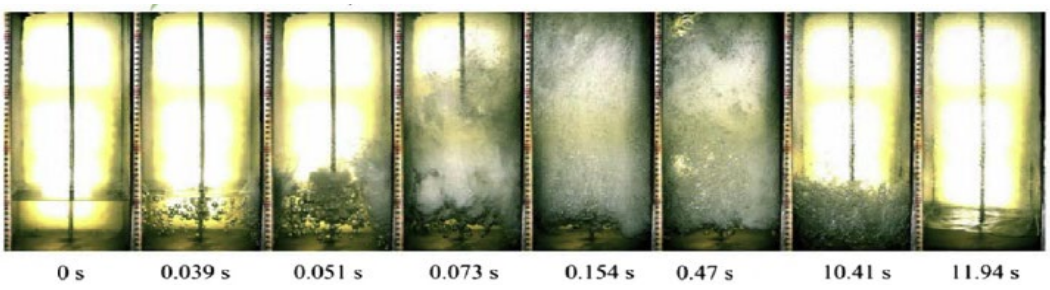

Figure 1.4 Experimental test of static flash evaporation by Zhang et al. [18]

Zhang et al. [22] performed exergy analysis on static flash evaporation by utilizing water. Efficiency exergy (EE) was introduced for a unit mass of water film as a ratio of delivered exergy to the released exergy. They conducted their experiment in temperature range of 46.5-104.6˚C, initial water film height of 0.1-0.3 m, superheat degree of 1.78-43.9K and found that EE could be modified by simultaneously raising the temperature and lowering down the superheat degree, flash speed and the initial height of water film.

A recent study by Gao et al. [23] involved a novel method instead of previous procedures. They injected a dilute solution of fluid into the vacuum area and analysed the influence of temperature variation on the fundamental theoretical analysis. This research indicated that the intensity of flash evaporation was enhanced by increasing the inlet temperature of droplets.

With reference to circulatory flash evaporation, numerous valuable works also have been done in recent years. Zhang et al. [24] used horizontal velocity in a flash evaporation and this is applicable to many industries. Multi-stage flash desalination is one of the most significant applications of circulatory flash evaporation. Their experiments were conducted with different flow rates, initial water film heights and pressures. The outcomes revealed that enhancing the superheat degree leads to a decline in the heat transfer coefficient. Non-equilibrium friction (NEF) was also another factor that was affected by operating conditions. The NEF dropped as the pressure and flow rate rose in the chamber, while it increased as the initial water film height climbed.

In order to identify the influence of liquid components on the performance of the circulatory flash evaporation, Zhang et al. [25] carried out their experiments by using different concentration of NaCl in pure water. These concentrations were 0, 5, and 10% with different ranges of flow rate, pressure and initial water film height. In comparison with their previous investigations, the same trend was observed in relation to NEF, pressure, flow rate and initial water film height. In addition, 10% NaCl solution had a coincident with NEF curve for pure water.

As a comparative research between static and circulatory flash evaporation, Junjie et al. [26] analysed these two types of flash evaporation based on two different experimental rigs and the same heat and mass transfer properties. One of the significant results of this research was the finding that the heat and mass transfer coefficient is a time-dependent function.

1.3.2 Spray and jet flash evaporation

It is now well established from a variety of studies that nozzles are widely used to control the inlet flow, speed, direction and many related parameters. Based on the orifice exit size of nozzles and their applications, it can be grouped into various

types: jet, propelling, magnetic, spray, etc. In the case of flash evaporation, the most common nozzles are spray and jet that liquid is injected through a different diameter into the vacuum area.

The jet nozzles inject liquid in a solid cone-shaped spray pattern which consist of medium droplets. This type of nozzles has a round impact area and uniform pattern. A wide variety of jet nozzles are available based on their configuration, capacity, and droplets sizes. The spray nozzles atomize liquid in a very fine droplet. The spray pattern depends on spray type. Many types of sprays are available but three of the most common types are: flat fan, cone spray, and streaming nozzles.

The primary research on this kind of flash evaporation was done by Miyatake et al. [27]. They experimentally conducted spray flash evaporation. They examined at 60˚C inlet temperature of liquid and the influence of flow rate, superheat degree and nozzle diameter. As a result, the empirical equation was appropriate for forecasting the changes of liquid temperature, and they concluded that spray flash evaporation has a much more intense heat transfer than pool boiling.

In the same year, additional experimental work related to spray flash evaporation was carried out by Miyatake et al. [28]. The difference was the range of inlet liquid temperatures which changed from 40˚C to 80˚C. By investigating the outcomes, more comprehensive and general equations were developed to predict of the variation in temperature along the centreline of the jet direction. It was also found that the performance of the spray flash evaporation was not affected by reducing the temperature compared to other flash evaporation systems.

Another successful study was carried out by Miyatake et al. [29] to enhance and develop the rate of flash evaporation with accurate analysis the influence of superheat, temperature and flow rate of liquid by changing nozzle diameter.

Detailed examination of the atomization model for the flash spray by Zeng and Lee [30] showed that the break-up originates from two mechanisms: bubble growth and aerodynamic force. Prediction of hollow-cone spray atomization was the next goal that indicated the tendency of drop size to fall by reducing the ambient pressure, thickness of spray cone and rate of fuel vaporization.

Ikegami et al. [31] compared the effect of injection direction on the performance of the system. For this purpose, they considered superheated water as a liquid at different temperatures of 24, 30, and 40˚C. The mean velocity was from 1.74 to 3.62 m/s with a nozzle diameter of 20 mm. The thermal resistances were installed along the nozzle exit to measure the fall in the temperature of the superheated liquid. The experimental procedure for both types of upward and downward injection was implemented, and the results were organised to compare the data and analysis. As a result, it was observed that upward flash evaporation took less time for completion than downward. Therefore, upward injection was recommended to improve the efficiency and performance of flash evaporation rigs.

In the case of a general analysis of spray and jet flash evaporation, several other experiments were studied in relation to nozzle size and nozzle geometry [32-34], the effect of operating conditions on the performance of the system [34-37].

Recently some researchers attempted to distinguish between studies involving general analysis and studies involving detailed analysis of spray flash evaporation. They tried to find a theoretical or empirical correlation between operating conditions and the characteristics of spray and jet flash evaporation. They also focused on the influence of operating conditions on the performance of the system. The outcomes showed that this kind of study will be more helpful for modification of the spray flash evaporation systems.

In order to study flash evaporation more in depth, some of the mathematical models are developed and proposed in different ways. Cai et al. [38] analysed temperature distribution against the travelled distance of droplets mathematically. They found a model based on the diffusion-controlled evaporation model to investigate flow velocity and droplet size of the downward jet flash evaporation. Another model with the capability of predicting spray flash speed was presented by Cai et al. [39]. Based on the model results, they concluded that higher Jacob number, Reynolds number, and Weber number all causes to increase of evaporation rate. Chen et al. [40] quantified a spray shattering inside a vacuum area by developing a mathematical model based on droplet motion. The effect of influential parameters on the flash evaporation was also studied and they revealed that the average size of droplets are several orders of magnitudes smaller than the nozzle diameter.

Mutair and Ikegami [41] and Mutair and Ikegami [42] presented the effect of factors such as inlet velocity of flow, initial temperature of water, super heat degree, and diameter of injection nozzle on the thermal characteristics of spray flash evaporation. They proposed exponential curve model in order to predict the temperature along the centreline of the jet inside the chamber. The direction of the jet was upward; the range of temperature was 24 to 40˚C and the pressure of the chamber was assumed below the boiling pressure that corresponds to the inlet water temperature. At the end of their survey, it was concluded that it would be possible to predict the end point of evaporation and the inflection point of evaporation using empirical equations which were derived during the tests. These correlations are useful for the design of a flash evaporation drum.

Liu et al. [10] experimentally investigated the flash evaporation process of saltwater droplets with salinity between 0 and 26%. The salt water droplets were released into the vacuum chamber. The suspended NaCl-water droplet was located at the junction of a thermocouple to measure the evolution of temperature during the experiment. On the other side, an infrared thermal imager was set to evaluate the variation in the surface temperature of the droplets. They also considered high speed camera to record changes in the height and diameter of the droplets shape. It was clear that different solutions of salt into the water had a significant effect on the rate of evaporation so that by raising the concentration of NaCl the evaporation rate decreased. The transition of droplet temperature was also determined based on changing some parameters such as surrounding pressure, initial temperature, and primary size of droplet. In follow-up research, Liu and Mi [43] reported theoretical research on the evaporation of droplet during depressurization. In order to simulate the temperature variation in a defined condition, a mathematical model was expanded. The numerical results were validated with experimental results and it would be valuable for deep understanding of the thermodynamic process of droplet evaporation.

Chen et al. [44] developed a theoretical model of flash evaporation of superheated liquid which was injected into the vacuum area. The droplet motion and size were two main parameters for deriving equations. While the discrepancy of numerical model with experimental works was 14%. This numerical model has the potential to predict the produced water and thermal efficiency of spray flash evaporation. In

addition, several significant design parameters had a key role to obtain a desirable outcome. The second major finding was that the smaller (size) and faster (velocity) droplets lead to further evaporation and higher water productivity, respectively.

The classification of pool evaporation and jet or spray evaporation which provides summary of the literature review with more related sources has been shown in Table 1.1.

Table 1.1 Summary of previous works

<table>
<tr><th>Authors</th><th>Type of system</th><th>Parameters Discussed</th><th>Remarks</th></tr>
<tr><td>Miyatake et al. [16]
Miyatake et al. [17]
Tay et al. [1]
Saury et al. [45]
Kim [12]
Fath [18]
Jin and Low [46]
Jin et al. [47]
Zhang et al. [24]
Junjie et al. [26]
Zhang et al. [22]
Augusto et al. [48]
Hahne and Barthau [49]
Reinke and Yadigaroglu [50]
Saury et al. [45]
Saury et al. [51]
Gopalakrishna et al. [52]
Gopalakrishna and Lior [53]
Zhang et al. [25]
Shao et al. [54]
Zhang et al. [55]
Dan et al. [19]
Zhang et al. [56]
Zhao et al. [57]
Zhang et al. [21]
Zhang et al. [20]
Zhang et al. [58]</td><td>Pool evaporation →</td><td>Superheat degree, initial temperature, film height, pressure, residence time, flash speed, initial water film concentration, flow rate, flash chamber pressure, pool boiling, bubble size and distribution of the vortex number</td><td>Proposed various correlation between the liquid evaporated by flashing and operating conditions.</td></tr>
<tr><td>Miyatake et al. [27]
Miyatake et al. [28]
Miyatake et al. [29]
Zeng and Lee [30]
Ikegami et al. [31]
Mutair and Ikegami [41]
Mutair and Ikegami [42]
El-Zahaby et al. [59]
El-Zahaby et al. [60]
Muthunayagam et al. [34]
El-Fiqi et al. [35]
Liu et al. [61]
Hou et al. [62]
Miyatake and Miki [63]
Peter et al. [64]
Chen et al. [44]
Mutair and Ikegami [65]
Balaji [32]
Liu and Mi [43]
Wellmann et al. [66]
Xuening et al. [67]
Liu et al. [10]
Gao et al. [36]
Hamawand et al. [37]</td><td>Jet or spray evaporation →</td><td colspan="2"><table>
<tr><th>Analysis based on jet or spray characteristics</th><th>Type of analysis</th><th>Operating conditions</th></tr>
<tr><td>Mutair and Ikegami [41]
Mutair and Ikegami [42]
Mutair and Ikegami [65]</td><td rowspan="2">Thermal characteristics</td><td>T_{in}=24˚C-40˚C
$P_{chamber}$=2.93kpa-7.26kp
U_{in}=0.8-3.56 m/s
ΔT=2-13
C= No info. (sea water)
Nozzle diameter=54.4107mm</td></tr>
<tr><td>Liu et al. [61]
Liu et al. [10]
Liu and Mi [43]</td><td>T_{in}=10˚C-12.5˚C
$P_{chamber}$=0.15kpa-4kpa
C= 0-26%</td></tr>
<tr><td>Chen et al. [44]</td><td>Dynamic and Thermal characteristics</td><td>T_{in}=50˚C
$P_{chamber}$ = 12kpa
U_{in}=5 m/s
ΔT=4
C= 0
Nozzle diameter=5 mm</td></tr>
</table></td></tr>
</table>

The next sections will consider the literature relating to the components of vacuum spray flash evaporation and the main characteristics of the spray and jet.

1.4 Process and components of spray and jet flash evaporation

Layout of low temperature spray and jet flash evaporation is shown in Figure 1.5. The water is heated up in a tank through the heater until desired temperature and then pumped to the chamber with the appropriate velocity which can be adjusted with the pump. The characteristics of fine droplets that break up in the drum is directly related to the diameter of the nozzle. Various types of nozzles in regard to their application could be applied to obtain the best result. By utilizing each type of nozzle, the heated water is injected to the vacuum area in which the pressure is maintained far below of the saturation pressure corresponds to the degree of heated water. The vacuum pump is connected to the drum through the condenser and at the beginning of every experiment it worked at full capacity. So, the vapour is produced as a result of the superheated water being exposed to the vacuum pressure. A part of the vapour transforms to the condenser and the non-evaporating part drains to the water reservoir. The shell and tube condenser cools the steam, and distilled water is stored in the fresh water tank [68].

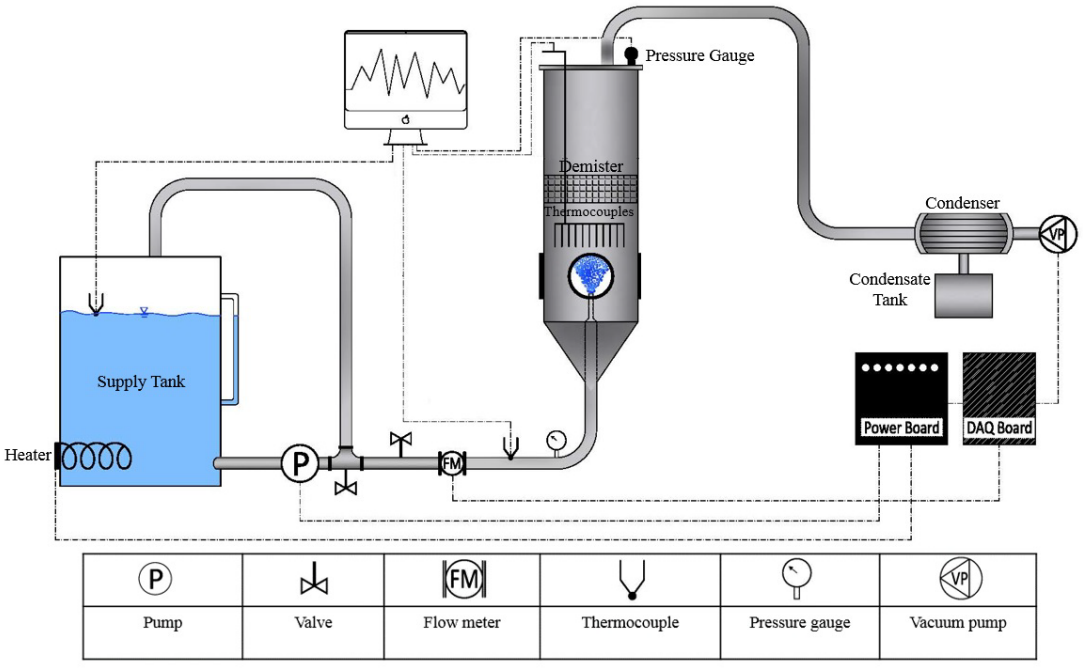

Figure 1.5 Layout of spray and jet low temperature flash evaporation

1.4.2 Spray characteristics

There is evidence that spray nozzle performance plays a crucial role in determining the characteristics of the spray. The inlet liquid is squeezed in the narrow pipe and shunted to the narrower part namely nozzle. The compressed liquid is sprayed out through the hole of nozzle and due to the sudden changes of pressure the liquid is tore and break up into fine droplets. Many different parameters, such as temperature, pressure, flow rate, nozzle diameter, properties of liquid affect the spray characteristics which are mainly: droplets velocity, droplets flux, droplets size, droplet sauter mean diameter, spray flow rate, and spray angle that base on the measuring instrument and application of the system could be measured and discussed. According to references [69, 70] droplet velocity and sauter mean diameter are the two most common and significant characteristics of spray.

1.4.2.1 Droplets flux

The variation of droplets flux in axial distance can be correlated by a Gaussian function as given below:

$$N = 953.66 + \frac{2.33\times10^{6}}{54.62\sqrt{\pi/2}} exp\left(\left(\frac{z-103.84}{54.62}\right)^{2}\right) \quad (1.1)$$

Where N is the droplets number in 10s spurt duration and Z is the spray axial distance.

1.4.2.2 Droplets mean velocity

The local droplets mean velocity in axial distance is defined as:

$$\bar{V} = \frac{\sum_{i=1}^{N} D_I^3 . V_i}{\sum_{i=1}^{N} D_I^3} \quad (1.2)$$

Where V_i is the velocity and of the ith droplet at the measuring point.

1.4.2.3 Sauter mean diameter (SMD)

In order to compare the different size of droplets measured by laser instruments, D_{32} (SMD) is defined as follows:

$$D_{32} = \frac{\sum_{i=1}^{N} D_i^3}{\sum_{i=1}^{N} D_i^2} \quad (1.3)$$

Where D_i is the diameter of the ith droplet, N is the total number of droplets [69].

Previous studies of the different applications of the spray such as cooling that droplets velocity which are distributed in a flow filed are not uniform vectors and also droplets sauter mean diameter is related to nozzle diameter which shows the importance of the size of nozzle diameter. Although these conclusions are general and were obtained for modifying spray cooling, they indicate that the study of the dynamic behaviour of droplets may lead to improving the design and optimizing the efficiency of related processes. The thermal characteristics of liquids droplets which spread in the atmosphere was another parameter. Researchers pay more attention on this feature to predicting the amount of energy that is released by the droplets. In order to determinate the characteristics of the droplets, the researchers used laser measuring instruments such as PDA (Phase Doppler Anemometry), LDV (laser Doppler Velocimetry), and a shadowgraph for dynamic features and thermocouples for thermal were utilized [71, 72].

1.4.3 Parameters affecting the process of flash evaporation

It is well established from a considerable amount of literature that there are significant parameters which affects the performance of the flash evaporation process. These parameters are derived from related literature relating to the topic and will be defined.

1.4.3.1 Non-equilibrium fraction (NEF)

NEF as a non-dimensional number is introduced by Miyatake et al. [16] and some authors called as non-equilibrium allowance. This number is characterized the degree of completion for flash evaporation and it was detected that higher evaporation take place when superheat degree increased appropriately. This number identified the variation of temperature during the flashing process.

$$NEF(t) = \frac{T(t)-T(e)}{T_0-T_e} \tag{1.4}$$

Where T(t) is the bulk-average temperature of the liquid at time t of starting flash evaporation, T(e) represents the equilibrium temperature after flash evaporation stopped that equals to the measured temperature in experimental method T_e. T_0 also,

represents the initial bulk-average temperature of the liquid before injection to the flash.

1.4.3.2 Inlet temperature

Miyatake et al. [28] revealed that various temperature of inlet liquid affected on the performance of the system. They also found that the performance of spray flash evaporation even at lower temperature is higher than pool flash evaporation system. For this purpose, the range of 40 to 80˚C was considered and meaningful changes observed on evaporation rate while the inlet temperature decreased.

1.4.3.3 Superheat degree

One of the most prominent parameter in flash evaporation is superheat. The phenomenon of flashing occurs when the temperature of liquid exceeds a certain degree of superheat. As discussed before, when the liquid expose to sudden pressure drop, it creates a new status with lower than its saturation condition, as a result the liquid at initial equilibrium becomes superheated. The energy released through this process could not be restricted and converted to the latent heat of vaporization. The difference of temperature between inlet liquid and saturation point is defined as the degree of superheat [35] :

$$\Delta T = T_{in} - T_{sat} \tag{1.5}$$

Where T_{in} is the temperature inlet and T_{sat} is the saturation temperature of evaporator.

1.4.3.4 Operating pressure

The study of previous works have identified that pressure play an important role to control the whole process of flash evaporation. Miyatake et al. [16] and Miyatake et al. [17] investigated the equilibrium pressure in the range of 74 to 463mbar (7.6 to 46.3kpa). The finding of Saury et al. [45] provide insights for the relation between inlet pressure and NEF. The inlet pressure range was 50 to 200mbar and decreasing the pressure with increasing inlet temperature was the function of final flashed mass. Peterson et al. [73] did their experiment in the range of 11.4 to 27kpa that shows normal evaporation occurred at low pressure and large changes in inlet pressure lead to more flash evaporation.

1.4.3.5 Actual heat

The actual heat is defined as the difference between the temperature of inlet liquid and outlet brine liquid exiting of the evaporator which is estimated as follows:

$$\Delta T_{actual} = T_{in} - T_{out} \tag{1.6}$$

Where T_{in} is the inlet temperature and T_{out} is the outlet temperature of liquid. Falling the sensible heat of feed liquid during flash evaporation is the reason of differences between inlet temperature and outlet brine temperature.

1.4.3.6 Evaporation rate

The most obvious equation to derive evaporation rate is the heat balance. The heat balance equation presents the equality of heat lost by the feed liquid and heat obtained by the evaporation of feed liquid [34]. According to the inlet liquid temperature and saturation pressure defines the mass of produced liquid vapour as:

$$M_f C_p \Delta T_{sup} - M_v h_{fg} = 0$$

$$\rightarrow \quad M_v = \frac{M_f C_p \Delta T_{sup}}{h_{fg}} \tag{1.7}$$

where M_v is the mass flow rate of generated vapour, M_f is the mass flow rate of feed liquid, C_p is the specific heat of liquid and h_{fg} is the enthalpy of vaporization.

It should be considered that above equation was derived based on utilizing the whole sensible heat of feed liquid for vaporization. El-Fiqi et al. [35] also, developed the above equation based on actual heat which is shown below:

$$M_f C_p T_{in} - M_f C_P T_{out} - M_v h_{fg} = 0 \tag{1.8}$$

The comparison result of experimental and the values were achieved by above equation shows a little discrepancy that discussed and investigated.

1.4.3.7 Evaporation ratio (Yield ratio)

The percentage of evaporation that was obtained from inlet liquid that was being injected to the evaporator was definedas evaporation ratio by [32]. It can be given as the following equation:

$$\frac{M_v}{M_f} = \frac{C_p \Delta T_{sup}}{h_{fg}} \tag{1.9}$$

1.4.3.8 Flashing efficiency

The flashing efficiency of the spray flash evaporation is presented as the ratio of actual evaporation which occurs inside the drum and super heat degree as a maximum possible evaporation for the inlet liquid corresponding to the saturation temperature. It also can be interpreted as the ratio of the vapour generation to the maximum vapour generation and the equation is shown below [6]:

$$\eta = \frac{\Delta T_{actual}}{\Delta T_{sup}} = \frac{T_{in} - T_{out}}{T_{in} - T_{sat}} \tag{1.10}$$

1.4.3.9 Non-equilibrium temperature difference (NETD)

NETD or thermal loss is the difference between the temperatures of outlet brine with saturation temperature of liquid from evaporator that defined as [6]:

$$NETD = T_{out} - T_{sat} \tag{1.11}$$

1.4.3.10 Nozzle

Literature reported that nozzle diameter is one of the most important factor for affecting the performance of spray flash evaporation systems. Miyatake et al. [27] experimentally analysed the effect of different nozzle diameter when superheated liquid injected into the low-pressure area. They considered 60˚C temperature for the feed water and the nozzles, were made of glass tube, and had a diameter range of 3.46 to 8.15 mm. By considering the experimental results, an empirical equation which depends on nozzle diameter derived. Also, Mutair and Ikegami [41] investigated the efficiency and performance of the jet flash evaporation by changing the nozzle diameter (54.4 to 107 mm). They found that nozzle diameter affects the position of inflection point (highest rate of flash evaporation) so that increasing the nozzle diameter lead to increase the height of inflection point.

1.5 Project motivation

There have been several investigations into the causes of spray flash evaporation and up today provided some useful information on the flashing. But further analysis shows that the outcomes have not given a comprehensive insight into the flashing spray desalination. Some detailed information such as the influence of operating conditions on the characteristics of spray or jet nozzles, the effect of droplets size, velocity, and flux which are the main feature of spray or jet nozzles on the

evaporation rate and performance of the system, the influence of different salinities of the inlet saltwater on the characteristics of the nozzle, and the effect of different types of nozzles or arrangements of nozzles on each other and on the overall performance of the system have not been investigated. Most of this research focused only on general process of flashing so offered prevalent conclusions at system level, and little or no information is available on the droplet analysis (micro scale) due to the difficulty of experimental investigation [44]. The difficulty of experimental analysis is the measuring droplets behaviour inside vacuum area. This problem has been addressed by mounting thermocouple holding bar inside a chamber and installing two windows along the chamber to observe the movement of droplets. Such information is essential for the more accurate design and optimization of spray evaporators. An in-depth investigation into the development of an experimental and theoretical spray evaporation model is necessary.

1.6 Research questions

The overview above clears existing challenges and unresolved problems in relation to flash evaporation desalination system. To accomplish this doctoral thesis three research questions are briefly described below:

RQ 1-1 What are the effects of initial temperature, inlet flow rate, superheat degree, nozzle diameter, and salinity of the saltwater on the formation and dynamic characteristics of the spray and jet nozzle?

RQ 1-2 What are the effects of initial temperature, inlet flow rate, superheat degree, nozzle diameter, and salinity of the saltwater on temperature variation of the spray and jet nozzle?

RQ 2 How do the characteristics of the spray and jet nozzle affect performance of flash evaporation?

RQ 3 How does using a single or multiple arrangement of spray and jet nozzles affect their characteristics and process efficiency in flash evaporation?

1.7 Research methodologies

The above research questions are addressed in this thesis by applying both experimental and numerical methodologies. An experimental setup for this work

has been designed and installed by other researchers [75] to simplify and hasten the process of the measurements and study. This setup is available in the laboratory of the school of engineering at Edith Cowan University. All the equipment that is used in flash evaporation system are electric heater, vacuum chamber, feed water tank, flow meter, feed pump, various type of nozzles, vacuum and injection pump, condenser, pressure gauge, and thermocouples. The experimental method includes temperature, pressure, flow rate, salinity, droplet size, velocity, and flux measurements.

There are numerous methods to measure the droplets size, velocity, and flux of atomized water particles. These can be divided into two categories: mechanical and optical methods. Based on development of science, the mechanical method is rarely used nowadays, but the optical methods are widely used. In this research, shadowgraph technique has been selected among the other methods. The shadowgraph technique is utilized to some modern applications such as visualisation of the fluid and surface flow characterization. This system is involved two main equipment: the light source and the recording element. The aim of using illumination source is to achieve homogenous background in front of recording element. A high-speed camera is also used as the recording sensor and LED will provide short duration illumination. Although the principle of this system seems simple, there are several parameters that should be adjusted and controlled to obtain effective images. Figure 1.6 shows the diagram of shadowgraph technique that highlights the difference in refractive index at the interface between a body and its surroundings. As can be seen the illumination doesn't have any interact with the object and produces a clear and bright background for capturing the photos [76].

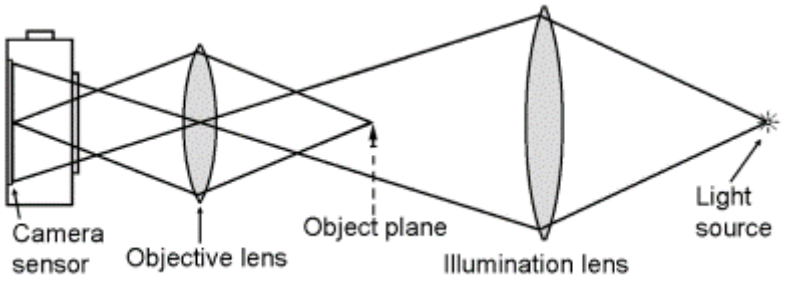

Figure 1.6 Public diagram of shadowgraph system [76]

In this study, MATLAB software (version 2015b) has been also employed to calculate droplet sizes and comparing the results with experimental measurement values obtained by shadowgraph technique.

1.8 Thesis structure

This thesis is presented and organised as "Thesis with publication" format[1]; and is structured in chapters as follows:

Chapter 1 presents the general overview of the project topic and defining flash evaporation desalination system, followed by project motivations, objectives of the thesis and methodology used in this research.

Chapter 2 discusses the effect of the operating parameters on the temperature distribution and evaporation rate of flashing spray. The dimensionless temperature introduced follows an exponential decaying curve and is found to also match temperature distributions in a range of other works covering different nozzles (sprays or jets), in both upward and downward flash evaporation.

Chapter 3 provides the effect of operational parameters on spray characteristics of flash evaporation system. Spray angle and droplet size are two important characteristics of spray nozzles.

Chapter 4 presents the performance improvement of the spray flash evaporation system using multi-nozzle head in various configurations.

Chapter 5 discusses the comparative study between the jet and spray flash evaporation system and analyses the effect of influential parameters on these nozzles by calculation of evaporation rate and gain output ratio.

Chapter 6 provides a general discussion of the results presented in each chapter and addresses the research questions for the overall project.

[1] "Thesis with Publication" is an acceptable format of thesis for postgraduate research at ECU policy. The current thesis has been written based on the guideline provided at http://www.ecu.edu.au/GPPS/policies_db/policies_view.php?rec_id=0000000434. In this format, the submitted thesis can consist of publications that have already been published, are in the process of being published, or a combination of these.

Chapter 7 integrates the findings of all chapters and also outlines directions for future research.

1.9 References

1. J. Tay, S. Low, and S. Jeyaseelan, *Vacuum desalination for water purification using waste heat.* Desalination. Vol. 106, 1996: p. 131-135.
2. W. Graves, *Water: The Power, Promise, and Turmoil of North America's Fresh Water*. 1993: National Geographic Society.
3. A.D. Khawaji, I.K. Kutubkhanah, and J.-M. Wie, *Advances in seawater desalination technologies.* Desalination. Vol. 221, 2008: p. 47-69.
4. Matt McGrath, Climate change and coronavirus, Retrieved from https://www.bbc.com/news/science-environment-52485712.
5. AFFA, *Introduction to desalination technologies in Australia.* AFFA publications. 2002.
6. M. Maria Antony Raj, K. Kalidasa Murugavel, T. Rajaseenivasan, and K. Srithar, *A review on flash evaporation desalination.* Desalination and Water Treatment. Vol. 57, 2016: p. 13462-13471.
7. U. Pliquett, R. Joshi, V. Sridhara, and K. Schoenbach, *High electrical field effects on cell membranes.* Bioelectrochemistry. Vol. 70, 2007: p. 275-282.
8. D. Johnson, J. Lott, and C. Sliepcevich, *The exchange crystallization freeze desalination process.* Desalination. Vol. 18, 1976: p. 231-240.
9. T. Efrat, *Utilizng available 'coldness' from liquefied natural gas (LNG) regasification process for seawater desalination*, in *DA World Congress – Perth Convention and Exhibition Centre (PCEC)* 2011.
10. L. Liu, Q.c. Bi, and H.x. Li, *Experimental investigation on flash evaporation of saltwater droplets released into vacuum.* Microgravity Science and Technology. Vol. 21, 2009: p. 255-260.
11. G.J.J. Wessley and P.K. Mathews, *Investigations on low temperature flash evaporation desalination for small-scale applications.* 2013.
12. D.H. Kim, *A review of desalting process techniques and economic analysis of the recovery of salts from retentates.* Desalination. Vol. 270, 2011: p. 1-8.
13. I. Aoki, *Water flash evaporation under low pressure conditions.* Previews of Heat and Mass Transfer. Vol. 6, 1995: p. 518.
14. P. Sebastian and J.P. Nadeau, *Experiments and modeling of falling jet flash evaporators for vintage treatment.* International journal of thermal sciences. Vol. 41, 2002: p. 269-280.
15. K. Al-Shayji, S. Al-Wadyei, and A. Elkamel, *Modelling and optimization of a multistage flash desalination process.* Engineering optimization. Vol. 37, 2005: p. 591-607.
16. O. Miyatake, K. Murakami, Y. Kawata, and T. Fujii, *Fundamental experiments with flash evaporation.* Heat Transfer-Jpn. Res. Vol. 2, 1973: p. 89-100.

17. O. Miyatake, T. Fujii, T. Tanaka, and T. Nakaoka, *Flash evaporation phenomena of pool water.* Heat Transfer Japanese Research. Vol. 6, 1977: p. 13.
18. H.E.S. Fath, *The non-equilibrium factor and the flashing evaporation rate inside the flash chamber of a multi-stage flash desalination plant.* Desalination. Vol. 114, 1997: p. 277-287.
19. Z. Dan, C. Daotong, Y. Junjie, and Z. Bingchao, *Experimental study on static flash evaporation of aqueous NaCl solution.* International Journal of Heat and Mass Transfer. Vol. 55, 2012: p. 7199-7206.
20. D. Zhang, B. Zhao, J. Yan, and Q. Yang, *Experimental study on static flash vaporization of aqueous NaCl solution at different flash speed: Steam-carrying effect.* International Journal of Heat and Mass Transfer. Vol. 79, 2014: p. 618-627.
21. D. Zhang, J. Yan, B. Zhao, and J. Feng, *Experimental study on energy conversion efficiency during static flash of aqueous NaCl solution.* International Journal of Heat and Mass Transfer. Vol. 83, 2015: p. 284-293.
22. D. Zhang, J. Yan, Y. Liu, and B. Zhao, *Preliminary exergy analysis of static flash of pure water.* International Journal of Heat and Mass Transfer. Vol. 86, 2015: p. 377-387.
23. W. Gao, W. Sun, K. Anderson, Y. Cheng, and A. Li, *Investigation on temperature distribution of flash evaporation of LiCl droplets released into vacuum.* International Journal of Heat and Mass Transfer. Vol. 74, 2014: p. 414-420.
24. Y. Zhang, J. Wang, J. Liu, D. Chong, W. Zhang, and J. Yan, *Experimental study on heat transfer characteristics of circulatory flash evaporation.* International Journal of Heat and Mass Transfer. Vol. 67, 2013: p. 836-842.
25. Y. Zhang, J. Wang, J. Yan, D. Chong, J. Liu, W. Zhang, and C. Wang, *Experimental study on non-equilibrium fraction of NaCl solution circulatory flash evaporation.* Desalination. Vol. 335, 2014: p. 9-16.
26. Y. Junjie, Z. Dan, C. Daotong, W. Guifang, and L. Luning, *Experimental study on static/circulatory flash evaporation.* International Journal of Heat and Mass Transfer. Vol. 53, 2010: p. 5528-5535.
27. O. Miyatake, T. Tomimura, Y. Ide, and T. Fujii, *An experimental study of spray flash evaporation.* Desalination. Vol. 36, 1981: p. 113-128.
28. O. Miyatake, T. Tomimura, Y. Ide, M. Yuda, and T. Fujii, *Effect of liquid temperature on spray flash evaporation.* Desalination. Vol. 37, 1981: p. 351-366.
29. O. Miyatake, T. Tomimura, and Y. Ide, *Enhancement of spray flash evaporation by means of the injection of bubble nuclei.* Journal of solar energy engineering. Vol. 107, 1985: p. 177.
30. Y. Zeng and C.-F.F. Lee, *An atomization model for flash boiling sprays.* Combustion Science and Technology. Vol. 169, 2001: p. 45-67.
31. Y. Ikegami, H. Sasaki, T. Gouda, and H. Uehara, *Experimental study on a spray flash desalination (influence of the direction of injection).* Desalination. Vol. 194, 2006: p. 81-89.
32. D. Balaji, *Experimental study on the effect of feed water nozzles on non-equilibrium temperature difference and flash evaporation in a single-stage evaporator and an investigation of effect of process parameters on the liquid flashing in a LTTD desalination process.* Desalination and Water Treatment. Vol. 57, 2016: p. 27152-27168.

33. U. Haruo, M. Akio, K. Toru, H. Masaki, and E. Stuhltrager., *A Study of the Spray Flash Desalination (Effect of Nozzle Shape).* Bulletin of the Society of Sea Water Science, Japan. Vol. 45, 1991.
34. A. Muthunayagam, K. Ramamurthi, and J. Paden, *Low temperature flash vaporization for desalination.* Desalination. Vol. 180, 2005: p. 25-32.
35. A.K. El-Fiqi, N.H. Ali, H.T. El-Dessouky, H.S. Fath, and M.A. El-Hefni, *Flash evaporation in a superheated water liquid jet.* Desalination. Vol. 206, 2007: p. 311-321.
36. W. Gao, C. Li, C. Xu, D. Wang, and D. Wu, *An experimental investigation of salt-water separation in the vacuum flashing assisted with heat pipes and solid adsorption.* Desalination. Vol. 399, 2016: p. 116-123.
37. I. Hamawand, L. Lewis, N. Ghaffour, and J. Bundschuh, *Desalination of salty water using vacuum spray dryer driven by solar energy.* Desalination. Vol. 404, 2017: p. 182-191.
38. B. Cai, X. Tuo, Z. Song, Y. Zheng, H. Gu, and H. Wang, *Modeling of spray flash evaporation based on droplet analysis.* Applied Thermal Engineering. Vol. 130, 2018: p. 1044-1051.
39. B. Cai, Y. Yin, Y. Zheng, W. Wang, H. Gu, J. Yao, and H. Wang, *Mathematical study of spray flash evaporation in a spray-assisted seawater desalination chamber.* Desalination. Vol. 465, 2019: p. 25-37.
40. Q. Chen, K.J. M, Y. Li, and K.J. Chua, *Experimental and mathematical study of the spray flash evaporation phenomena.* Applied Thermal Engineering. Vol. 130, 2018: p. 598-610.
41. S. Mutair and Y. Ikegami, *Experimental study on flash evaporation from superheated water jets: Influencing factors and formulation of correlation.* International Journal of Heat and Mass Transfer. Vol. 52, 2009: p. 5643-5651.
42. S. Mutair and Y. Ikegami, *Experimental investigation on the characteristics of flash evaporation from superheated water jets for desalination.* Desalination. Vol. 251, 2010: p. 103-111.
43. L. Liu and M.-L. Mi, *Theoretical investigation on rapid evaporation of a saline droplet during depressurization.* Microgravity Science and Technology. Vol. 25, 2014: p. 295-302.
44. Q. Chen, K. Thu, T. Bui, Y. Li, K.C. Ng, and K. Chua, *Development of a model for spray evaporation based on droplet analysis.* Desalination. Vol. 399, 2016: p. 69-77.
45. D. Saury, S. Harmand, and M. Siroux, *Experimental study of flash evaporation of a water film.* International Journal of Heat and Mass Transfer. Vol. 45, 2002: p. 3447-3457.
46. W.X. Jin and S.C. Low, *Investigation of single-phase flow patterns in a model flash evaporation chamber using PIV measurement and numerical simulation.* Desalination. Vol. 150, 2002: p. 51-63.
47. W.X. Jin, S.C. Low, and S.C.M. Yu, *Some experimental observations on the single and multi-phase flow patterns in a model flash evaporation chamber.* International Communications in Heat and Mass Transfer. Vol. 26, 1999: p. 839-848.
48. C. Augusto, J. Ribeiro, A. Gaspar, and J. Costa, *Physical and experimental calibration of a mathematical model of the low-pressure-vaporization of free water.* Journal of Food Engineering. Vol. 138, 2014: p. 23-34.

49. E. Hahne and G. Barthau, *Evaporation waves in flashing processes.* International Journal of Multiphase Flow. Vol. 26, 2000: p. 531-547.
50. P. Reinke and G. Yadigaroglu, *Explosive vaporization of superheated liquids by boiling fronts.* International Journal of Multiphase Flow. Vol. 27, 2001: p. 1487-1516.
51. D. Saury, S. Harmand, and M. Siroux, *Flash evaporation from a water pool: Influence of the liquid height and of the depressurization rate.* International Journal of Thermal Sciences. Vol. 44, 2005: p. 953-965.
52. S. Gopalakrishna, V.M. Purushothaman, and N. Lior, *An experimental study of flash evaporation from liquid pools.* Desalination. Vol. 65, 1987: p. 139-151.
53. S. Gopalakrishna and N. Lior, *Analysis of bubble translation during transient flash evaporation.* International Journal of Heat and Mass Transfer. Vol. 35, 1992: p. 1753-1761.
54. Y. Shao, Y. Li, L. Yang, X. Zhang, L. Yang, H. Wu, and R. Xu, *New experimental system for high pressure and high temperature flashing evaporation experiments.* Applied Thermal Engineering. Vol. 66, 2014: p. 148-155.
55. D. Zhang, D. Chong, J. Yan, and B. Zhao, *Experimental study on static flash evaporation of aqueous NaCl solution at different flash speed: Heat transfer characteristics.* International Journal of Heat and Mass Transfer. Vol. 65, 2013: p. 584-591.
56. Y. Zhang, J. Wang, J. Yan, D. Chong, and J. Liu, *Experimental study on energy transformation and separation characteristic of circulatory flash evaporation.* International Journal of Heat and Mass Transfer. Vol. 99, 2016: p. 862-871.
57. B. Zhao, D. Zhang, Q. Yang, and J. Yan, *Experimental study on equilibrium waterfilm concentration in static flash evaporation of aqueous NaCl solution.* Desalination. Vol. 353, 2014: p. 109-117.
58. D. Zhang, D. Chong, J. Yan, and Y. Zhang, *Study on steam-carrying effect in static flash evaporation.* International Journal of Heat and Mass Transfer. Vol. 55, 2012: p. 4487-4497.
59. A. El-Zahaby, A. Kabeel, A. Bakery, E. Agouz, and O. Hawam. *Enhancement of solar desalination still productivity using flash evaporation*. in *Thirteenth International Water Technology Conference, IWTC*. 2009.
60. A. El-Zahaby, A. Kabeel, A. Bakry, S. El-Agouz, and O. Hawam, *Augmentation of solar still performance using flash evaporation.* Desalination. Vol. 257, 2010: p. 58-65.
61. L. Liu, Q. Bi, and G. Wang. *Dynamics of evaporation and cooling of a water droplet during the early stage of depressurization*. in *ASME 2009 International Mechanical Engineering Congress and Exposition*. 2009. American Society of Mechanical Engineers.
62. J. Hou, H. Cheng, D. Wang, X. Gao, and C. Gao, *Experimental investigation of low temperature distillation coupled with spray evaporation.* Desalination. Vol. 258, 2010: p. 5-11.
63. O. Miyatake and Y. Miki, *Simplified expression for efficiency of spray flash evaporation*. 1987, Soc chemical Eng japan kyoritsu p. 252-256.

64. E.M. Peter, A. Takimoto, and Y. Hayashi, *Flashing and shattering phenomena of superheated liquid jets.* JSME International Journal Series B Fluids and Thermal Engineering. Vol. 37, 1994: p. 313-321.
65. S. Mutair and Y. Ikegami, *On the evaporation of superheated water drops formed by flashing of liquid jets.* International Journal of Thermal Sciences. Vol. 57, 2012: p. 37-44.
66. J. Wellmann, K. Neuhäuser, F. Behrendt, and M. Lehmann, *Modeling an innovative low-temperature desalination system with integrated cogeneration in a concentrating solar power plant.* Desalination and Water Treatment. Vol. 55, 2015: p. 3163-3171.
67. F. Xuening, C. Lei, D. Yuman, J. Min, and F. Jinping, *CFD modeling and analysis of brine spray evaporation system integrated with solar collector.* Desalination. Vol. 366, 2015: p. 139-145.
68. A.H. Araghi, M. Khiadani, M. Sadafi, and K. Hooman, *A numerical model and experimental verification for analysing a new vacuum spray flash desalinator utilising low grade energy.* Desalination. Vol. 413, 2017: p. 109-118.
69. Z. Zhifu, W. Weitao, C. Bin, W. Guoxiang, and G. Liejin, *An experimental study on the spray and thermal characteristics of R134a two-phase flashing spray.* International Journal of Heat and Mass Transfer. Vol. 55, 2012: p. 4460-4468.
70. J. Xie, Z. Gan, F. Duan, T. Wong, S. Yu, and R. Zhao, *Characterization of spray atomization and heat transfer of pressure swirl nozzles.* International Journal of Thermal Sciences. Vol. 68, 2013: p. 94-102.
71. M. Sadafi, S.G. Ruiz, M. Vetrano, I. Jahn, J. van Beeck, J. Buchlin, and K. Hooman, *An investigation on spray cooling using saline water with experimental verification.* Energy Conversion and Management. Vol. 108, 2016: p. 336-347.
72. J. Xie, Z. Gan, T. Wong, F. Duan, S. Yu, and Y. Wu, *Thermal effects on a pressure swirl nozzle in spray cooling.* International Journal of Heat and Mass Transfer. Vol. 73, 2014: p. 130-140.
73. R. Peterson, S. Grewal, and M. El-Wakil, *Investigations of liquid flashing and evaporation due to sudden depressurization.* International journal of heat and mass transfer. Vol. 27, 1984: p. 301-310.
74. M. Sadafi, I. Jahn, and K. Hooman, *Nozzle arrangement effect on cooling performance of saline water spray cooling.* Applied Thermal Engineering. Vol. 105, 2016: p. 1061-1066.
75. A.H. Araghi, M. Khiadani, K. Hooman, and G. Lucas, *Efficiency of a Combined Desalination and Power System Utilising a Two-Phase Flow Multi-Stream Heat Exchanger.* Heat Transfer Engineering. Vol. 38, 2016: p. 1000-1007.
76. Husted, B.P., *Experimental Measurements of Water Mist Systems and Implications for Modelling i CFD*. 2007: Department of Fire Safety Engineering, Lund University.

Chapter 2

Evaporation Rates and Temperature Distributions in Fine Droplet Flash Evaporation Sprays [1]

Abstract

This study reports an experimental investigation of a flash evaporation system based on low-temperature thermal desalination (LTTD) technology. Low temperature liquid in the range of 60 to 80˚C becomes superheated by injecting it through a nozzle into a depressurized chamber. Previous studies have not attempted to establish a correlation model between the temperature distributions and the evaporation rate. Moreover, this study presents for the first time the temperature distribution in fine droplets (small nozzle, 0.8mm) sprays upward flash evaporation sprays over a range of conditions. The effect of the operating parameters on the temperature distribution and evaporation rate of flashing spray is also investigated and comparisons are made between the results of the present experiments and flash evaporation jets.

The dimensionless temperature introduced (Θ_{emp}) follows an exponential decaying curve and is found to also match temperature distributions in a range of other works covering different nozzles (sprays or jets), in both upward and downward flash evaporation. It is also found that flow rate has a different effect on the evaporation rate depending on whether spray or jet flash evaporation is taking place. Increasing the flow rate in sprays leads to higher flash evaporation but lowers the evaporation rate in jets.

Keywords: Flash evaporation, fine droplets, superheated, model, evaporation rate

---

[1] This chapter has been published as a full research paper:
F. Fathinia, Y.M. Al-Abdeli, and M. Khiadani, *Evaporation rates and temperature distributions in fine droplet flash evaporation sprays.* International Journal of Thermal Sciences. Vol. 145, 2019: p. 106037. https://doi.org/10.1016/j.ijthermalsci.2019.106037
Whilst efforts were made to retain original content of the article, minor changes such as number formats, font size and style were implemented in order to maintain consistency in the formatting style of the thesis.

2.1 Introduction

Water is an essential part of mankind's life and many processes have been constructed for the purpose of producing potable water. Rapid population growth, use of water for agricultural irrigation, and pollution of water resources have caused researchers to continually seek effective processes to address freshwater scarcity. Desalination separates fresh water from the nearly inexhaustible supply of seawater, but most of its technologies are energy intensive [1]. In this context, seawater desalination has been the subject of many studies aiming to develop reliable and economical technologies, as well as resolving the factors affecting process efficiency.

Flash evaporation desalination is a process which involves rapidly vaporizing (saturated liquid) water in a vacuum chamber due to a sudden drop in the surrounding pressure. Low Temperature Thermal Desalination (LTTD) technologies use the principle of flash evaporation whereby sprays are injected under vacuum conditions thereby causing the liquid to quickly superheat. In order to regain thermodynamic equilibrium, the saline liquid is vaporized and pure water is condensed. Ocean Thermal Energy Desalination (OTED) [2, 3] and Discharge Thermal Energy Combined Desalination (DTECD) [4] are two variant processes constructed based on the LTTD method which have attracted attention because of their ability to utilize waste heat and reduce CO_2 emission level [5]. Fundamental insight into the thermodynamics and structure of flash evaporation sprays is essential for process designers to improve system efficiency. For this reason, some research has focused on the atomization part of LTTD systems in order to correlate operating parameters to performance [5-10]. The current study resolves the effects of several process parameters on the centreline temperature distribution which has a significant impact on the atomization characteristics of saline sprays under vacuum.

The general flashing process based on the thermodynamic phase diagram of water is described in

Figure 2.1 Before injection, pressurized water is stable and held in the sub-cooled region at the inlet temperature (T_{in}). The liquid is decompressed isothermally at the

nozzle exit when it is in the superheated state. This region of injection is called the nucleation region and is where small bubbles are produced due to the low chamber pressure (P_{out}). The bubbles then expand precipitously under the vacuum pressure until they reach the spray breakup point, whereby very fine droplets are atomized inside the vacuum chamber. These small droplets do not remain in equilibrium but turn into vapour due to the fluid existing above its saturated temperature (T_{sat}). The latent heat of vaporization is the energy consumed by flash evaporation and manifests itself as a temperature reduction of droplet temperature to saturation point and continues until droplets return to the surrounding temperature inside the chamber [11]. This causes spatial variation in temperature throughout the spray and forms an important means of characterising the flash evaporation process (as occurs in the present study).

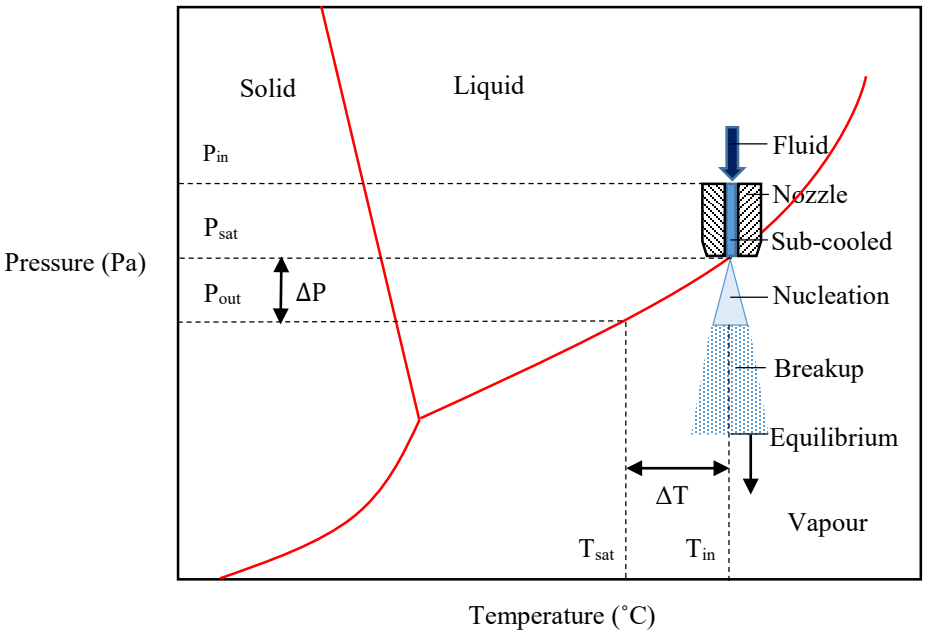

Figure 2.1 Thermodynamic phase diagram of fluid states and the characteristic regions of the jet in flash evaporation.

In this context, the superheat degree (ΔT) is the difference between the inlet temperature (T_{in}), which is measured at the point of introducing the nozzle into the vacuum chamber, and saturation temperature (T_{sat}) which varies based on the concentration of the saline fluid at a given vacuum pressure. It is expressed by Equation 2.1 [12]:

$$\Delta T = T_{in} - T_{sat} \tag{2.1}$$

Research in to flash evaporation has tackled two main approaches; pool evaporation or spray and jet evaporation [12]. In pool evaporation, a liquid that is dispersed over a surface area is subjected to a controlled vacuum pressure within a sealed chamber, while in spray and jet evaporation, the liquid is injected through a nozzle having an orifice into the vacuum chamber. In the present study, the term "jet" is differentiated from "spray" based on the likely centreline temperature profile as shown in Figure 2.2, whereby jets do not immediately experience breakup near the nozzle exit point (z=0), unlike sprays that atomize very near the nozzle exit. The present study focuses on the latter.

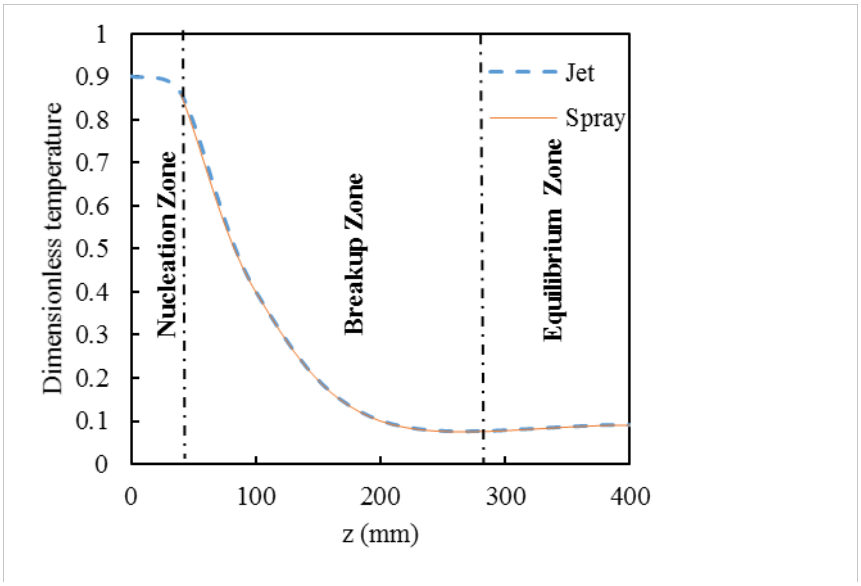

Figure 2.2 Dimensionless centreline temperature profiles in jets and sprays (adapted from [13])

In relation to spray flash evaporation, Miyatake et al. [14] experimentally examined the flash evaporation phenomenon using different nozzle diameters at T_{in}=60˚C and concluded that spray flash evaporation has much more intense heat transfer than pool boiling. In a follow up work, Miyatake et al. [15] applied a different range of temperatures (T_{in}=40˚C-80˚C) and developed empirical models to predict the variation in centreline temperature for downward saline injected sprays. However, more work is warranted to resolve the temperature distribution in upward flowing sprays since the direction of injecting sprays affects the characteristics of the flashing process. In this regard, Ikegami et al. [16] observed that upward flashing from fairly large orifices of the order d=20mm took less time for evaporation

compared to those injected downwards (T_{in} =24, 30, and 40˚C; u=1.74 to 3.62 m/s). As such, this study focuses on developing an empirical model for the spatially resolved temperatures in much finer nozzle upward sprays over a range of steady-state operating conditions, in both saline and pure water.

Additionally, a number of models have been presented to describe the underlying physics of droplet evaporation. Some of these have been utilized to study droplet evaporation in fuel sprays [17, 18], reacting sprays [19, 20], cooling sprays [21, 22], or (liquid) pool evaporation [23-25]. These models have provided generalised mathematical, empirical or other descriptions of (non-reacting) sprays under flash evaporation. Mutair and Ikegami [26] modelled surface evaporation from superheated droplets in the upward flow when exposed to vacuum. Mutair and Ikegami [13, 27] also presented their results in terms of a non-dimensionalised temperature as well as deriving a Boltzman sigmoid model for predicting thermal behaviour of upward superheated water jets (not sprays) under low chamber pressure (T_{in} =24-40˚C) and they concluded it would be possible to empirically predict the end point and inflection point of evaporation. Although their study supported the significance of resolving the temperature distribution and structure in flash evaporation of large diameter nozzles, their results and proposed equations did not involve or give any specifications about flash evaporation from small diameter nozzles as used in this research. In follow-up research, Liu and Mi [28] reported a mathematical model for single droplet, not spray, evaporation when suspended on a thin wire, with empirical predictions validated against experimental data. Chen et al. [29] also developed a theoretical model of spray flash evaporation (superheated liquid) using droplet velocity and size as the main parameters to predict the fraction of condensed (pure) water (compared to the total brine water sprayed) as well as thermal efficiency of the process. Cai et al. [30] developed a model to analyse the influence of the injection pressure, evaporation chamber pressure and flow velocity on the energy utilization efficiency and spray flash speed. Alghamdi et al. [31] visualised flash-boiling atomization of a flash evapoaration jet when released into a depressuized area and helped resolve the bubble expansion mechanism. Their results showed that atomized droplets achieve much larger speeds than the jet velocity. Whilst most of these works used nozzles with relatively large orifice diameters for spraying superheated water, Chen et al.

[32] reported that smaller droplets enhance the evaporation rate due to increased surface area. However, the temperature distribution of these fine droplets (achieved with a smaller nozzle orifice) in the vacuum chamber and its correlation to the evaporation rate has not been comprehensively clarified. Hence why the present study adds new insights into flash spray evaporation in finer droplet sprays unlike earlier works with much larger droplet sizes [16]. Finally, whilst most of these studies [13, 27-29, 32] have focussed on flash evaporation from saline nozzles, no studies have attempted to derive such empirical models in fine droplets (nozzle orifice of 0.8mm) upward flowing pure water sprays. This is important particularly as Liu et al. [33] have experimentally confirmed that, over varied concentration (NaCl salinity=0%, 10%, 26%), the evaporation rate in flash evaporation sprays changes.

To summarise, little or no information is available in the published literature on models to describe the temperature distribution in single nozzle upward projected fine droplets sprays under flash evaporation conditions, with concentrations from potable (0%NaCl) to sea water (3.5%NaCl). Parameters varied will also show the effects of four process factors, namely initial temperature (T_{in}), salinity (C), superheat degree (ΔT), and inlet flow rate of inlet liquid (Q). Comparisons will also be made between the results of the current experiment and other flashing coarse droplets ejected from jet nozzles.

2.2 Methodology

2.2.1 Vacuum chamber

Figure 2..3a shows the vacuum spray flash evaporator which operates on the DTECD principle [5]. It is a single stage flash evaporation process comprised of a supply tank, the spray chamber (operated at P_{vac}), a data acquisition system to log temperatures, shell and tube condenser for water evaporated in the spray chamber, a condensate tank, the cooling water tank connected to the condenser, and a vacuum pump (creating vacuum pressure inside chamber). Due to the challenges of souring filtered seawater of uniform qualities and the limited capacity of the feed tank, a mixture of tap water and NaCl is instead applied throughout the experiments. The spray liquid is heated up in the water tank until the desired temperature (T_{in}) is reached then pumped to the vacuum chamber. The flow rate (Q=1-2l/min) can be

adjusted using the variable speed pump (Southern Cross, SBI-9T). By utilizing the spray nozzle (H.Ikeuichi, JJXP 014 303), the heated water is injected into the vacuum chamber, where the pressure is maintained below the saturation pressure (P_{sat}) at the corresponding T_{in}. According to the nozzle manufacture's specification [34], the free pass diameter of the nozzle is 0.8mm, the spray pattern is full cone (included angle of 55˚), and the nozzle has a spray capacity which can be varied between 0.79 to 2.89l/min over inlet pressures 0.3bar to 10bar. Over these nominal specific actions, the mean droplet diameter is also estimated to be in the range of 290 to 410μm. The vacuum pump (Speck, V-30-55.0012) is connected to the chamber via the condenser and can be valve regulated to create a constant vacuum pressure. Vaporization is produced in the chamber as a result of the superheated water being exposed to the vacuum pressure. This vapour is sucked to the shell and tube condenser, where cooling by the recirculating tank takes place to condense the vapour. The distilled water is then directed to the condensate tank.

The top of the vacuum chamber also includes a demister in the form of a steel mesh layer. The demister (Harver Standard) and its specifications are summarized in Table 2.1.

Table 2.1 Specifications of the wire mesh demister [**35**]

Type	Diameter (mm)	Thickness (mm)	Bulk density (kg/m^3)	Surface area (m^2/m^3)	Voidage (%)
MOC:SS304	400	100	144	265.09	98.18

It is installed to trap any (saline, non-vaporized) water droplets whose trajectory may take them to the top of the vacuum chamber. Since it is positioned 320mm above the nozzle, it prevents saline water to entrain in the vapour flow and only water condensate that is desired from flash evaporation emerges from the shell and tube heat exchanger. This allows accurate calculation of the evaporation rate (E) for the flash evaporator. Figure 2.3b illustrates the radial distances between thermocouples on the holding bar, which can be translated to different axial

locationS in the axial z-direction. Figure 2.3c also shows all the components and main dimensions of vacuum spray flash evaporator.

(a)

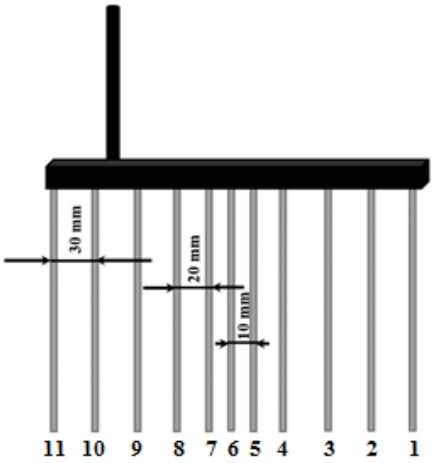

(b)

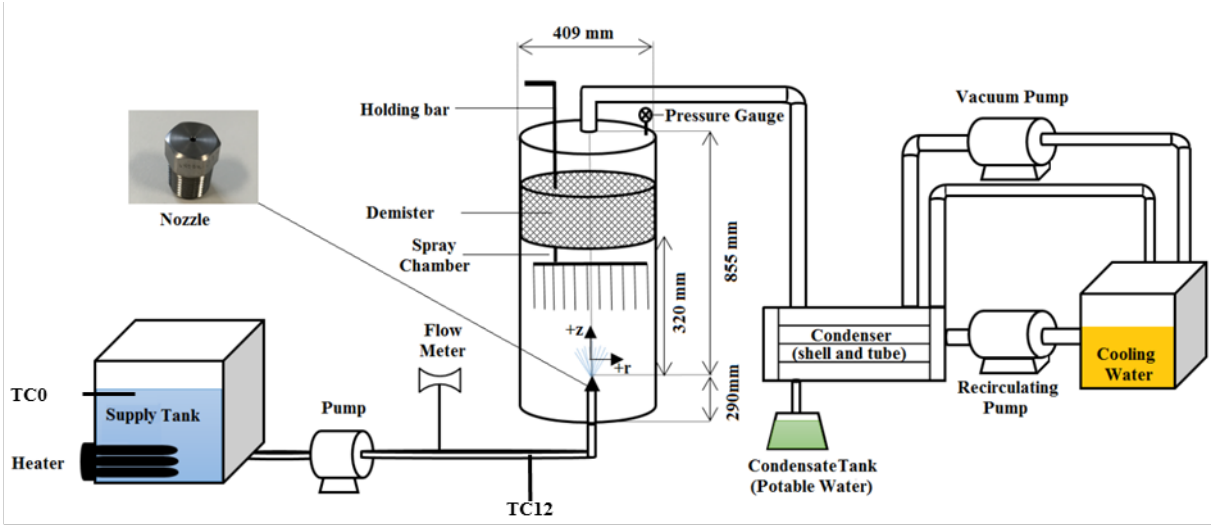

(c)

Figure 2.3 (a) The vacuum spray flash evaporator and its instrumentation; (b) thermocouple distribution on the holding bar; and (c) components and main dimensions

A flow meter (MFS Magmaster) with ±0.2% (l/min) accuracy is placed in the pipeline before injection. A vacuum pressure transmitter (General Electric, UNIK 5000, PTX-5-0-6-2-TA-A3-CA-H0-PE, and range 0 to 6bar gauge) with ±0.04% (bar) accuracy is attached at the top of the vacuum chamber. A thermocouple was

also used before the nozzle to measure the supply water temperature (T_{in}). All data acquired by these instruments are logged by a National Instrument LabVIEW V.2014. For each test condition, data acquisition of process parameters occurs only when the vacuum chamber is operated in steady state mode. Over this stable period, temperatures are acquired and the final volume of water collected into the condensate tank is measured. This is the process for establishing the evaporation rate and for this purpose, a graduated glass beaker is used to measure the condensate having a minimum scale increment of 1ml.

2.3 Temperature measurements

Temperature inside the vacuum chamber is measured over the axial distance of z=0 to 200mm. By moving the holding bar along the streamwise direction, the temperature can be measured at 13 axial stations: 0, 5, 10, 15, 20, 30, 40, 60, 80, 100, 140, 180, and 200mm. Eleven thermocouples (TC Measurement, type T-Class1) with the accuracy of ±0.75% are applied for measuring the radial and axial distribution of temperature in sprays (TC1-TC11) inside the chamber. In addition, two thermocouples with the same configuration are installed outside of the chamber, (TC0) for monitoring the temperature of the tank and (TC12) for measuring T_{in} before the injection. The calibration for all the thermocouples was done for 0˚C and 100˚C by using a thermocouple calibration device (Armfield, TH1 Temperature Measurement and Calibration). The procedure involved inserting the thermocouples into a bath of ice or boiling water so as to establish the melting point of ice and boiling point of water as reference temperatures, respectively [36].

In establishing the temperature distribution for sprays, a steady state operating condition had to first be established. This is significant because of the relatively large thermal mass of the (steel) vacuum chamber and measurements in liquid and vapour phases. Once stable operating conditions are established temperature changes are negligible. Figure 2.4 illustrates that four minutes are required to achieve a steady operation period over different test conditions. All temperatures reported (in the results) are averages established over a10min interval within the stable operating period at a data acquisition sampling period of 2.5s.

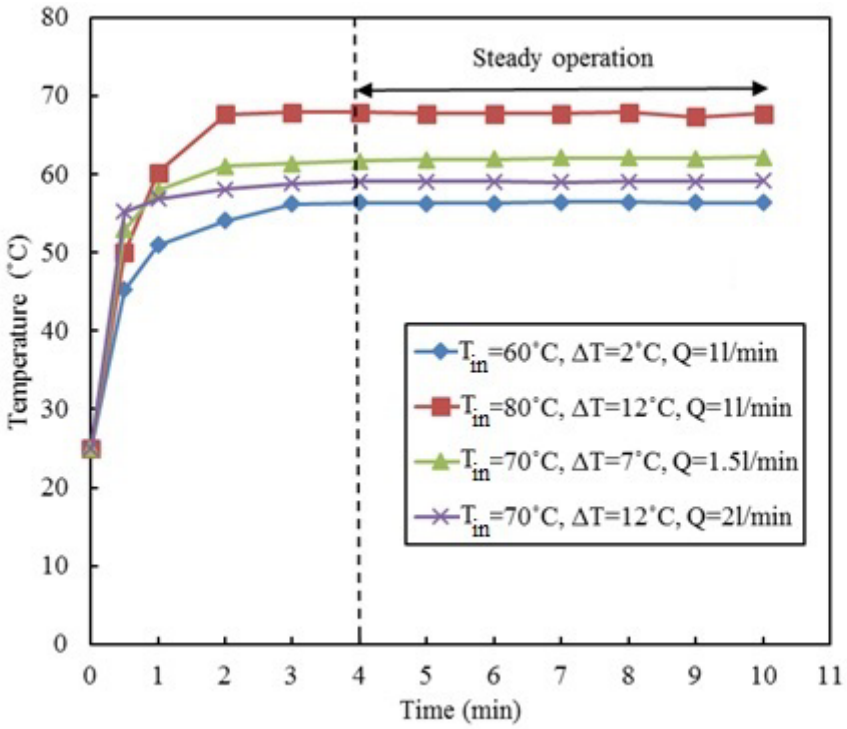

Figure 2.4 Time series of temperatures at the nozzle exit plane (T_{in} (0,0)). Data also shows the duration to reach the steady operation period

In order to non-dimensionalise various measured spray temperatures, it is necessary to define a dimensionless parameter for temperature. Other researchers have suggested Equation 2.2 to express a dimensionless temperature for the jet nozzle [8, 12, 13], where T(r,z) denotes the temperatures in the radial and axial points, T_{sat} is the saturation temperature that depends on both the chamber pressure and purity of water (concentration of saline solution), and T_{in} in the present is the feed water temperature.

$$\theta = \frac{T(r,z) - T_{sat}}{T_{in} - T_{sat}} \tag{2.2}$$

However, it is notable that whilst this expression has been used for jets before, it has not been applied to (fine droplet) sprays. This is likely because the spatially resolved temperature T(r,z) measured in such sprays can be less than T_{sat}, thereby rendering the (numerator) negative. Moreover, in contrast to Equation 2.2 in which its denominator does not consider the effects of nozzle type or atomization characteristics (T_{sat} and T_{in} are nozzle/spray independent), these parameters are

reflected in Equation 2.3 by considering T_{equ}. The modified dimensionless temperature (Θ_{exp}) used in the present study is given by Equation 2.3:

$$\theta_{\exp} = \frac{T(r,z) - T_{equ}}{T_{in} - T_{equ}} \tag{2.3}$$

where T(r,z) is the radial and axial temperature in the chamber, T_{in} is the inlet temperature of saline water and T_{equ} is the equilibrium temperature. By introducing T_{equ} instead of T_{sat}, spray temperatures are normalized by the effects of superheating in each spray nozzle. This is because the spatial location at which localised superheating occurs (in the droplets) depends not only on (T_{in}) and (T_{sat}) but also the spray pattern. The advantage of using T_{equ} instead of T_{sat} is the applicability of the proposed equation in both spray and jet nozzles. This is mainly due to the fact that when jet nozzles are used, a greater volume of water in liquid state hits the thermocouples making T_{equ} equal to T_{sat}. Therefore, Equation 2.3 is capable of covering both types of nozzles.

Figure 2.5 shows a graphical representation of the equilibrium temperature (T_{equ}) in a test condition. It can be seen that radially resolved temperatures in the spray continue to change with axial distance (indicating physical spray evaporation), but remain relatively unchanged at 200mm (evaporation is complete). Therefore, in the test condition depicted within Figrue 2.5, T_{equ}=54˚C which is achieved at z=200mm.

To further emphasize the merit of using T_{equ} in Equation 2.3 (denominator) as the parameter to normalise the spatially resolved temperatures T(r,z), Table 2 presents the axial station at which various T_{equ} are observed, where these locations (z_{equ}) have been derived graphically from the axial distribution of centreline temperature over z=0 to z=200mm.

Table 2.2 The equilibrium temperature (T_{equ}) for water (C=0%) and saline sprays (C=3.5%, NaCl) at Q=1 l/min

ΔT(˚C)	T_{in}(˚C)	C (%)	T_{equ}(˚C)	Z_{equ}(mm)
	60	3.5	46.2	197.8
	60	0	47.8	197.1
	70	3.5	53.4	200.4
2	70	0	54.3	198.2
	80	3.5	58.9	204.1
	80	0	60.8	201.1
	60	3.5	43.7	197.2
	60	0	44.8	196.9
	70	3.5	50.4	202.1
12	70	0	50.8	202.0
	80	3.5	56.6	203.4
	80	0	58.2	200.3

These data show that the equilibrium height is fairly constant at z equal 200mm. In other words, the evaporation is complete in this height (z_{equ}) and the equilibrium temperature of the droplets (T_{equ}) does not change further of this point which justifies the measurements done in this research to be limited to z=200mm. Figure 2.6 also summarises the data for two sprays at a single flow rate (Q= 1l/min); a saline spray (C=3.5%) and pure water spray (C=0%) when operated at different saturation temperatures. It is evident from this that whilst multiple sprays can have the same values of T_{sat} and T_{in}, T_{equ} varies between sprays. As such, normalization by T_{sat} in Equation 2.2 (as has occurred in earlier research) means that the spatial variation of sprays, as defined by T_{equ}, is not considered. Normalization by T_{equ} therefore allows the characteristics of each spray to be considered when deriving

Θ. Based on this, it is obvious that for the same inlet flow temperature (T_{in}) and comparable T_{equ}, a slower rate of evaporation is likely when higher temperatures T(r,z) are observed throughout the spray due to a weakened effect from the latent heat of vaporisation, Consequently, higher values of Θ_{exp} arise from weaker flash evaporation and a diminished evaporation rate.

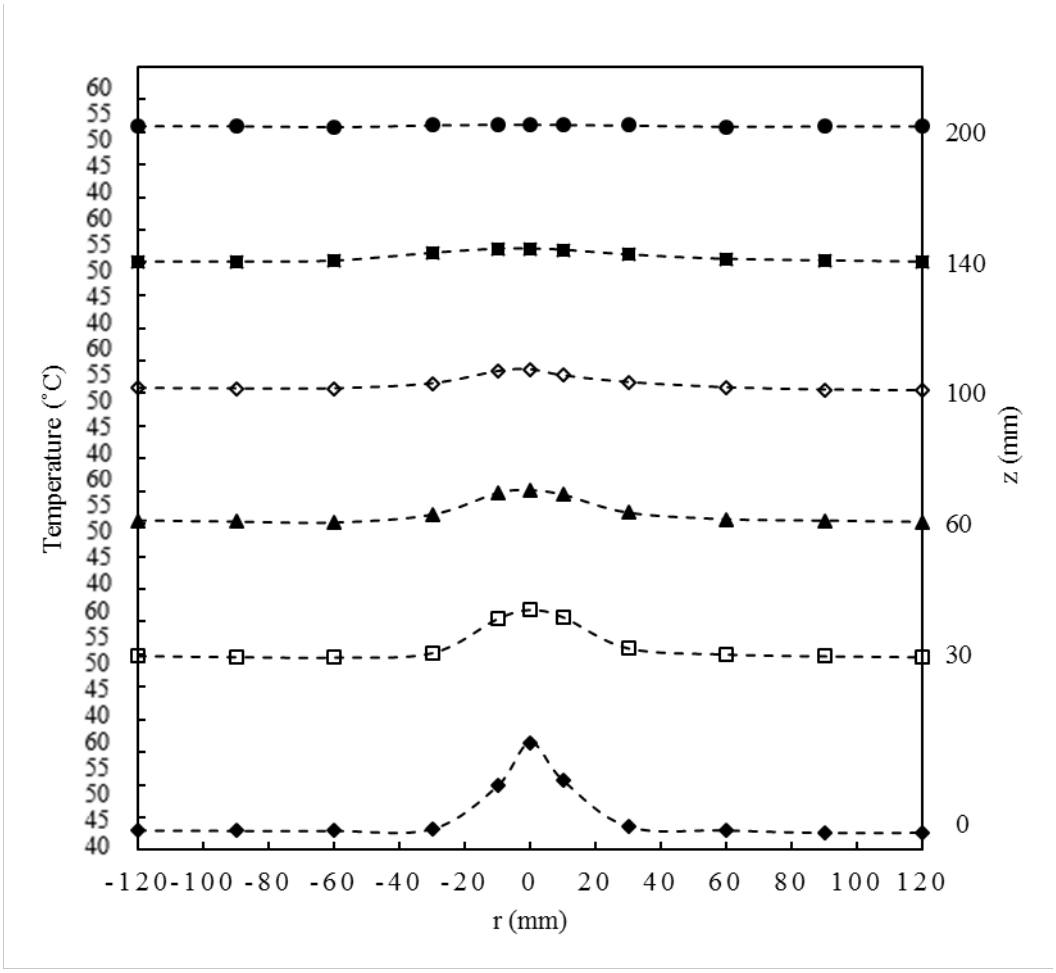

Figure 2.5 Distribution of spray temperature (T_{in}(r,z)) and the equilibrium temperature (T_{equ}) resolved at z=200 mm and condition of C=3.5%, T_{in}=70˚C, Q=1 L/min, and ΔT=2˚C

Measuring the distilled water condensed by the heat exchanger has been applied for calculating the evaporation rate. As such, the evaporation rate (E) is defined as follows [37]:

$$E = \frac{m_{dis}}{m_{in}} \tag{2.4}$$

where m_{dis} is the mass of distilled product (potable water) and m_{in} is the mass of inlet brine water.

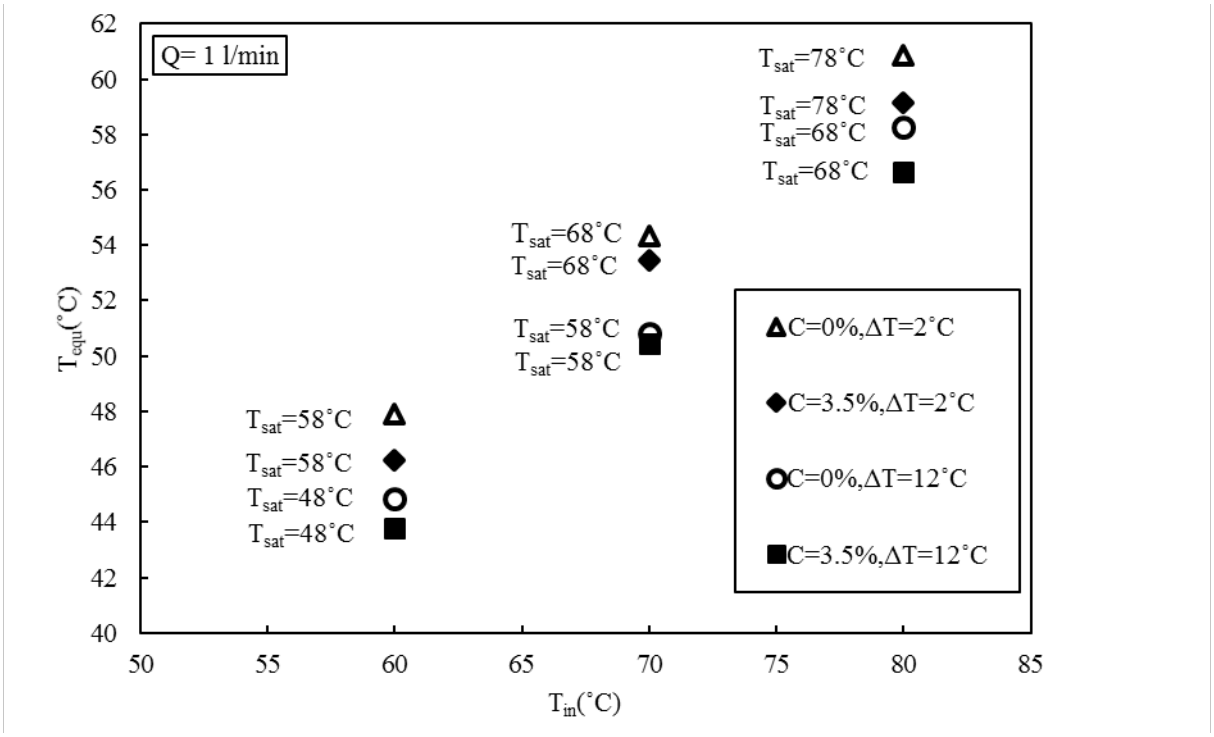

Figure 2.6 Variation of equilibrium temperature (T_{equ}) in sprays with varying (T_{in})

2.4 Uncertainty analysis

In this study, the experimental uncertainty is calculated as a function of systematic and random error [38], where ε is the total uncertainty, ε_s is the systematic error and ε_r is the random error:

$$\varepsilon = \pm\sqrt{\varepsilon_s^2 + \varepsilon_r^2} \tag{2.5}$$

Systematic errors are a constant value during an experiment and are normally introduced by the measuring instrument accuracy that manufacturers report. Random errors come from the measured data and are derived from repeating measurements and then estimated by the standard error. The random error is calculated using Equation 2.6 [39] ,where s is the sample variance for the n groups of measurements and calculated by Equation 2.7:

$$\varepsilon_r = \frac{s}{\sqrt{n}} \tag{2.6}$$

$$s^2 = \frac{\sum_{i=1}^{n}(x_i - \overline{x})^2}{n-1} \tag{2.7}$$

The $\overline{x}$ sample average is obtained by Equation 2.8:

$$\overline{x} = \frac{\sum_{i=1}^{n} x_i}{n} \tag{2.8}$$

where, x_i is the ith specific data. In the experiments, the uncertainty of results was quantified based on each test having three repetitions (n=3). Therefore, the calculated total uncertainty values of the temperature, flow rate, and vacuum pressure are presented in Table 2.3.

Table 2.3 Uncertainty of measured parameters

Parameter	ε_s, Systematic uncertainty (± %)	ε_r, Random uncertainty (± %)	ε, Total uncertainty (± %)
TC0	0.75	0.21	0.77
TC1	0.75	0.23	0.78
TC2	0.75	0.27	0.79
TC3	0.75	0.26	0.79
TC4	0.75	0.29	0.80
TC5	0.75	0.17	0.77
TC6	0.75	0.17	0.77
TC7	0.75	0.32	0.81
TC8	0.75	0.20	0.77
TC9	0.75	0.29	0.80
TC10	0.75	0.28	0.80
TC11	0.75	0.22	0.78
TC12	0.75	0.18	0.77
Flow rate	0.20	0.05	0.21
Vacuum pressure	0.04	0.00	0.04
Evaporation rate	0.20	0.02	0.20

Sample calculations are also presented in Table A-1 and A-2 within the supplemental material.

2.5 Results and discussion

The primary task of this study is to develop an empirical model from analysing the temperature distribution and evaporation rate of upward flash evaporation sprays from a single nozzle inside a vacuum chamber. The research will explore the effects of four factors, namely inlet temperature (T_{in}), salinity (C), inlet flow (Q), and superheat degree (ΔT) on the spatially resolved temperature distribution T(r, z) and evaporation rate (E).

2.5.1 Effect of inlet temperature and salinity

Figure 2.7a shows the empirical centreline dimensionless temperature (Θ_{exp}) and its exponential fit (Θ_{emp}) over the axial distance (z=0mm to 200mm). A set of inlet temperatures ranging from 60˚C to 80˚C is considered while other conditions are kept constant. The value of R-squared is demonstrated which quantifies the accuracy of the fit curve (Θ_{emp}). The closer the value of R-squared is to 1, the more accurate the fitness of Θ_{emp}. The data shows that the inlet temperature does not affect the centreline temperature distribution significantly as long as the superheat degree, flow rate, and salinity are held constant. To further support, experimental data relating to the evaporation rate for this set of conditions are shown in Figure 2.7b.

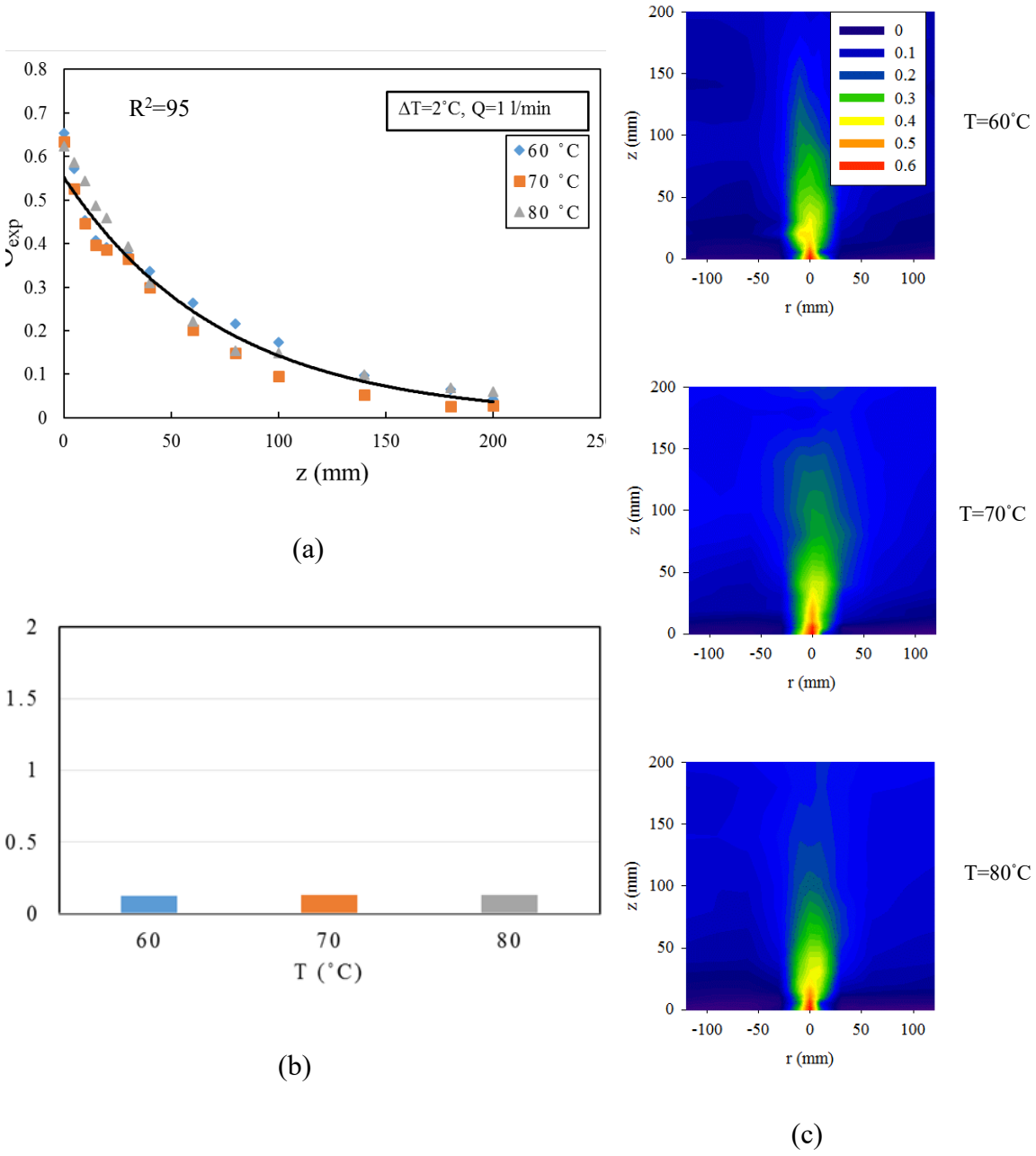

Figure 2.7 (a) Centreline variation of dimensionless temperature (Θ_{exp}) and its exponential fit, (b) The evaporation rate, and (c) False colour maps of spatial distribution at different inlet temperatures (T_{in}=60, 70, 80˚C) of saline water sprays (C=3.5%, ΔT =2˚C, Q=1l/min)

It is apparent that when the inlet temperatures of 3.5% saline water are in the range of 60 to 80˚C, the superheat degree of 2˚C results in evaporation rate of about 0.13%. To spatially visualize the temperature distribution of flash evaporation sprays, two dimensional (r, z) temperature contour plots are presented in Figure 2.7c based on the data obtained from temperature measurement within the spray distance of 200mm. The most striking observation to emerge from this data is the steep temperature gradients within 100mm from the start point of injection which

indicates the rapid evaporation of saline water. Interestingly, the temperature distributions in these three flash evaporation sprays are roughly the same for all inlet temperatures under the constant superheat degree of 2˚C. Taken together, these findings suggest a role for linking Θ_{emp} to E, so that the slope of the exponential fit is an indicator of the evaporation rate.

Figures 2.8a and b also indicate the effect of same inlet temperature (60 to 80˚C) under two different set of conditions in which the superheat degree and flow rate are changed to 12˚C and 1.5l/min, respectively. The same behaviour for the centreline temperature profile is also seen for these set of conditions. In other words, the exponential fit does not show any significant difference over various inlet temperatures in the range of 60 to 80˚C. Miyatake et al. [15] also noted the influence of liquid inlet temperature (30˚C, 40˚C, 60˚C) at 12˚C superheat degree in downward flash evaporation and reported that the dimensionless temperature is unchanged for different inlet temperatures. This deduction is also observed for the upward spray flash evaporation because increasing the inlet temperature and decreasing the vacuum pressure neutralize the effects of each other at the same time. Raising the inlet temperature decreases the surface tension and viscosity of the saline water leading to flash evaporation enhancement [40]. On the other hand, decreasing the vacuum pressure to keep the superheat degree constant reduces the flash evaporation [13]. As a result, changing the inlet temperature under constant superheat degree is ineffective to change Θ_{exp}.

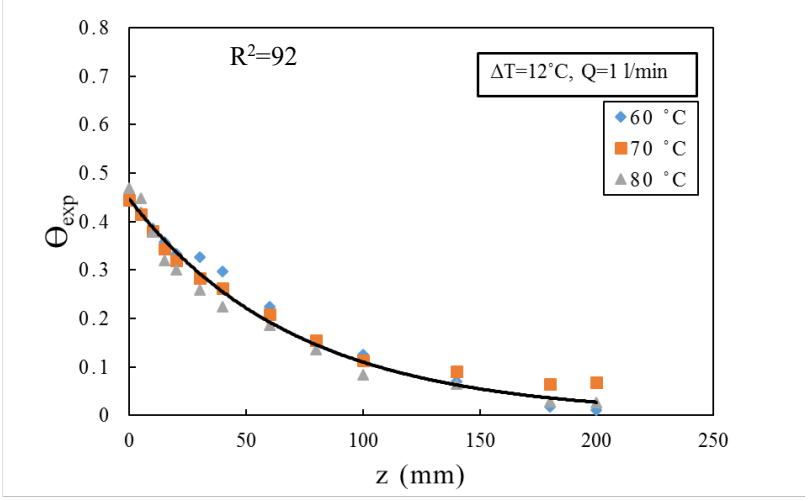

(a)

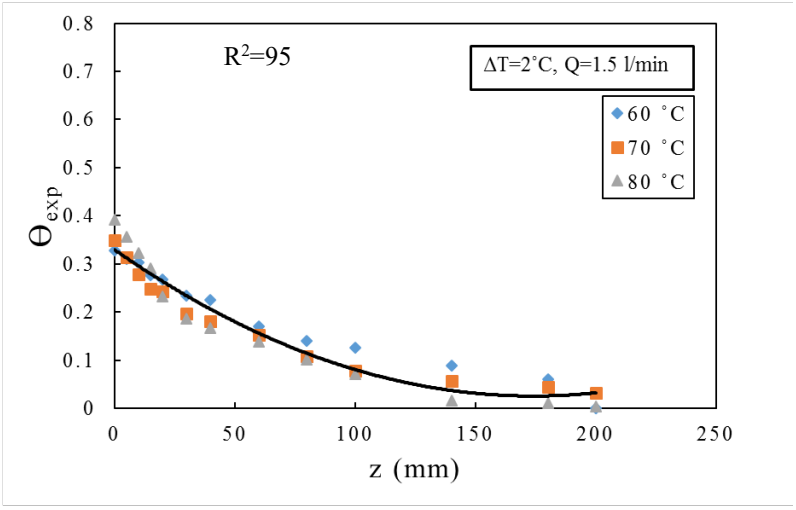

(b)

Figure 2.8 Centreline variation of dimensionless temperature (Θ_{exp}) at different inlet temperatures (T_{in}=60, 70, 80˚C) of saline sprays (C=3.5%).

Figure 2.9a-b, delineate the centreline temperature variations with the same conditions but for pure water sprays (tap water). As can be seen, no evidence is found to indicate a significant difference between the trends of 3.5% and 0% salt concentration. This behaviour is attributed to the fact that the boiling point elevations of 3.5% saline water for the temperatures of 60˚C, 70˚C, and 80˚C are 0.40, 0.42, and 0.45, respectively [41]. These values are very small and could not have any meaningful effect on the flash evaporation process. In summary, one can

conclude a strong similarity in the centreline temperature distribution between saline and pure water upward sprays.

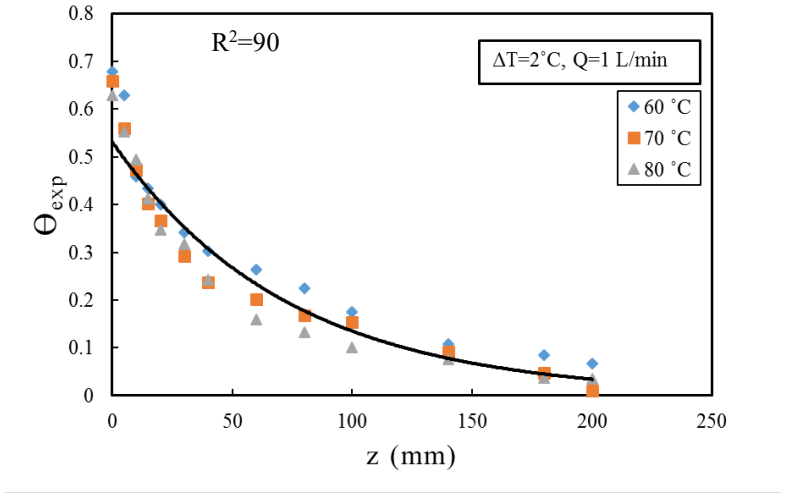

(a)

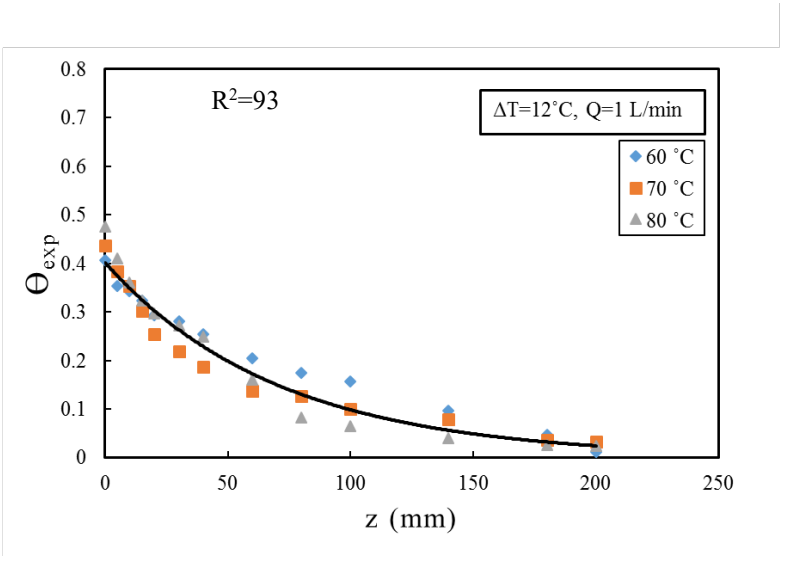

(b)

Figure 2.9 Centreline variation of dimensionless temperature (Θ_{exp}) at different inlet temperatures (T_{in}=60, 70, 80˚C) of tap water sprays (C=0%).

2.5.2 Effect of superheat degree

Figure 2.10a indicates that changes in superheat degree have an impact on the slope of Θ_{emp}. An increase in the superheat degree results in the slope reduction of Θ_{emp} and consequently hastens the flash evaporation particularly within 200mm of the nozzle exit. As shown in this figure, the initial values of Θ_{exp} (z=0) for various superheat degrees have the largest differences in comparison with other vertical distances, which was possibly related to the droplets concentration at the exit point. As Figure 2.10b shows, the evaporation rate jumps from 0.13% for the superheat degree of 2˚C to 1.2% for the superheat degree of 12˚C. This proves the link between the slope reduction of Θ_{emp} and the enhancement value of E. Careful analysis of the temperature contour plot for this set of experiments (T=70˚C, and Q=1l/min, C=3.5%), in Figure 2.10c, shows the pronounced influence of the nature of superheat degree. As the superheat degree increases, the value of Θ_{exp} falls, and this results in a noticeably quicker flash evaporation. A possible explanation for this might be that increasing vacuum pressure (higher superheat degree) leads to greater difference in the vapour density between droplet surface and the surrounding vapour. In addition, increasing the superheat degree causes a faster drop in the environmental pressure and more intensive air movement around the droplets [29]. The integration of these effects results in higher evaporation rate. The effect of superheat degree on spray flash evaporation was also similar to the one on jet flash evaporation [13].

Figure 2.11a and b also consider the influence of superheat degree in the range of 2 to 12˚C when the inlet temperature and flow rate are changed to T_{in}=80˚C and Q=1.5l/min, respectively. The behaviour of Θ_{emp} is repeated under these conditions and validates the aforementioned statement that improving superheat degree improves flash evaporation. Another explanation for this factor is

that a higher superheat degree threshold supplies more thermal energy for droplet growth and leading to increase in evaporation [11]. As a result, the mean droplet diameter decreases for the same volume of emerging fluid leading to better spray atomization. Smaller droplet size is considered to promote evaporation and also shorten the vertical distance (Z_{equ}) taken to complete evaporation [11]. The most

important finding is that the superheat degree plays an important role in controlling the process of flash evaporation.

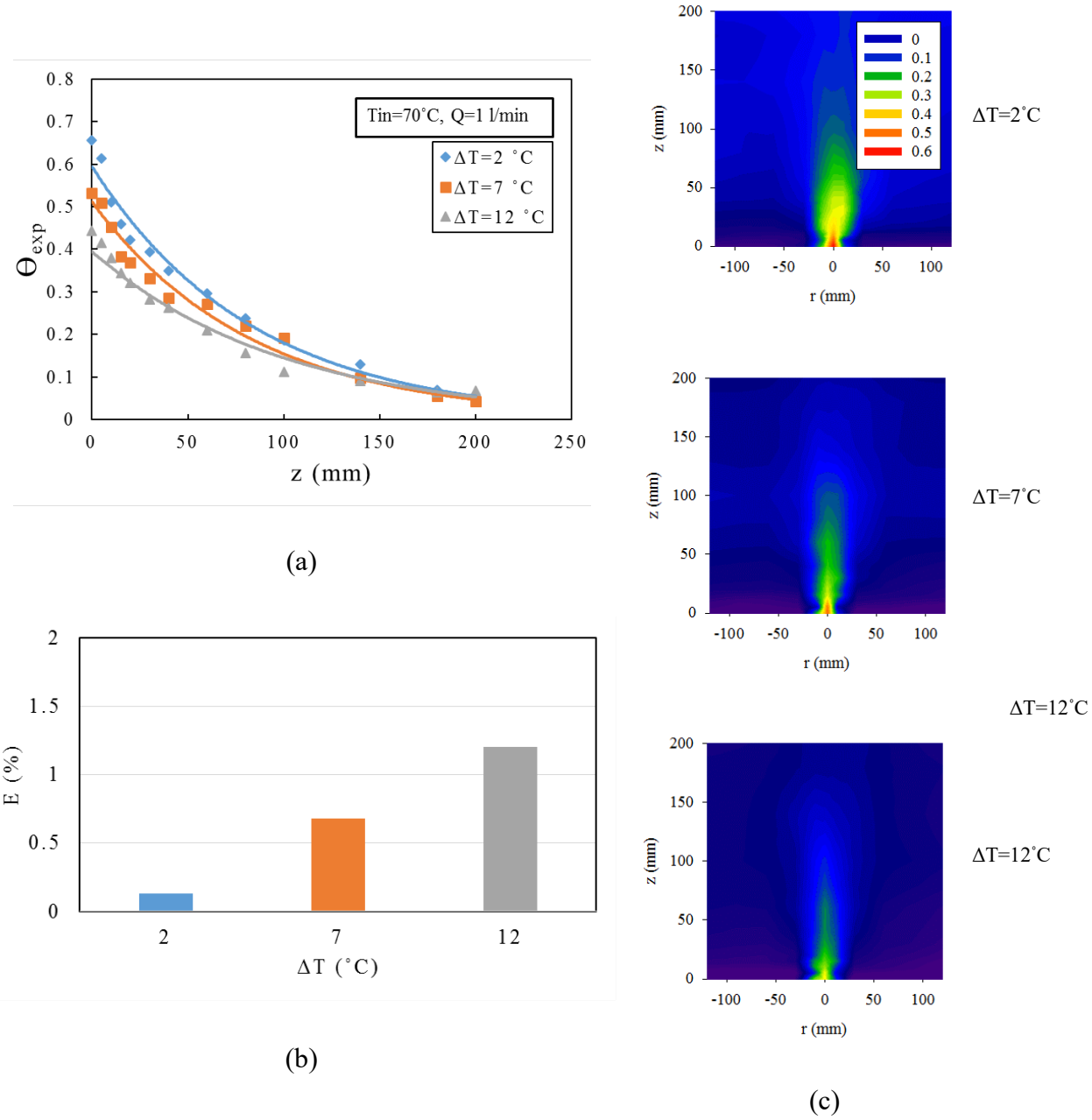

Figure 2.10 (a) Centreline variation of dimensionless temperature (Θ_{exp}) and its exponential fit, (b) The evaporation rate, and (c) False colour maps of spatial distribution at different superheat degree (ΔT=2, 7, 12˚C) of saline water sprays (C=3.5%, T_{in}=70˚C, Q=1l/min)

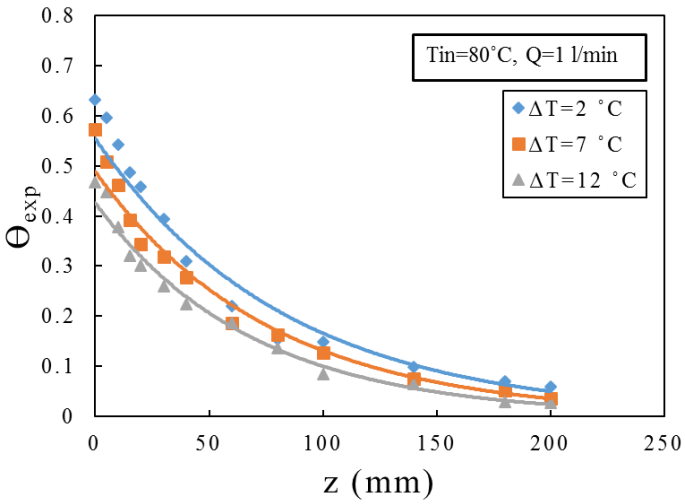

(a)

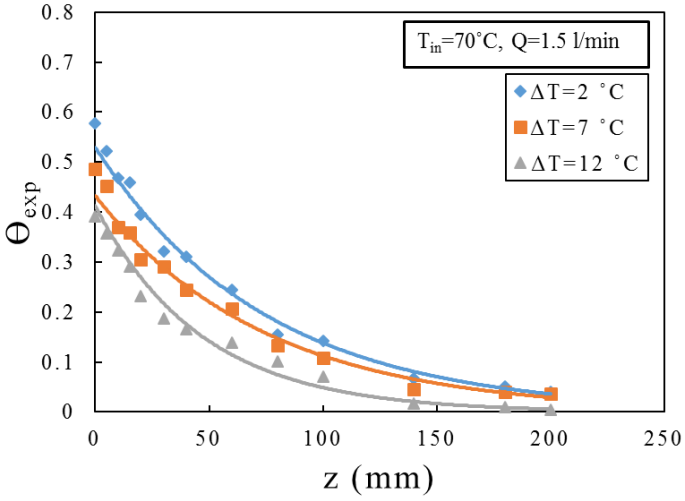

(b)

Figure 2.11 Centreline variation of dimensionless temperature (Θ_{exp}) at different super heat degree (ΔT) of saline water sprays (C=3.5%)

2.5.3 Influence of flow rate

Figure 2.12a shows the variations in the temperature profiles which lie along the centreline of the spray for a set of experiments in the flow rate range of 1l/min to 2l/min. The general trend of the cooling curve (Θ_{emp}) for the flash evaporation phenomenon is illustrated in this figure. As can be seen, the temperature, superheat

degree, and concentration are maintained at 60˚C, 7˚C, and 3.5%, respectively. It is clear that a certain enhancement of flow rate results in a decrease in the slope of cooling curve and spraying higher flow rates attain lower Θ_{exp} values at the same axial distance. This reduction of slope and Θ_{exp} are interpreted as a promotion of flash evaporation.

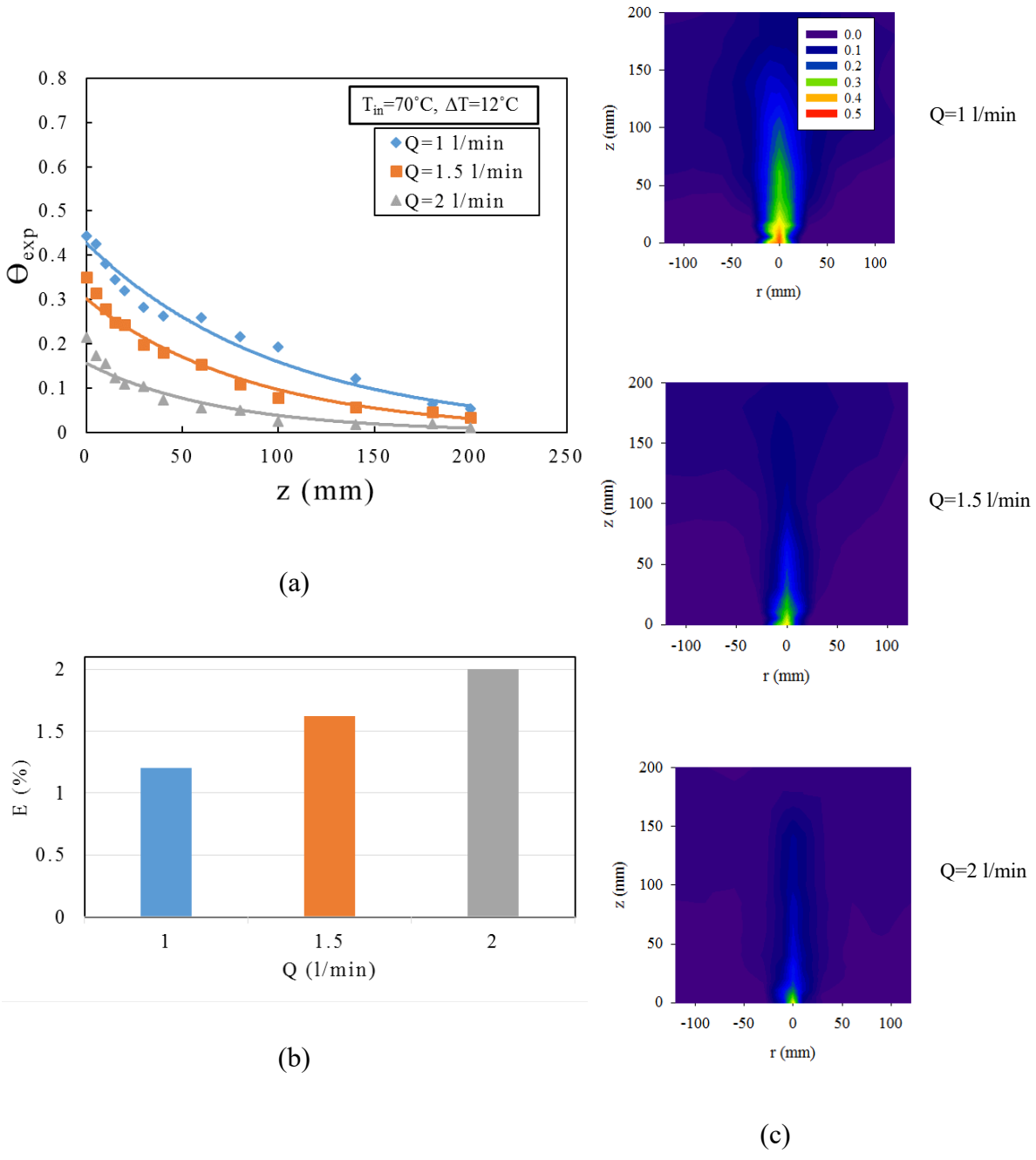

Figure 2.12 (a) Centreline variation of dimensionless temperature (Θexp) and its exponential fit, (b) The evaporation rate, and (c) False colour maps of spatial distribution at different flow rate (Q=1, 1.5, 2l/min) of saline water sprays (C=3.5%, ΔT=12˚C, and Tin=70˚C)

Figure 2.12b also illustrates that by increasing the flow rate from 1l/min to 2l/min, the evaporation rate promotes from 1.2% to 1.94%. To obtain a better visualization, Figure 2.12c displays the temperature distribution of the spray nozzle under these conditions. Whilst the line plots denote the centreline variation of (non-dimensionlized) temperature, these color maps provide additional information on the spatial temperature distribution within the wider body of the spray. It is apparent that a greater area of the completed evaporation (indicated by the blue colour) can be observed when the flow rate is raised from 1 to 2l/min. This trend is attributed to the fact that higher inlet flow rate provides a greater amount of kinetic energy that is required for the break-up of droplets. In addition, the higher energy leads to instability of water and increasing the interfacial turbulences between vapour and water. Therefore, smaller droplets [42] and consequently more evaporation are the expected to occur.

In order to investigate the effect of flow rate under other conditions, Figure 2.13a and b show the temperature profile while the inlet temperature and superheat degree are increased. It is clear that the behaviour of the profile is similar to Figure 2.12a. It is worth noting that the behaviour of the spray nozzle differs from the jet nozzle in the work carried out by Mutair and Ikegami [13]. They argued that higher flow rate leads to less flash evaporation due to the increase in inertia of the jet which denotes as a retarding force. The enhancement of this force keeps the jet unshuttered, while there is no unshuttered area in the spray nozzle and all the liquid is atomized completely.

2.6 Modelling of centreline temperature variation

Based on the range of conditions tested, it is possible to establish an empirical fit. By analyzing these experiments, it is observed that an exponential decay in dimensionless centreline temperature is a common pattern. The dimensionless centreline temperature shows initially an almost exponential decay with the fastest drop in the temperature taking place near the nozzle exit. The rate of temperature drop slows down as the spray further develops due to what is expected to be from

rapid droplet evaporation. The exponential decay presented for saline and pure water temperatures is derived using data analysis. By considering all temperatures under different experimental conditions, it was found that most of the data fit Equation 2.9 well, where Θ_{emp} defines the dimensionless centreline temperature and k is a coefficient (0.010 to 0.014).

$$\theta_{emp} = \frac{0.9(T(0,0) - T_{equ})}{T_{in} - T_{equ}} e^{-kz} \tag{2.9}$$

To emphasise the relevance of the non-dimensionalised temperature derived in the present study (Θ_{exp}) in small orifice upward flowing saline and pure water sprays, Figure 2.14 shows a compilation of other published data using Equation 2.2. It is observed that experimental data for both Mutair and Ikegami [13, 27] (upward flowing large orifice jets, d=54-81mm) as well as that by Miyatake et al. [15] (downward flowing small orifice sprays, d=5mm) show good agreement with the fit which is derived from the present study (Equation 2.9).

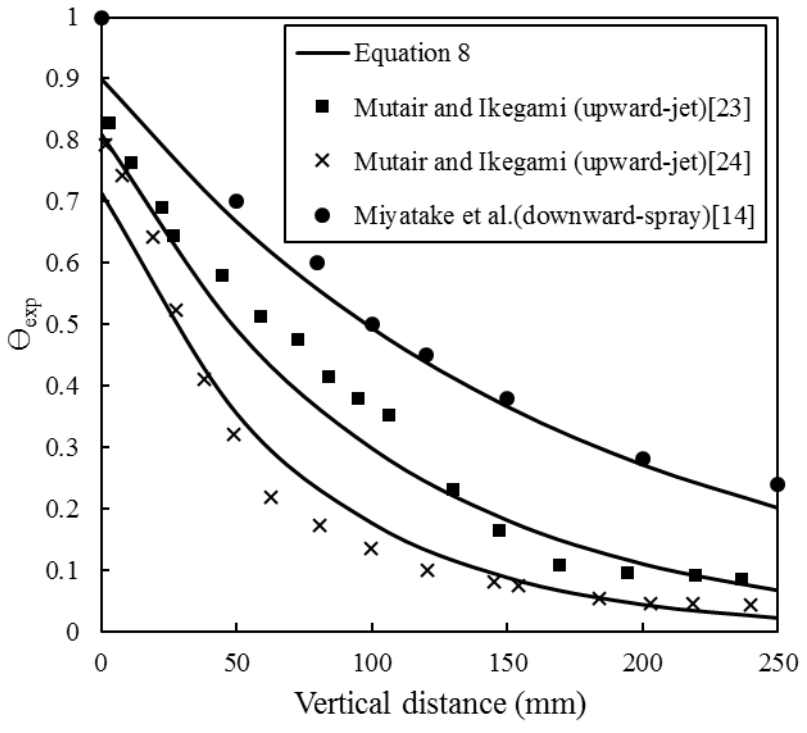

Figure 2.13 Centreline variation of dimensionless temperature (Θ_{exp}) at different flow rate (Q=1, 1.5, 2l/min) of saline water sprays (C=3.5%).

The current study has not only provided an insight for the first time into the temperature distributions in upward flowing fine droplet (d=0.8mm) saline and pure

water sprays, but also presented an empirical fit (Equation 2.9) that appears to satisfy a range of differently sized nozzles, in both upward and downward flowing spray/jet flash evaporation.

2.7 Conclusions

Flash evaporation of saline (water) sprays is strongly dependent on the localised and chamber pressure. The present study has resolved the temperature distribution in saline sprays (C=0 to 3.5%) under a range of conditions (T_{in}=60-80˚C, Q=1-2l/min, ΔT=2-12˚C). These measurements have been done during the steady state operating period of a (vacuum) chamber, with the accuracy of measurements also be reported by an uncertainty analysis. The main findings may be summarised as:

A dimensionless temperature, described by an exponential fit, was found to be well correlated to the evaporation rate in the saline sprays. This relationship, established herein for the first time in fine droplet sprays (orifice diameter 1.5mm), also describes the temperature distribution in previous published works covering other jets and sprays, both upward and downward flowing. The significance of this dimensionless temperature (Θ_{emp}) which can be established using centre line measurements only, is that it serves as an indirect indicator of the evaporation rate within the conditions tested.

Both inlet temperature and salinity (in the range 0 to 3.5%) do not significantly affect the evaporation rate as long as other conditions are kept constant. However, both higher superheat degrees and greater inlet flow rates increase the evaporation rate. This observation which has not been reported before in fine orifice sprays is likely attributed to the increase in spray shattering (at a greater superheat degree and inflow) but requires further research using flow visualisations for confirmation.

The study also confirms that both the inlet temperature and superheat degree have similar influence on the dimensionless temperature and evaporation rate. This is in agreement with earlier studies into (large orifice) jets. However, changing flow rate in (fine orifice) sprays is seen to have a different effect compared to (large orifice) jets, whereby increasing the flow rate results in a higher evaporation rate in spray (but lower in jets).

Acknowledgment

The author acknowledges ECU for awarding School of Engineering scholarship to pursue a PhD research program.

2.8 References:

1.A.D. Khawaji, I.K. Kutubkhanah, and J.-M. Wie, *Advances in seawater desalination technologies.* Desalination. Vol. 221, 2008: p. 47-69.

2.N. Noda, Y. Ikegami, and H. Uehara, *Extraction condition of OTEC using the Uehara cycle*. 2002: The International Society of Offshore and Polar Engineers. 26-31.

3.H. Uehara, A. Miyara, Y. Ikegami, and T. Nakaoka, *Performance Analysis of an OTEC Plant and a Desalination Plant Using an Integrated Hybrid Cycle.* Journal of Solar Energy Engineering. Vol. 118, 1996: p. 115-122.

4.A. Hosseini Araghi, M. Khiadani, K. Hooman, and G. Lucas, *Optimised exergy efficiency of a combined flash spray desalinator recovering discharge thermal energy.* Desalination and Water Treatment. Vol. 57, 2016: p. 18588-18596.

5.A.H. Araghi, M. Khiadani, and K. Hooman, *A novel vacuum discharge thermal energy combined desalination and power generation system utilizing R290/R600a.* Energy. Vol. 98, 2016: p. 215-224.

6.A. El-Zahaby, A. Kabeel, A. Bakry, S. El-Agouz, and O. Hawam, *Augmentation of solar still performance using flash evaporation.* Desalination. Vol. 257, 2010: p. 58-65.

7.A. Muthunayagam, K. Ramamurthi, and J. Paden, *Low temperature flash vaporization for desalination.* Desalination. Vol. 180, 2005: p. 25-32.

8.A.K. El-Fiqi, N.H. Ali, H.T. El-Dessouky, H.S. Fath, and M.A. El-Hefni, *Flash evaporation in a superheated water liquid jet.* Desalination. Vol. 206, 2007: p. 311-321.

9.D. Balaji, *Experimental study on the effect of feed water nozzles on non-equilibrium temperature difference and flash evaporation in a single-stage evaporator and an investigation of effect of process parameters on the liquid flashing in a LTTD desalination process.* Desalination and Water Treatment. Vol. 57, 2016: p. 27152-27168.

10.A.H. Araghi, M. Khiadani, K. Hooman, and G. Lucas, *Efficiency of a Combined Desalination and Power System Utilising a Two-Phase Flow Multi-Stream Heat Exchanger.* Heat Transfer Engineering. Vol. 38, 2016: p. 1000-1007.

11.Q. Chen, K.J. M, Y. Li, and K.J. Chua, *Experimental and mathematical study of the spray flash evaporation phenomena.* Applied Thermal Engineering. Vol. 130, 2018: p. 598-610.

12.M. Maria Antony Raj, K. Kalidasa Murugavel, T. Rajaseenivasan, and K. Srithar, *A review on flash evaporation desalination.* Desalination and Water Treatment. Vol. 57, 2016: p. 13462-13471.

13.S. Mutair and Y. Ikegami, *Experimental investigation on the characteristics of flash evaporation from superheated water jets for desalination.* Desalination. Vol. 251, 2010: p. 103-111.

14.O. Miyatake, T. Tomimura, Y. Ide, and T. Fujii, *An experimental study of spray flash evaporation.* Desalination. Vol. 36, 1981: p. 113-128.

15.O. Miyatake, T. Tomimura, Y. Ide, M. Yuda, and T. Fujii, *Effect of liquid temperature on spray flash evaporation.* Desalination. Vol. 37, 1981: p. 351-366.

16.Y. Ikegami, H. Sasaki, T. Gouda, and H. Uehara, *Experimental study on a spray flash desalination (influence of the direction of injection).* Desalination. Vol. 194, 2006: p. 81-89.

17.H. Ma, X. Wu, F. Feng, D. Wang, C. Yang, and C. Zhuo, *An experimental study on fuel spray-induced vortex-like structures.* Experimental Thermal and Fluid Science. Vol. 57, 2014: p. 335-343.

18.S.S. Sazhin, *Advanced models of fuel droplet heating and evaporation.* Progress in Energy and Combustion Science. Vol. 32, 2006: p. 162-214.

19.M. Orain and Y. Hardalupas, *Droplet characteristics and local equivalence ratio of reacting mixture in spray counterflow flames.* Experimental Thermal and Fluid Science. Vol. 57, 2014: p. 261-274.

20.S. De and S.H. Kim, *Large eddy simulation of dilute reacting sprays: Droplet evaporation and scalar mixing.* Combustion and Flame. Vol. 160, 2013: p. 2048-2066.

21.J.-X. Wang, Y.-Z. Li, X.-K. Yu, G.-C. Li, and X.-Y. Ji, *Investigation of heat transfer mechanism of low environmental pressure large-space spray cooling for near-space flight systems.* International Journal of Heat and Mass Transfer. Vol. 119, 2018: p. 496-507.

22.J.-X. Wang, Y.-Z. Li, G.-C. Li, and X.-Y. Ji, *Ground-Based Near-Space-Oriented Spray Cooling: Temperature Uniformity Analysis and Performance Prediction.* Journal of Thermophysics and Heat Transfer. 2019: p. 1-10.

23.S.Y. Misyura, *The effect of Weber number, droplet sizes and wall roughness on crisis of droplet boiling.* Experimental Thermal and Fluid Science. Vol. 84, 2017: p. 190-198.

24.S. Gopalakrishna, V.M. Purushothaman, and N. Lior, *An experimental study of flash evaporation from liquid pools.* Desalination. Vol. 65, 1987: p. 139-151.

25.C. Wang, R. Xu, X. Chen, P. Jiang, and B. Liu, *Study on water flash evaporation under reduced pressure.* International Journal of Heat and Mass Transfer. Vol. 131, 2019: p. 31-40.

26.S. Mutair and Y. Ikegami, *On the evaporation of superheated water drops formed by flashing of liquid jets.* International Journal of Thermal Sciences. Vol. 57, 2012: p. 37-44.

27.S. Mutair and Y. Ikegami, *Experimental study on flash evaporation from superheated water jets: Influencing factors and formulation of correlation.* International Journal of Heat and Mass Transfer. Vol. 52, 2009: p. 5643-5651.

28.L. Liu and M.-L. Mi, *Theoretical investigation on rapid evaporation of a saline droplet during depressurization.* Microgravity Science and Technology. Vol. 25, 2014: p. 295-302.

29.Q. Chen, K. Thu, T. Bui, Y. Li, K.C. Ng, and K. Chua, *Development of a model for spray evaporation based on droplet analysis.* Desalination. Vol. 399, 2016: p. 69-77.

30.B. Cai, Q. Wang, S. Yin, H. Gu, H. Wang, H. Zhen, and L. Zhang, *Energy analysis of spray flash evaporation from superheated upward jets.* Applied Thermal Engineering. Vol. 148, 2019: p. 704-713.

31.T. Alghamdi, S.T. Thoroddsen, and J.F. Hernández-Sánchez, *Ultra-high speed visualization of a flash-boiling jet in a low-pressure environment.* International Journal of Multiphase Flow. Vol. 110, 2019: p. 238-255.

32.Q. Chen, Y. Li, and K.J. Chua, *On the thermodynamic analysis of a novel low-grade heat driven desalination system.* Energy Conversion and Management. Vol. 128, 2016: p. 145-159.

33.L. Liu, Q.c. Bi, and H.x. Li, *Experimental investigation on flash evaporation of saltwater droplets released into vacuum.* Microgravity Science and Technology. Vol. 21, 2009: p. 255-260.

34.H. Ikeuchi. *Hydraulic Spray Nozzles (Full Cone Spray Pattern)*. 2018; Available from: https://www.kirinoikeuchi.co.jp/eng/products/spray/03/.

35.A. Hosseini Araghi, *A novel discharge thermal energy combined desalination and power cycle utilising a vacuum spray flash evaporator.* Retrieved from https://ro.ecu.edu.au/theses/1945. 2016.

36.F.J. Förster, S. Brack, R. Poser, J. von Wolfersdorf, and B. Weigand, *A novel surface-integrated spray-on thermocouple for heat transfer measurements.* Experimental Thermal and Fluid Science. Vol. 93, 2018: p. 356-365.

37.A.H. Araghi, M. Khiadani, M. Sadafi, and K. Hooman, *A numerical model and experimental verification for analysing a new vacuum spray flash desalinator utilising low grade energy.* Desalination. Vol. 413, 2017: p. 109-118.

38.R.J. Moffat, *Describing the uncertainties in experimental results.* Experimental Thermal and Fluid Science. Vol. 1, 1988: p. 3-17.

39.H.W. Coleman and W.G. Steele, *Experimentation and Uncertainty Analysis for Engineers* Quality and Reliability Engineering International. Vol. 6, 1990: p. 231-231.

40.M.H. Sharqawy, J.H. Lienhard, and S.M. Zubair, *Thermophysical properties of seawater: a review of existing correlations and data.* Desalination and Water Treatment. Vol. 16, 2010: p. 354-380.

41.K.G. Nayar, M.H. Sharqawy, L.D. Banchik, and J.H. Lienhard V, *Thermophysical properties of seawater: A review and new correlations that include pressure dependence.* Desalination. Vol. 390, 2016: p. 1-24.

42.M. Razzaghi, *Droplet size estimation of two-phase flashing jets.* Nuclear Engineering and Design. Vol. 114, 1989: p. 115-124.

Chapter 3

Experimental and mathematical investigations of spray angle and droplet sizes of a flash evaporation desalination system [1]

Abstract

The aim of this research is to study experimentally the effect of operational parameters on spray characteristics of flash evaporation system which is the key component of the discharge thermal energy combined desalination (DTECD) system. Spray angle and droplet size under vacuum condition are two important characteristics of spray nozzles that can be used to aid the design of flash chamber and estimating the evaporation rate, respectively. For this purpose, initially the effect of superheat degree, inlet pressure, and inlet temperature on the spray angle of three different types of full cone spray nozzles was investigated using a high-speed camera. Moreover, a force balanced mathematical model was developed to calculate droplet sizes and the results were compared with experimentally measured values using shadowgraph technique. The results show that the spray angle was largely affected by the superheat degree regardless of nozzle type. In addition, an empirical equation was suggested to correlate inlet pressure, saturation pressure, and spray angle. Further, a model was proposed to estimate the variation of droplet sizes along the spray centreline and concluded that the spray capacity significantly influenced the droplets' lifetime.

[1] This chapter has been published as a full research paper:
F. Fathinia, M. Khiadani, and Y.M. Al-Abdeli, *Experimental and mathematical investigations of spray angle and droplet sizes of a flash evaporation desalination system.* Powder Technology. Vol. 355, 2019: p. 542-551. https://doi.org/10.1016/j.powtec.2019.07.081
Whilst efforts were made to retain original content of the article, minor changes such as number formats, font size and style were implemented in order to maintain consistency in the formatting style of the thesis.

3.1 Introduction

The phenomenon of flashing sprays occurs when a liquid is injected into a low pressure zone through an exhaust valve, jet or throttling device such as spray nozzle. Due to a sudden drop in surrounding pressure, rapid and volatile atomization of the liquid appears which is then termed as superheated. Some of the industrial applications of this process involve fuel spray [1, 2], reacting spray [3, 4], and spray flash desalination[5, 6].

The study of the spray formed by such a process has received considerable attention due to its practical significance [7]. In the early 1960s, Brown and York [8] conducted experiments to study the mechanism of spray flashing with a cylindrical jet. Water and Freon-11 were used as a working fluid for atomization, where a high speed camera assisted to visualize the spray pattern. Ultimately, the authors explained shattering of liquid as sudden bubble growth. In follow up works, research approaches to study spray characteristics have focused on spray angle [9], droplet size [10], spray impact [11], and spray pattern [12]; where spray angle and droplet size have attracted the most attention [7].

Spray angle, obtained from high quality images, is a significant factor influencing both spray pattern and droplet size. Gong and Fu [13] analysed the influence of structural parameters and viscosity on spray angle of a swirling atomizer used in combustion. They used oil in their experiments and developed empirical relationships to determine discharge coefficient and spray angle. Chen and Lefebvre [14] used spray drying food and found that decreasing the surface tension and viscosity of liquid enlarged the spray angle. Sovani et al. [15] also surveyed the effects of pressure, liquid properties and atomizer design on spray angle in fuel injection and concluded that the spray angle becomes wider as pressure increases. Several studies have also found that the spray angle is directly proportional to the pressure of injection [16-18]. Wang et al. [19] employed spray cooling to compare the spray angle between R404 and R134. They concluded that the R404 spray angle is more concentrated and also has better spatial selectivity than R134. These studies provide a clear direction on the design of relevant spray applications. However, insufficient coverage of this subject on spray flash evaporation and desalination using saltwater (less volatile) as a working fluid is noticeable.

In recent years, the development of advanced measuring instruments has facilitated growing research in the subject of measuring droplet size [20-24]. Tratnig and Brenn [25] measured the droplet size produced by pressure swirl atomization using Phase Doppler Anemometry (PDA) to establish a relationship between the global droplet size and Sauter mean droplet size. A Phase Doppler Laser Interferometer was employed as the main measurement device for investigating the spatial distribution characteristics of multiple factors in the spray field by Yang et al. [26] and for experimentally validating the effectiveness of the spray field by Liu et al. [27]. In another research, Li et al. [28] used a high speed camera and Phase Doppler Particle Analyser (PDPA) to study atomization of 5-hole direct injector. They found that the size distribution of droplets changed in relation to the bifurcation of the target jet. PDPA was also used to accurately measure droplet sizes and velocities of a solid-cone spray for dust reduction [29] and compare the spray performance for typical water-based dust reduction media [30]. In another work, shadowgraph technique for measuring the droplet size and comparison with other techniques was developed by Zhou et al. [31]. They revealed that the use of shadowgraph for in-line measurements of wide distribution of droplet size was more effective than other methods. The same approach has been used in this study to measure the droplet sizes in flash evaporation using saltwater.

In the area of flash evaporation, previous researchers have mainly investigated the effect of nozzle shape [32]; direction of injection [33]; initial temperature, superheat degree and flow rate [34, 35]; large nozzle diameter [36]; and injection of bubble nuclei [37]. In these studies the flow was injected into a flash environment via a nozzle and none of them specifically investigated the effects of operating parameters when the flow is injected into the flash chamber via spray. Recently, Chen et al. [38] proposed that analysing spray characteristics such as droplet size would be beneficial for more in-depth understanding of evaporation process and optimization of a spray evaporator. In addition, Cai et al. [39] and [40] developed a model based on the droplet analysis to estimate temperature distribution along the centreline of the jet nozzle and investigate the influence of initial parameters such as injection pressure, vacuum pressure, and flow velocity on thermal utilization. However, unlike sprays, jets do not immediately experience breakup near the nozzle exit point. Therefore, it is expected that their model produces more accurate results

for the spray nozzles. Hence, their model has been modified (particles distance and size) and validated experimentally for predicting the evaporation rate of three different spray nozzles to show its usability. This comparison between the calculated evaporation rate and measured distilled water was not made before which was necessary to show the applicability of the proposed model.

Lack of substantial information about the spray angle and droplet sizes in flash evaporation processes due to the infeasibility of experimental exploration motivated the authors to install visualising windows on the sides of the vacuum chamber to observe the behaviour of droplets. First, the spray angle of three different types of nozzles under vacuum were compared to understand the relation between the influential parameters such as superheat degree, inlet pressure, and inlet temperature on upward saline water spray characteristics. In the second part, the droplet sizes of saline water were measured by changing vacuum pressure. Then, a mathematical model for calculating the droplet size due to evaporation was modified and verified using the experimental results. Finally, an empirical correlation between droplet size changes and evaporation rate was explored.

3.2 Experimental setup and measurement

3.2.1 Vacuum spray flash evaporator

The experimental setup and control instrumentation of the vacuum flash evaporator used in this study is illustrated in Figure 3.1. The system is operated on the discharge thermal energy combined desalination (DTECD) principle proposed by Araghi et al. [41]. This is a single stage vacuum spray flash evaporator for desalination. Due to challenges of sourcing seawater of uniform qualities, saline water is artificially prepared by adding 35g NaCl (Chem-supply, SA046) per litre to normal tap water and a heater (Model: OMEGA, Type: Immersion CTS-75, 7.5kW) is installed in the supply tank to raise the temperature to the desired inlet temperature.

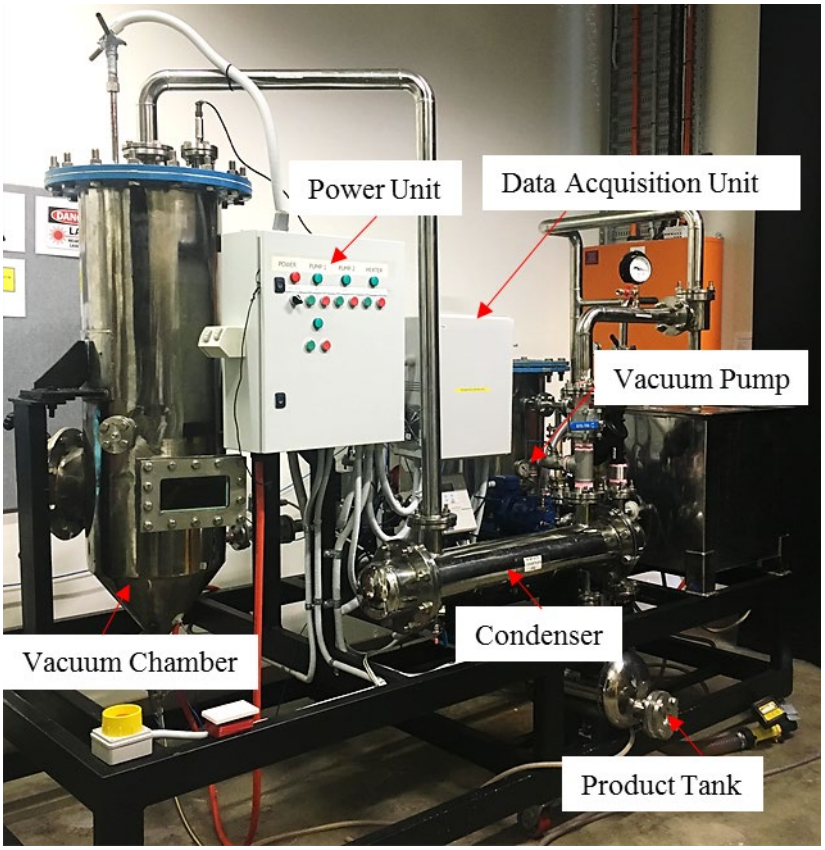

Figure 3.1 Experimental set up of single stage vacuum spray flash evaporator

The heated saline water is sprayed upward through a spray nozzle into the vacuum chamber using a variable speed pump (Model: Southern Cross SBI-9T). Three different nozzles with the manufacturer's specification are presented in Table 3.1 are used to carry out the experiments.

Table 3.1 Specifications of full cone spray nozzles at 2 bar pressure [64]

Nozzle Number	Type	Spray angle (degree)	Spray capacity (l/min)	Free pass Dia. (mm)
1	JJRP	65	2	1.5
2	JJXP-PP	65	1	0.8
3	JJXP	65	1.5	0.8

All these nozzles spray fine droplets which enhance the evaporation rate due to increased surface area. In addition, all of them have a similar spray angle under ambient conditions. Therefore, every two nozzles have at least one similar main characteristic. The flow rate is measured by an electromagnetic flow meter (Model: MFS Magmaster) with an accuracy of ±0.2%. Thermocouples (Model: TC Measurement, type T- Class1) with an accuracy of ±1 (˚C) are used to measure temperature at different locations. A vacuum pump (Model: Speck, V-30-55.0012) capable of lowering the absolute pressure to 0.033bar is installed after a shell and tube condenser to depressurise the flash chamber. A vacuum pressure transmitter (Model: General electric, UNIK 5000, PTX-5-0-6-2-TA-A3-CA-H0-PE, Range 0 to 6bar gauge) with ±0.04% accuracy is installed at the top of the chamber to measure the inside pressure. The heated liquid flow starts to become superheated when the pressure inside the chamber falls below the liquid's saturation pressure. A demister (Model: Haver Standard) with 98% voidage is installed inside the chamber (before the exit point of vapour) to trap any (saline) water whose trajectory may take them to the top of the vacuum chamber. Produced vapour is transferred to the shell and tube condenser which is cooled with tap water to condense the vapour. The distilled water is later collected to the condensate tank. A National Instrument data acquisition system alongside LabVIEW V.2014 is used to record flow rates, temperatures, and vapours pressure.

3.2.2 Imaging technique for measuring spray angle

A high speed camera (SpeedSense1040/CMC-4000) with 100mm f/2.0 lens was employed to capture the spray pattern of flash evaporator at a resolution of 2320×1726 pixels (full resolution). A 9080X7302 LED light source positioned perpendicular to the camera was used to illuminate the field of view (FOV). A transparent and smooth plate was placed between LED and measuring window to diffuse light for a more uniform light source. Snapshots of spray injection under vacuum condition was instantaneously captured at 193 frame per second. In reference to the work of Wang et al. [19], spray angle (α) is expressed as the angle between two lines connecting the nozzle exit centre and periphery of the spray at 15mm distance from the nozzle exit point as shown in Figure 3.2. Droplets become sparse near the boundary which brings uncertainty to the measurement of spray angle. For this reason, the ImageJ software was used to define a grayscale threshold

and eliminate this uncertainty by extracting the spray contour from the binary images. In a grayscale threshold the pixel was from 0 to 225 which represents the weakest (white) and strongest (black) intensity, respectively [42]. In the current study, 396 images were obtained within 2s with 10000µs exposure time to calculate the average spray angle in each condition.

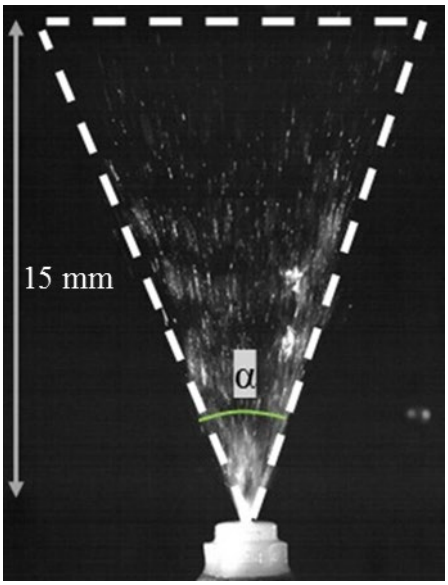

Figure 3.2 Definition of spray angle (α)

3.2.3 Measurement of droplet size

Imaging method analysis (IMA) was applied to measure different droplet sizes using shadowgraph technique. A long-distance microscope (QM 1 long mouth) with resolution of 3microns at 55.9cm was coupled with the camera to capture the droplet images as shown in Figure 3.3. The LED light source was positioned opposite to the camera to illuminate the field of view. Images of the droplets projected through the lens of microscope with magnification of *m* were taken using a high speed camera. Based on the condition of experiments, the camera and light source could be operated in single frame and double frame modes. In this experiment, since the droplets speed were high, double mode was employed to capture the droplets. In this mode, the light source pulses were at the end of the first frame and the beginning of the next frame and time between pulses was set to 50µs while the exposure time of frame 1 and 2 was 100µs. Although there were droplets out of the depth of field (DOF) in the entire area between microscope lens and light

source which is termed out of focus, image processing could be controlled and moderated these errors. For this purpose, ImageJ software was employed for processing all the captured images in the DOF to acquire the size of droplets in focus. General image processing algorithms do introduce non-negligible errors for defocused images.

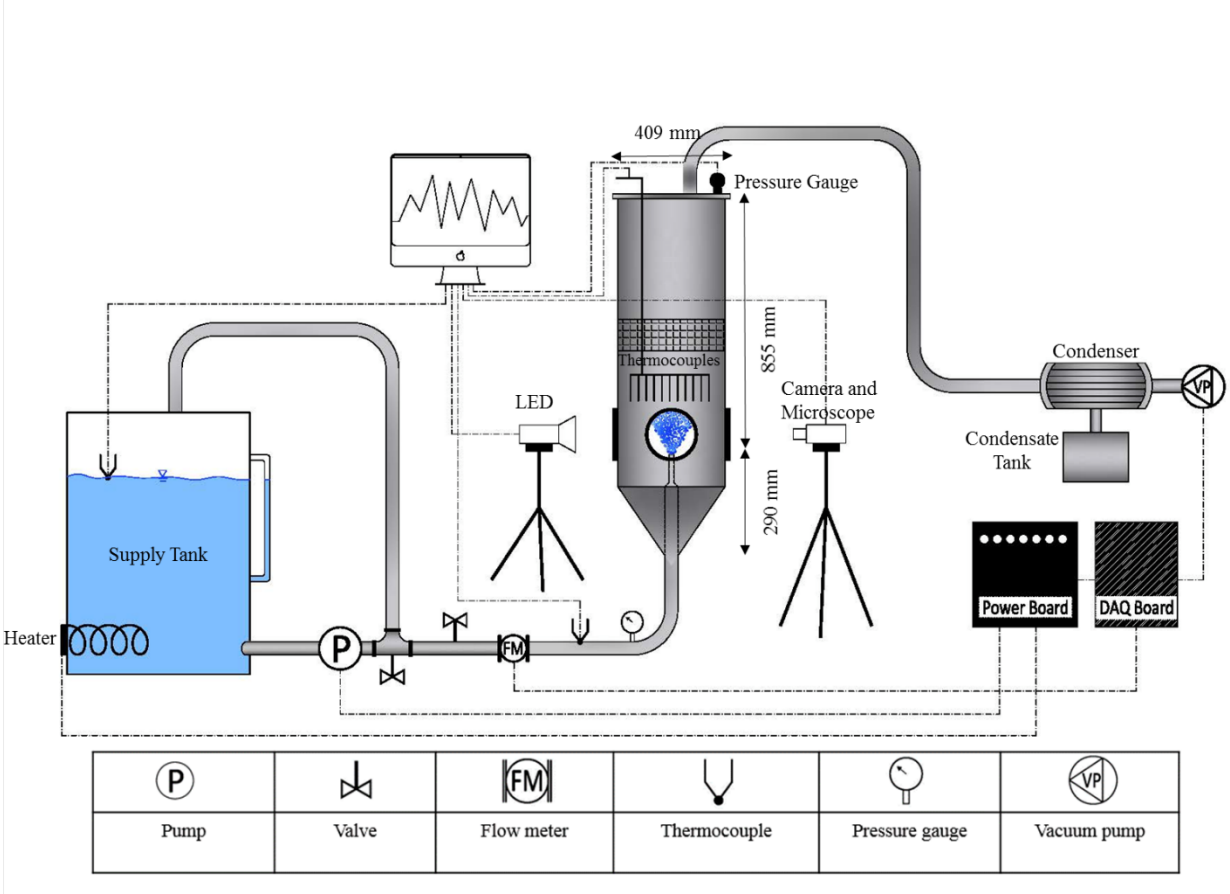

Figure 3.3 Integrated sketch of the flash evaporation system and configuration of shadowgraph.

In order to get more accurate results, it is required to increase the contrast and quality of images prior to the recognition of particles. Hence, image pre-processing is necessary for better extraction of data which includes image enhancement, binarization, denoising, illumination correction, elimination of defocused and imperfect droplets, and filling of the holes. For comparing the droplet sizes measured by shadowgraph technique with the calculated one, Sauter mean diameter (SMD) $D_{32,}$ was determined for the results obtained from the experimental and theoretical. Chin and Lefebvre [43] Pointed out that the SMD is the best indicator

to characterize the mean size of spray droplets. The SMD is established as the surface volume mean diameter and it is defined as follows [44]:

$$D_{32} = \frac{\sum n_i d_i^3}{\sum n_i d_i^2} \tag{3.1}$$

where n_i is the number of droplets with d_i diameter.

3.2.4 Equilibrium height and evaporation

In this work, eleven thermocouples (TC Measurement, type T- Class1) are applied inside the chamber for measuring the radial and axial temperature distributions of spray and determining the equilibrium height (Figure 3.1). This height is measured based on the definition of Mutair and Ikegami [36]. They argued that the evaporation is completed at the equilibrium height (saturation zone) where the radial temperature distribution remains relatively unchanged. At this height the droplet sizes remain unchanged [45] and the percentage decrease of droplet sizes are considered as the evaporated saline water. Muthunayagam et al. [46] proposed an equation for calculating the evaporation rate in flash evaporation system and it is defined as:

$$E = \frac{C\Delta T}{h_{fg}} \tag{3.2}$$

where C is the heat capacity of saline water, h_{fg} is the latent heat of vaporization and ΔT is the superheat degree which is given by:

$$\Delta T = T_{in} - T_{sat} \tag{3.3}$$

Here T_{in} is the inlet temperature and T_{sat} is the saturation temperature corresponding to the vacuum pressure.

3.2.5 Calibration and uncertainty analysis

This study is intended to analyse the collected data from an image based on real spatial unit (micrometre), rather than in pixels. Therefore, the authors needed to spatially calibrate the image before measuring the size of droplets. For this purpose, a calibration process was implemented using a calibrated image with known value.

This image was captured by the camera aimed at a calibration target, then applied to all uncalibrated images.

The calibration of thermocouples was performed for 0˚C and 100˚C using thermocouple calibration device by inserting the thermocouples into a bath of ice for the melting point of water and boiling water for the boiling point of water as a temperature reference [47]. The experimental uncertainty is calculated as a function of systematic and random errors [48]:

$$\varepsilon = \pm\sqrt{\varepsilon_s^2 + \varepsilon_r^2} \tag{3.4}$$

where ε is the total uncertainty, ε_s is the systematic error, and ε_r is the random error. Systematic errors are constant values during an experiment, and are normally attributed to the measuring instrument accuracy reported by the manufacturer. The random errors come from the measured data and derived from standard deviation as [49]:

$$\varepsilon_r = \frac{s}{\sqrt{n}} \tag{3.5}$$

where s is the standard deviation of a sample mean and s2 is variance of a sample for the n groups of measurement and calculated by:

$$s^2 = \frac{\sum_{i=1}^{n}(x_i - \bar{x})^2}{n-1} \tag{3.6}$$

in which $\bar{x}$ is the sample average and obtained by:

$$\bar{x} = \frac{\sum_{i=1}^{n} x_i}{n} \tag{3.7}$$

where, x_i is the ith specific data. In this experiment, the uncertainty of experimental results were analysed according to the mentioned method for three measurement repetition (n=3) for each set of experiments. Sample calculation is reported in Table A-1 within the supplemental material. Therefore, the calculated total uncertainty values of the temperature, flow rate, and vacuum pressure are presented in Table 3.2.

Table 3.2 Uncertainty of measured parameters

Parameter	Systematic uncertainty (± %)	Random uncertainty (± %)	Total uncertainty (± %)
TC1(tank)	0.75	0.21	0.77
TC2(Inlet)	0.75	0.18	0.77
Flow meter	0.20	0.05	0.21
Vacuum pressure transmitter	0.04	0.00	0.04

3.3 Mathematical modeling

The basic concept of the mathematical model for calculating the droplet size was proposed by Hinds [50] and has been modified for the purpose of this study. In this modified model, the time dependent velocity changes of droplets should be acquired for a high accuracy calculation of droplet sizes. For the simplicity of calculation, it is assumed that the upward movement of the droplets are only affected by the gravity force F_g, buoyancy force F_b, and drag force F_d as illustrated in Figure 3.4 and while the velocity of droplet rotation in this study is neglected, the effect of other forces such as Magnus lift and Saffman lift forces are considered negligible.

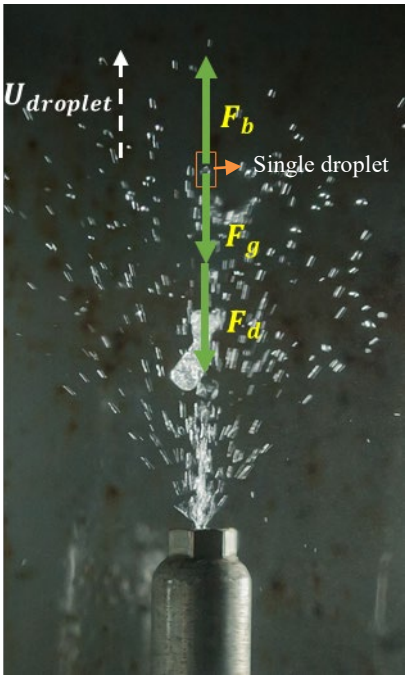

Figure 3.4 Force balance of a single droplet

These forces are defined as:

$$F_g = mg \tag{3.8}$$

$$F_b = \rho_V g V \tag{3.9}$$

$$F_d = \frac{A\rho_V C_D u(t)_d^2}{2} \tag{3.10}$$

where m is the mass, g is the gravitational constant, ρ_v is the vapour density, V is the volume, A is the area, u_d is the velocity of droplet, and C_D is the drag coefficient calculated from the Lapple-Shepherd correlation [51] expressed by:

$$C_D = \frac{24}{\mathrm{Re}_d}(1 + 0.125\,\mathrm{Re}_d^{0.72}) \tag{3.11}$$

where $\mathrm{Re_d}$ expressed as:

$$\mathrm{Re}_d = \frac{u(t)_d r}{\upsilon} \tag{3.12}$$

Based on Newton's second law, the force balance can be written as:

$$\frac{d(mu_d)}{dt} = F_b - F_d - F_g \tag{3.13}$$

By substituting Equations 3.8-10 in Equation 3.13, the final form of the equation for calculating the change of velocity with time is obtained from:

$$\frac{du_d}{dt} = (\frac{\rho_V}{\rho_L} - 1) - \frac{3C_D\rho_V}{R_L\rho_L} \tag{3.14}$$

where ρ_L and R_L are the density and radius of droplet, respectively. In this equation, it is assumed that the droplets density changes are negligible. Once the velocity of the droplet is calculated, the travelled distance along centerline at a particular time is obtained from:

$$s = \int_0^t u_d(t)dt \tag{3.15}$$

It is assumed that the evaporation occurs only on the surface of droplet and can be expressed by diffusion-controlled evaporation [52]. So, the mass variation of the droplet is defined as:

$$\dot{m} = \frac{\pi}{2} \rho_d D^2 \frac{dD}{dt} \tag{3.16}$$

where ρ_d and D are the density and diameter of the droplet. The mass reduction of droplet is calculated by [50]:

$$\dot{m} = -2\pi D D_V \frac{M}{R}\left(\frac{P_d}{T_d} - \frac{P_\infty}{T_\infty}\right) \tag{3.17}$$

where M is the molecular weight , R is the gas constant, P_d is the pressure of droplet, T_d is the temperature of droplet, P_∞ and T_∞ are the pressure and temperature inside the chamber, respectively. The value of self-diffusion coefficient (D_V) is determined from Chapman-Enskog theory [53]:

$$D_V = \frac{1.86\times10^{-3} T^{3/2} (2/M)^{1/2}}{p\sigma^2 \Omega} \tag{3.18}$$

where σ and Ω are the collision diameter and integral for mass diffusion, respectively. By summarising Equations 3.16-18, the variation droplet size variation at any time after the exit of the nozzle is calculated from:

$$\frac{dD}{dt} = -\frac{4 D_V M}{\rho_d D R}\left(\frac{P_d}{T_d} - \frac{P_\infty}{T_\infty}\right) \tag{3.19}$$

It is essential to consider the mass diffusion in the droplet, therefore a correction factor (ϕ) proposed by Davies [54] as defined by Equation 3.20 should be applied;

$$\phi = \frac{2\lambda + D}{D + 5.35\left(\frac{\lambda^2}{D} + 3.42\lambda\right)} \tag{3.20}$$

where λ is the molecular mean free path. Therefore, the final equation for calculating variation of the droplet size is obtained as:

$$\frac{dD}{dt} = -\frac{4D_V \phi M}{\rho_d DR}\left(\frac{P_d}{T_d} - \frac{P_\infty}{T_\infty}\right) = -\frac{4D_V \phi M}{\rho_d DR}\left(\frac{P_d}{T_d} - \varphi\frac{P_\infty^{sat}(T_\infty)}{T_\infty}\right) \tag{3.21}$$

In Equation 3.21 the saturation pressure of vapour (P_∞^{sat}) is given by [55]:

$$P_\infty^{sat}(T) = \frac{2}{15}\exp\left(18.5916 - \frac{3991.11}{T_\infty - 39.31}\right)\times 10^3 \tag{3.22}$$

In order to solve Equation 3.21, it is required to determine initial diameter of droplet (D_0) as an input which is defined as follows [56]:

$$D_0 = 0.833\times 10^{-3} - 0.0734\times 10^{-3}\ln(E_p) \tag{3.23}$$

where E_p (partial expansion energy) is calculated from:

$$E_p = \begin{cases} -\Delta h - [p_\infty^{sat}(T_0) - P_\infty]v_0 + [P_0 - p_\infty^{sat}(T_0)]v_0 & P_\infty \rangle p_\infty^{sat}(T_0) \\ (P_0 - P_\infty)v_0 & p_\infty^{sat}(T_0)\langle P_\infty \end{cases} \tag{3.24}$$

The droplet diameter in the present study is established in the non-dimensional flash evaporation model and solved based on a code was written in MATLAB. The first order differential equation (Equation 3.21) is solved using explicit Runge-Kutta method and an explicit numerical calculation. The solution algorithm for solving this equation is illustrated in Figure 3.5.

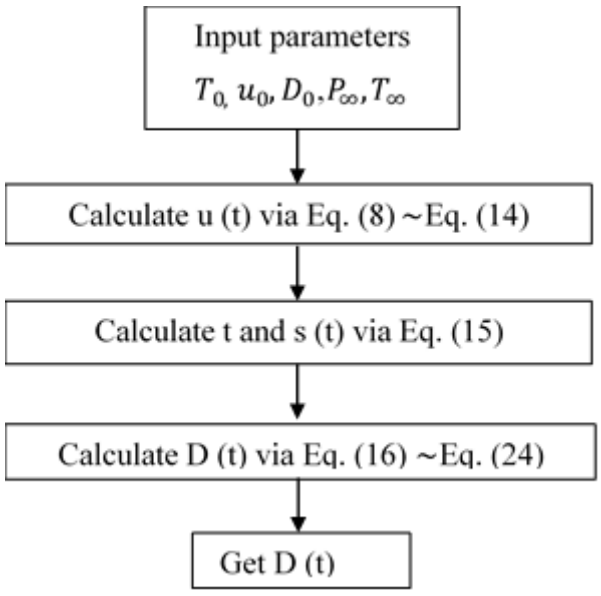

Figure 3.5 Solution algorithm procedures

It is required to define the initial conditions to solve the equations including initial temperature, velocity, and droplet diameter. In addition, ambient pressure and temperature should be added as input parameters. Properties of saline water were calculated based on the formulations proposed by Nayar et al. [57] and vapour properties were estimated based on the correlations formula developed by Wagner and Kretzschmar [58].

3.4 Results and discussion

The results and discussion section consists of two parts. The first part reports on the variation of measured spray angle operated under different conditions for three different types of full cone spray nozzles. The second part reports on the measurement of droplet size along the centreline of the spray nozzles, where the results are compared with the calculated values from the mathematical model discussed earlier. The results are further validated by comparing the calculated droplet size changes with the measured evaporation rate.

3.4.1 Spray angle

The effect of superheat degree on spray angle of three different types of nozzles is presented in Figure 3.6. For better visualization, only a snapshot of Nozzle 2 with the increment of superheat degree is shown in this figure. The same inlet temperature (Tin=70˚C), flow rate (Q=1l/min), and salinity (C=35g/l) are applied for all measurements. In case of ΔT=2˚C, the spray angle is broadened, but the spray break-up is not complete. Considerable enlargement of the disintegration performance is obvious at ΔT=12˚C, while a further increase of superheat degree (ΔT=22˚C) promotes the widening of the spray angle. As illustrated in Figure 3.7, there is a positive correlation between superheat degree and spray angle in spray flash evaporation. The higher the superheat temperature, the broader is the spray angle. For Nozzles 1 to 3, the spray angle is increased from 68˚ to about 75˚, 101˚, and 92˚, respectively.

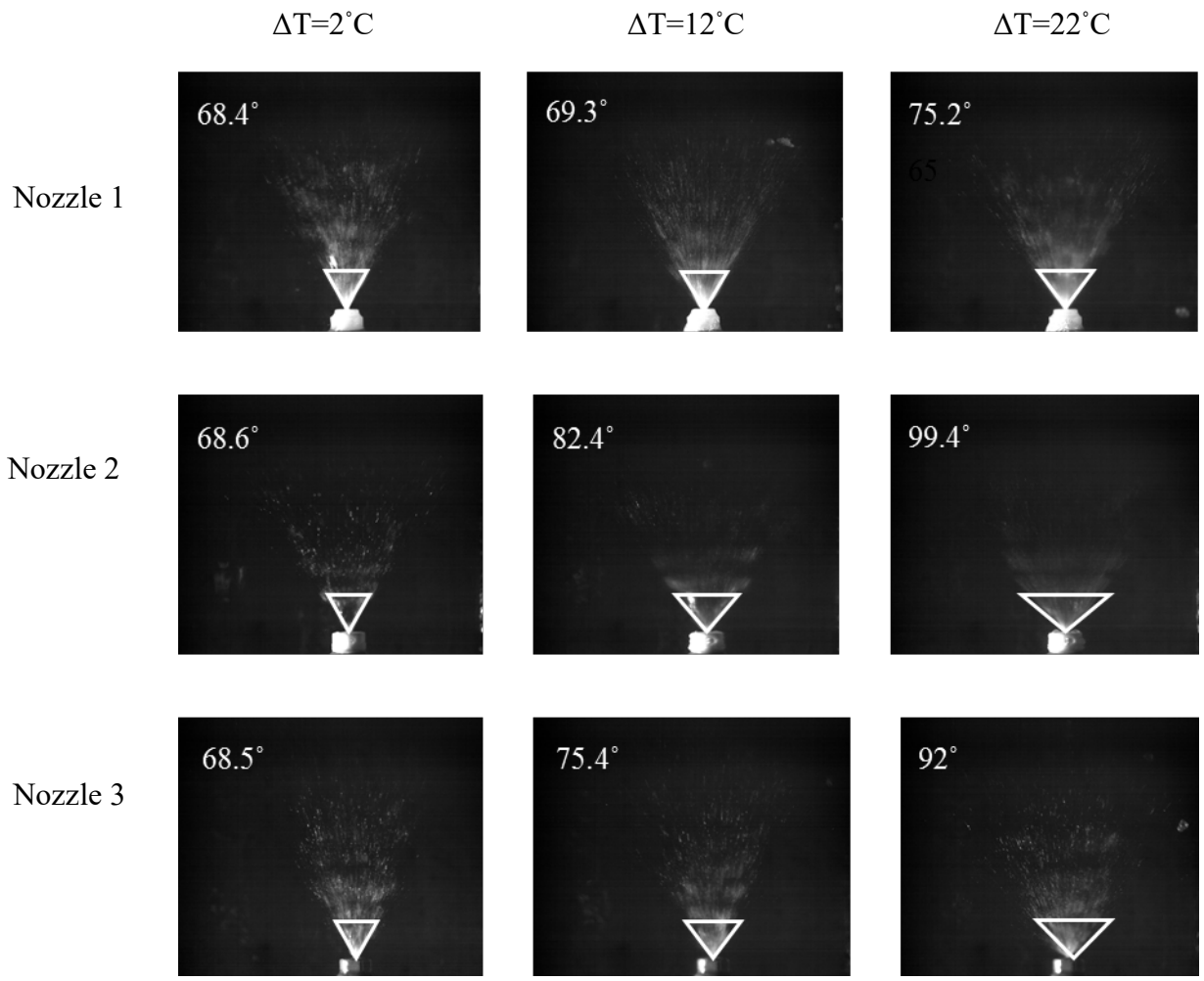

Figure 3.6 Variation of spray pattern and nozzle angles with superheat degree

It can be seen that by employing the same superheat degree, Nozzle 2 has the largest angle while Nozzle 1 has the least value. These differences among the nozzles are attributed to different droplet sizes produced by each nozzle. Hence, it is expected that Nozzle 2 has produced smaller droplet sizes which will be discussed in the next section.

The influence of the superheat degree on the spray angle can be attributed to the intensified evaporation. Higher superheat degrees are due to a higher vacuum pressure inside the chamber, which influences the droplet sizes. The droplets burst as they leave the nozzle and come in contact with the surroundings, whereby very fine droplets are atomized inside the vacuum chamber. Hence, the breakup is strengthened and the spray angle becomes wider. Similar results were found by Steelant [59] who used the acetone and ethanol as a working fluid.

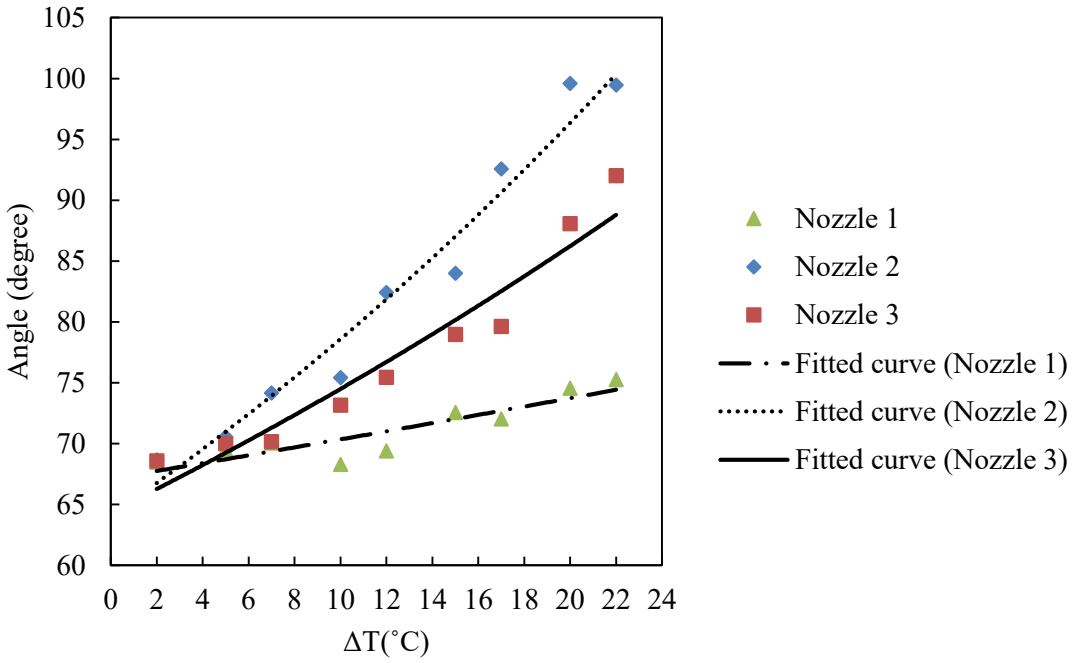

Figure 3.7 Variation of spray angle with superheat degree (T_{in}=70˚C, Q=1l/min)

It is worth mentioning that with respect to coalescence process when the droplets are injected, the spray broadening enhance the evaporation. The larger distance between the droplets reduces the interactions between them and smaller droplets enhance the evaporation due to increased surface area [60] .

Figure 3.8a shows variations of the spray angle (α) with the dimensionless inlet pressure which is normalized by saturation pressure (P_{in}/P_{sat}) for inlet temperature of 70˚C, flow rate of 1l/min, and salinity of 35g/l. The results were compared for all three nozzles.

A significant increase of the spray angle for all nozzles was illustrated when the dimensionless pressure was about 3-27. With increase of the dimensionless pressure (beyond 27), the spray angle remains fairly stable. It can be observed that by raising the pressure, Nozzle 2 finally has a wider angle (101˚) in comparison with Nozzle 1 (75˚) and Nozzle 3 (92˚). Moreover, the dimensionless spray angle (α/α_{max}) with the dimensionless inlet pressure is also illustrated in Figure 3.8b. The data for all three types of the nozzles follow similar trend and approximately fall into almost a single curve which can be used to calculate the spray angle regardless of nozzle type. The equation for this curve is defined as:

$$\frac{\alpha}{\alpha_{\max}} = 0.44 + 0.53(1 - e^{-\frac{P_{in}}{P_{sat}}}) \tag{3.25}$$

where α and α_{max} , respectively, represents the spray angle and maximum spray angle for each nozzle under various inlet pressure.

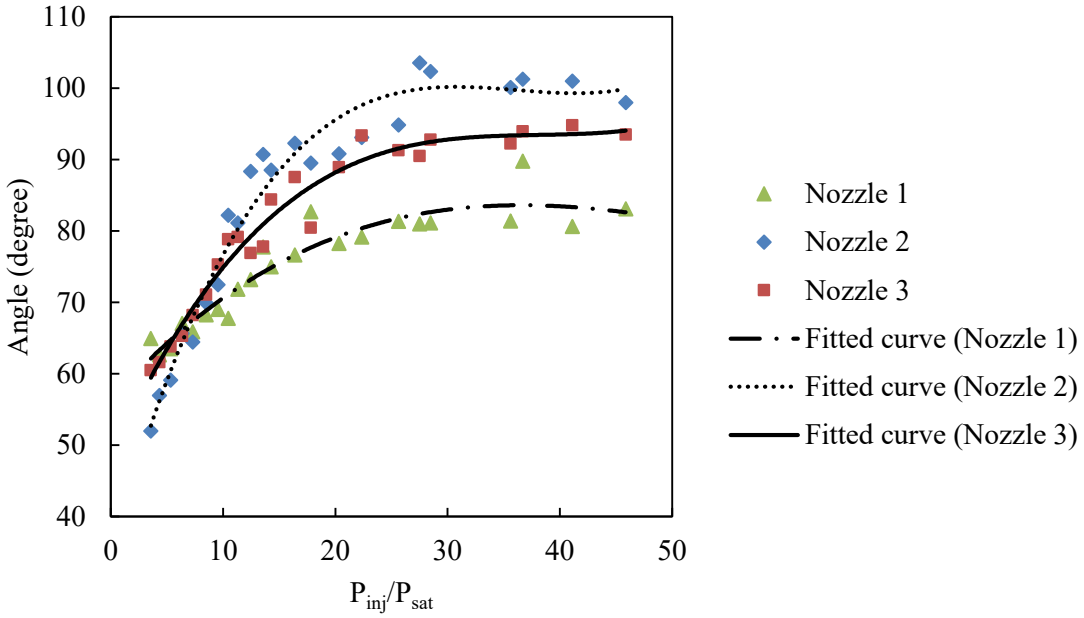

(a) Original spray angle

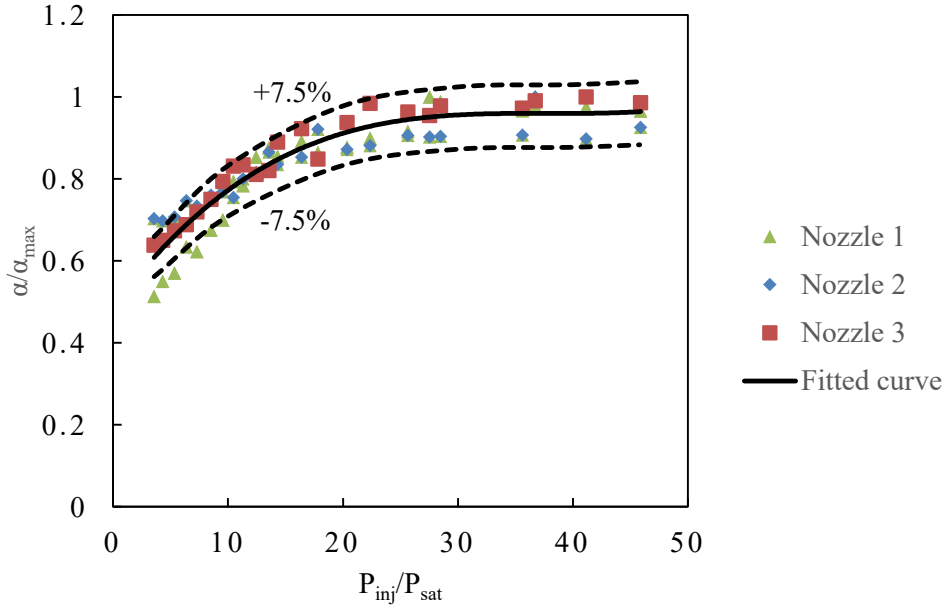

(b) Dimensionless spray angle

Figure 3.8 Variation of spray angle with pressure

The maximum angle of each spray can be extracted from the manufacturer's specification. For most situations, the prediction by Equation 3.25 agrees with experimental data to within ±7.5%. This equation would be beneficial for the purpose of designing a chamber to make sure the droplets won't interact with the wall.

The variations of the temperature and the spray angle are also illustrated in Figure 3.9. It can be seen that the spray angles are not significantly change when the inlet temperature of 35g/l saltwater are 20 to 80˚C for similar conditions (Q=1l/min and P_{sat}=1bar). Since Weber number in spray injection describes the dependency of spray atomization on liquid properties, therefore, any change in the spray angle is expected to be effectively dependent on the value of Weber number [61].

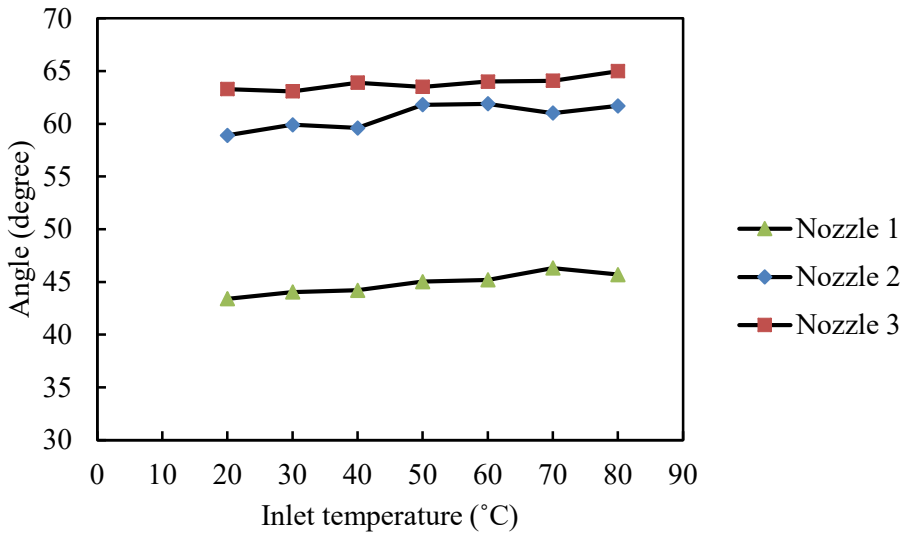

Figure 3.9 Variation of spray angle with inlet temperature (P_{sat}=1bar, Q=1l/min)

The Weber number defines as the ratio of the inertia forces (ρdv^2) to forces due to surface tension (σ) [62]. During these experiments, the inertia forces remained constant while the surface tension due to an increase of saltwater temperature from 20 to 80˚C would yield less than 5% decrease [63]. Therefore, for low changes in the Weber number, the spray angle does not vary significantly with increasing temperature when the other conditions are remained constant.

3.4.2 Experimental and theoretical study of the droplet sizes

As discussed earlier, the droplet sizes change along the centreline of the upward spray flash evaporation were calculated by the proposed mathematical model developed from the force balanced concept. In order to investigate the effect of key parameters on the droplet sizes, the model was validated by comparing the calculated and measured droplet sizes for Nozzle 2 assuming T_{in}=70˚C, ΔT=7˚C, C=35g/l, and Q=1l/min. The experimental values were calculated in the form of Sauter mean diameter (Equation 3.1) obtained by the shadowgraph technique and analysed by ImageJ software at 30mm, 120mm, 150mm, 180mm, 210mm, and 300mm above the nozzle exit. It is assumed that the system has reached the steady state condition and humidity is 100%. Figure 3.10 presents the experimental results versus calculated values and it reveals a good agreement between the two. The calculated values of the droplet sizes by the model are within 3-4% of the experimental values. This slight discrepancy is attributed to the accuracy of the measurements which was previously reported. Moreover, the results of the proposed model are compared with the measurements of evaporation rates which will be discussed later.

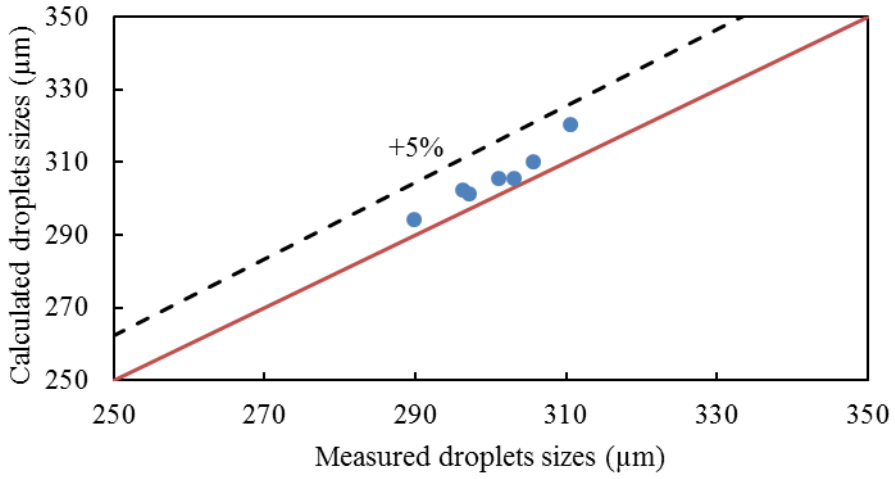

Figure 3.10 Comparison between measured and calculated droplets sizes

Figure 3.11 shows the calculated droplet sizes versus time for the superheat degrees 7, 14, and 21˚C for all three nozzles, and for selected humidities φ=0, 20, 40, 60, 80, and 100%; while the following conditions were kept constant: T_{in}=70˚C, C=35g/l, and Q=1l/min. Figure 3.11a shows the lifetime of the droplets which were sprayed by Nozzle 1. It can be seen that the droplets for ΔT=7˚C and φ=20% take about 0.27s to evaporate completely while for ΔT=14˚C this value is 0.24s. It is obvious that increasing the superheat degree leads to reduction of the droplets' lifetimes. From this figure, it can be also observed that increase of humidity delays the completion of evaporation. For example, in the case of ΔT=21˚C, the droplets' lifetimes for 0% humidity is about 0.21s while for 100% humidity is around 0.30s.

Figure 3.11b presents the data for Nozzle 2, where although the conditions are similar to Nozzle 1, the droplets' lifetimes are shorter. The difference can be attributed to the fact that Nozzle 2 has a smaller orifice in comparison with Nozzle 1 and requires more pressure for squeezing out the droplets at the same flow rate of 1l/min. As a result, finer droplets are injected at a higher injection pressure [18] and smaller droplets have more surface area which lead to more evaporation and as a result the droplets' lifetimes are shorter [60]. Figure 3.11c also illustrates the droplet sizes variation against time for Nozzle 3. This nozzle has more spray capacity than Nozzle 2 while their orifice size is the same. This comparison is significant because Mutair and Ikegami [36] suggested for the jet (droplets are coarser than spray nozzles) that nozzle's diameter as an important parameter as it affects the performance of flash evaporation. For this reason, it is expected to have comparable results between spray capacity and spray diameter for finding the most important factor in changing the droplet sizes of sprays.

Comparing Figure 3.11b and 11c one can see that, the lifetime for the droplets which are produced through Nozzle 2 is less than Nozzle 3. As an example, for the same ΔT=7 ˚C and φ=0%, the injected droplets from Nozzle 3 require 0.03s more time than Nozzle 2 to evaporate completely. Whilst the flow rate is equal for both nozzles with similar diameter, more pressure should be exerted for the one with smaller spray capacity (Nozzle 2) which leads to improve the atomization and evaporation. This comparison reveal that the spray capacity plays a more important role than nozzle diameter in spray flash evaporation systems.

In this study the reduction of the droplet sizes along the centreline of the spray is assumed as a flash steam. In order to analyse the reliability and validity of this assumption, the amount of evaporation was measured by condensing the vapours from final volume of water collected into the condensate tank and also calculated theoretically from Equation 3.2 and are compared with the calculated reduction size of droplets. For calculating the percentage decrease in the droplet sizes, it is required to determine this reduction from the exit point of the nozzle to the equilibrium height. Given the fact that there is no established model available to predict the equilibrium height, this vertical distance is measured experimentally from the exit point of the nozzle to the saturation zone.

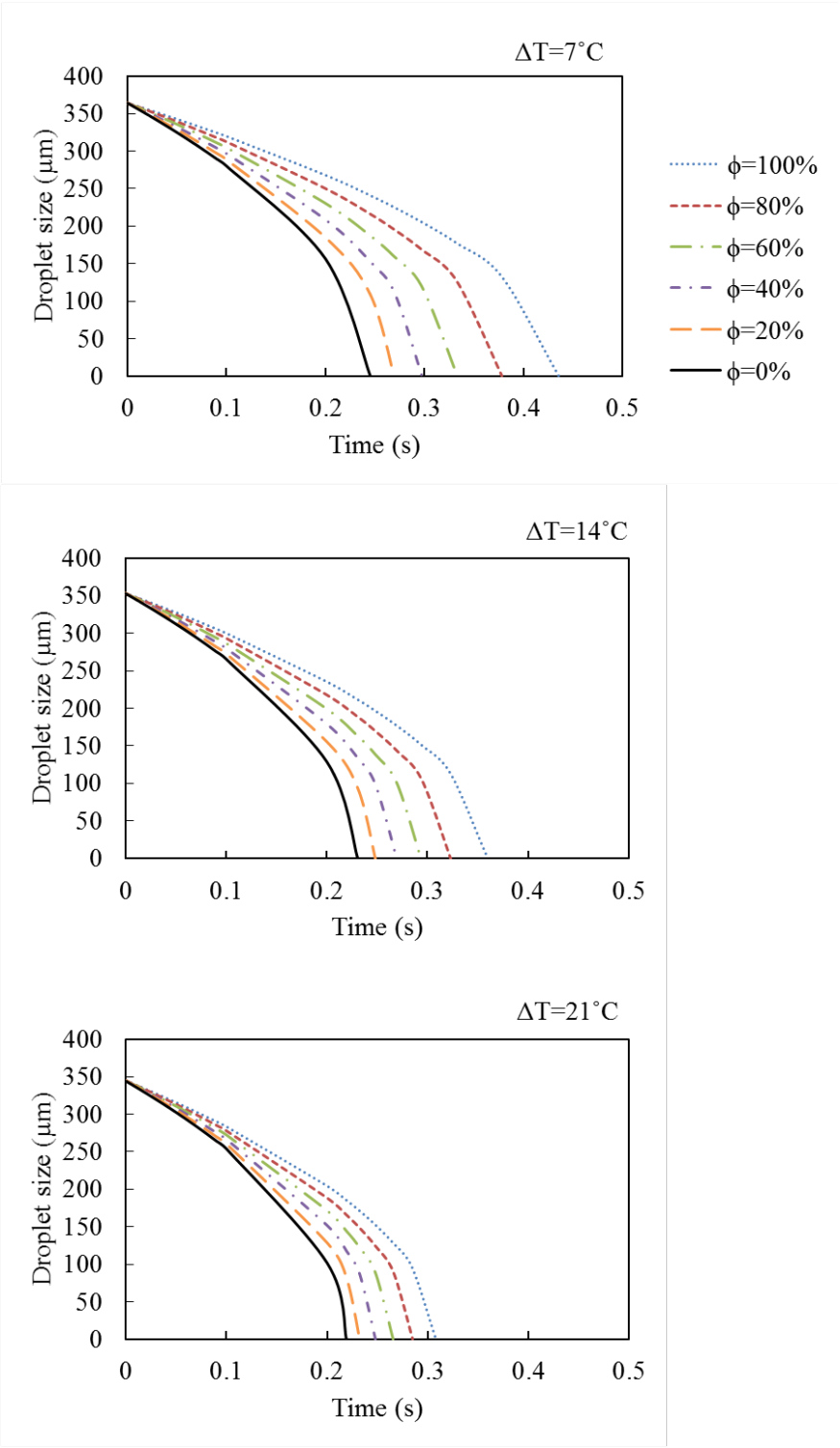
ΔT=7˚C
Droplet size (μm)
400
350
300
250
200
150
100
50
0
0
0.1
0.2
0.3
0.4
0.5
Time (s)
ϕ=100%
ϕ=80%
ϕ=60%
ϕ=40%
ϕ=20%
ϕ=0%
ΔT=14˚C
Droplet size (μm)
Time (s)
ΔT=21˚C
Droplet size (μm)
Time (s)

(a)

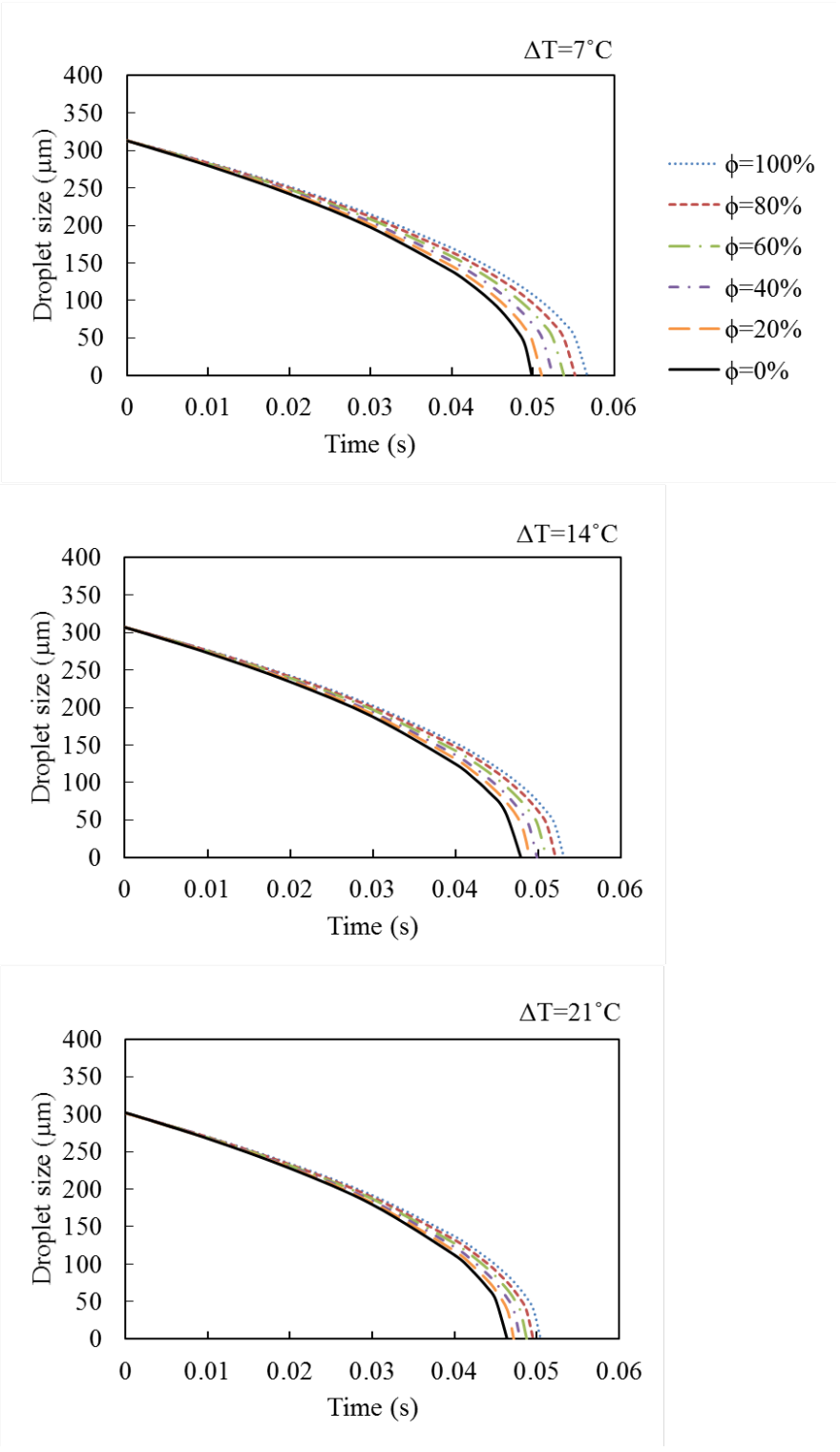
ΔT=7˚C
Droplet size (μm)
400
350
300
250
200
150
100
50
0
0
0.01
0.02
0.03
0.04
0.05
0.06
Time (s)
ϕ=100%
ϕ=80%
ϕ=60%
ϕ=40%
ϕ=20%
ϕ=0%
ΔT=14˚C
Droplet size (μm)
Time (s)
ΔT=21˚C
Droplet size (μm)
Time (s)

(b)

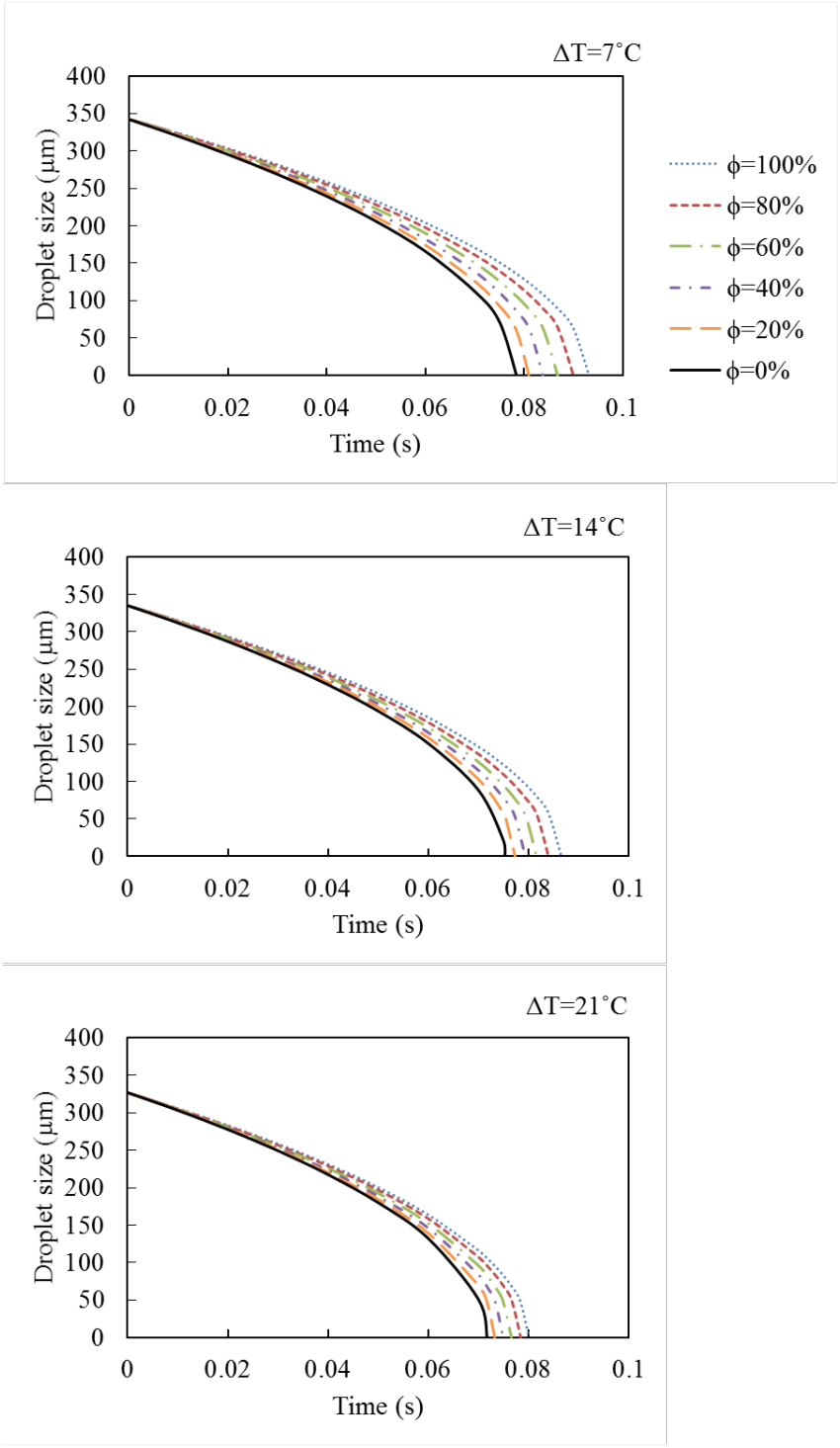

(c)

Figure 3.11 Calculated lifetime of droplets sizes at different humidity from the exit point of (a) Nozzle 1, (b) Nozzle 2, and (c) Nozzle 3

Figure 3.12 indicates the comparison of the percentage decrease in droplet sizes and the evaporation rate both experimentally and theoretically (red line) at different superheat degrees. According to the data obtained from Equation 3.2, the

evaporation rate is independent of nozzle type. These data represent the maximum possible evaporation under various superheat degrees in a flash evaporation system. The reduction of droplet sizes that are calculated separately for each nozzle type and the measured evaporation, indicate that although these changes follow the same trend as the one estimated theoretically, the quantitative values are different. Increasing superheat degree enhances the decrease in droplet size for all nozzle types by different values. For instance, when Nozzle 1 is used, the calculated droplet size changes for superheat degree of 7, 14, and 21 obtained to be 0.8, 2.1, and 3.2%. These values are 1, 2.3, and 3.5% for nozzle type 3. Moreover, having a constant superheat degree of 14 result in evaporation of 2.1, 2.4, and 2.3% in nozzle types 1, 2, and 3, respectively. Similar trend is also observed for the measured evaporation with a maximum difference of 12% from the calculated droplet size variation. Taken together, these findings suggest a role for reduction of the droplet sizes and lifetime in promoting evaporation. By looking at the performance of the nozzles, it can be concluded that data for Nozzle 2 are in a good agreement with the evaporation rate due to the finer droplet sizes produced by this nozzle and less lifetime in comparison with the other two nozzles.

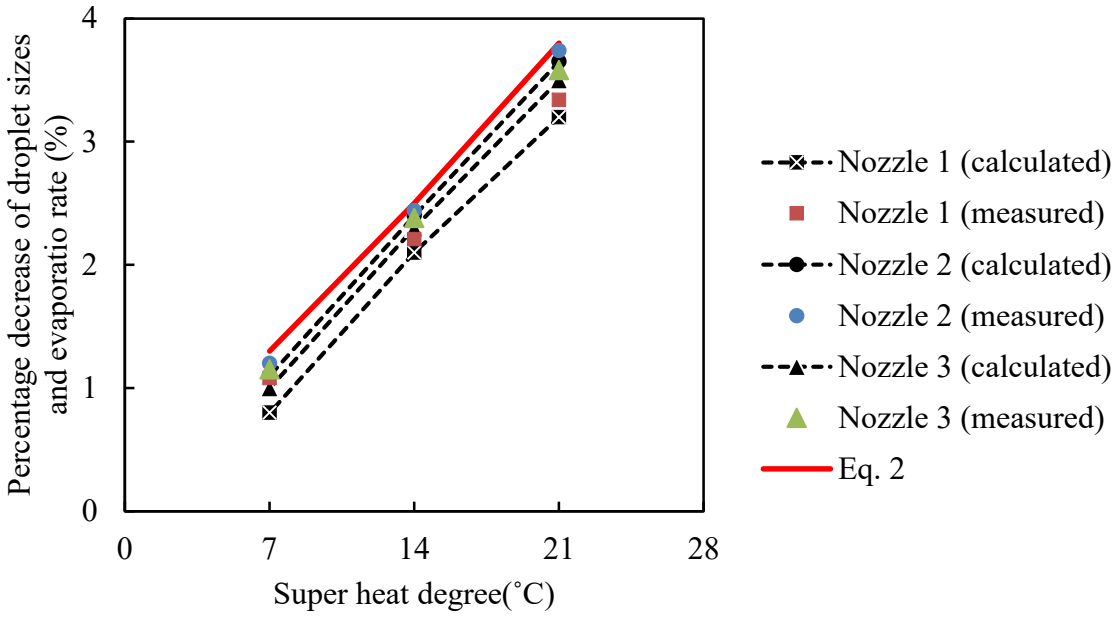

Figure 3.12 Comparison of the evaporation rate with the percentage decrease of droplets sizes for Nozzle 1, 2, and 3

3.5 Conclusions

In this study, the external morphology of spray flash evaporation for three different types of nozzles were recorded and the influence of input parameters on the spray angle were analysed. In addition, a mathematical model was proposed to estimate the variation of droplet sizes along the centreline of the spray with time and was validated experimentally by using shadowgraph technique. Lastly, the percentage decrease in droplet sizes of spray flash evaporation were calculated and compared with measured and calculated evaporation rate.

The main conclusions from this study are:

- The spray angle is directly affected by the superheat degree regardless of type of nozzle while it does not significantly influenced by change of inlet temperature.
- Based on the experimental results an empirical equation was proposed to predict the spray angle in vacuum chamber, showing an exponential growth of dimensionless spray angle with dimensionless pressure.
- The modified mathematical model for calculating the droplet size change along the centreline of the spray flash evaporation produces a good level of accuracy.
- Based on the results of mathematical model, contrary to humidity, increasing superheat degree reduces the droplets' lifetimes.
- Under the exact same operational conditions, spray nozzles with lower capacity, produces wider spray angle and finer droplet sizes which lead to more evaporation rate. This implies that the spray capacity is largely influenced the droplets' lifetime.

Acknowledgements

This research was supported by the School of Engineering at Edith Cowan University. The first author acknowledges the School of Engineering for awarding a scholarship to pursue his PhD study.

3.6 References:

1.H. Ma, X. Wu, F. Feng, D. Wang, C. Yang, and C. Zhuo, *An experimental study on fuel spray-induced vortex-like structures.* Experimental Thermal and Fluid Science. Vol. 57, 2014: p. 335-343.

2.S. Wu, M. Xu, D.L.S. Hung, and H. Pan, *In-nozzle flow investigation of flash boiling fuel sprays.* Applied Thermal Engineering. Vol. 117, 2017: p. 644-651.

3.S. De and S.H. Kim, *Large eddy simulation of dilute reacting sprays: Droplet evaporation and scalar mixing.* Combustion and Flame. Vol. 160, 2013: p. 2048-2066.

4.M. Orain and Y. Hardalupas, *Droplet characteristics and local equivalence ratio of reacting mixture in spray counterflow flames.* Experimental Thermal and Fluid Science. Vol. 57, 2014: p. 261-274.

5.Q. Chen, K.J. M, Y. Li, and K.J. Chua, *Experimental and mathematical study of the spray flash evaporation phenomena.* Applied Thermal Engineering. Vol. 130, 2018: p. 598-610.

6.A. Hosseini Araghi, *A novel discharge thermal energy combined desalination and power cycle utilising a vacuum spray flash evaporator.* (Doctoral dissertation). 2016, Edith Cowan University, Perth.

7.A.H. Lefebvre and V.G. McDonell, *Atomization and sprays*. 2017: CRC press.

8.R. Brown and J.L. York, *Sprays formed by flashing liquid jets.* AIChE Journal. Vol. 8, 1962: p. 149-153.

9.P. Cheng, Q. Li, S. Xu, and Z. Kang, *On the prediction of spray angle of liquid-liquid pintle injectors.* Acta Astronautica. Vol. 138, 2017: p. 145-151.

10.A. Bodaghkhani, B. Colbourne, and Y.S. Muzychka, *Prediction of droplet size and velocity distribution for spray formation due to wave-body interactions.* Ocean Engineering. Vol. 155, 2018: p. 106-114.

11.D. Kalantari and C. Tropea, *Spray impact onto flat and rigid walls: Empirical characterization and modelling.* International Journal of Multiphase Flow. Vol. 33, 2007: p. 525-544.

12.O.M. Ondimu, V.A. Ganesan, M.J. Gatari, J.C.M. Marijnissen, and L.L.F. Agostinho, *Modeling simple-jet mode electrohydrodynamic-atomization droplets' trajectories and spray pattern for a single nozzle system.* Journal of Electrostatics. Vol. 89, 2017: p. 77-87.

13.J.-S. Gong and W.-B. Fu, *The experimental study on the flow characteristics for a swirling gas–liquid spray atomizer.* Applied Thermal Engineering. Vol. 27, 2007: p. 2886-2892.

14.S.K. Chen and A.H. Lefebvre, *Spray cone angles of effervescent atomizers.* Atomization and Sprays. Vol. 4, 1994: p. 291-301.

15.S.D. Sovani, P.E. Sojka, and A.H. Lefebvre, *Effervescent atomization.* Progress in Energy and Combustion Science. Vol. 27, 2001: p. 483-521.

16.R. A. Wade, J. M. Weerts, P.E. Sojka, and J. Gore, *Effervescent atomization at injection pressures in the MPa range*. Vol. 3. 1999.

17.A. Amoresano, C. Allouis, M. Di Santo, P. Iodice, G. Quaremba, and V. Niola, *Experimental characterization of a pressure swirl spray by analyzing the half cone angle fluctuation.* Experimental Thermal and Fluid Science. Vol. 94, 2018: p. 122-133.

18.X. Liu, R. Xue, Y. Ruan, L. Chen, X. Zhang, and Y. Hou, *Effects of injection pressure difference on droplet size distribution and spray cone angle in spray cooling of liquid nitrogen.* Cryogenics. Vol. 83, 2017: p. 57-63.

19.R. Wang, Z. Zhou, B. Chen, F. Bai, and G. Wang, *Surface heat transfer characteristics of R404A pulsed spray cooling with an expansion-chambered nozzle for laser dermatology.* International Journal of Refrigeration. Vol. 60, 2015: p. 206-216.

20.M. Sadafi, S.G. Ruiz, M. Vetrano, I. Jahn, J. van Beeck, J. Buchlin, and K. Hooman, *An investigation on spray cooling using saline water with experimental verification.* Energy Conversion and Management. Vol. 108, 2016: p. 336-347.

21.S. Gepperth, R. Koch, and H.J. Bauer, *Analysis and Comparison of Primary Droplet Characteristics in the Near Field of a Prefilming Airblast Atomizer.* 2013: p. V01AT04A002.

22.J.B. Greenberg, *Droplet size distribution effects in an edge flame with a fuel spray.* Combustion and Flame. Vol. 179, 2017: p. 228-237.

23.L. Zhao, M. Wang, P. Wang, X. Zhu, Q. Qiu, and S. Shen, *SSExperimental Study on the Internal Flow Field and Spray Characteristics of Hollow Nozzle.* Applied Thermal Engineering. 2018.

24.H. Peng, W. Nie, P. Cai, Q. Liu, Z. Liu, and S. Yang, *Development of a novel wind-assisted centralized spraying dedusting device for dust suppression in a fully mechanized mining face.* Environmental Science and Pollution Research. Vol. 26, 2019: p. 3292-3307.

25.A. Tratnig and G. Brenn, *Drop size spectra in sprays from pressure-swirl atomizers.* International Journal of Multiphase Flow. Vol. 36, 2010: p. 349-363.

26.S. Yang, W. Nie, S. Lv, Z. Liu, H. Peng, X. Ma, P. Cai, and C. Xu, *Effects of spraying pressure and installation angle of nozzles on atomization characteristics of external spraying system at a fully-mechanized mining face.* Powder Technology. Vol. 343, 2019: p. 754-764.

27.Z. Liu, W. Nie, H. Peng, S. Yang, D. Chen, and Q. Liu, *The effects of the spraying pressure and nozzle orifice diameter on the atomizing rules and dust suppression performances of an external spraying system in a fully-mechanized excavation face.* Powder Technology. Vol. 350, 2019: p. 62-80.

28.Y. Li, H. Guo, X. Ma, J. Wang, and H. Xu, *Droplet dynamics of DI spray from sub-atmospheric to elevated ambient pressure.* Fuel. Vol. 179, 2016: p. 25-35.

29.H. Wang, J. Wu, Y. Du, and D. Wang, *Investigation on the atomization characteristics of a solid-cone spray for dust reduction at low and medium pressures.* Advanced Powder Technology. Vol. 30, 2019: p. 903-910.

30.H. Wang, Y. Du, X. Wei, and X. He, *An experimental comparison of the spray performance of typical water-based dust reduction media.* Powder Technology. Vol. 345, 2019: p. 580-588.

31.W. Zhou, J. Hu, M. Feng, B. Yang, and X. Cai, *Study on imaging method for measuring droplet size in large sprays.* Particuology. Vol. 22, 2015: p. 100-106.

32.U. Haruo, M. Akio, K. Toru, H. Masaki, and E. Stuhltrager., *A Study of the Spray Flash Desalination (Effect of Nozzle Shape).* Bulletin of the Society of Sea Water Science, Japan. Vol. 45, 1991.

33.Y. Ikegami, H. Sasaki, T. Gouda, and H. Uehara, *Experimental study on a spray flash desalination (influence of the direction of injection).* Desalination. Vol. 194, 2006: p. 81-89.

34.O. Miyatake, T. Tomimura, Y. Ide, M. Yuda, and T. Fujii, *Effect of liquid temperature on spray flash evaporation.* Desalination. Vol. 37, 1981: p. 351-366.

35.S. Mutair and Y. Ikegami, *Experimental investigation on the characteristics of flash evaporation from superheated water jets for desalination.* Desalination. Vol. 251, 2010: p. 103-111.

36.S. Mutair and Y. Ikegami, *Experimental study on flash evaporation from superheated water jets: Influencing factors and formulation of correlation.* International Journal of Heat and Mass Transfer. Vol. 52, 2009: p. 5643-5651.

37.O. Miyatake, T. Tomimura, and Y. Ide, *Enhancement of spray flash evaporation by means of the injection of bubble nuclei.* Journal of solar energy engineering. Vol. 107, 1985: p. 177.

38.Q. Chen, K. Thu, T. Bui, Y. Li, K.C. Ng, and K. Chua, *Development of a model for spray evaporation based on droplet analysis.* Desalination. Vol. 399, 2016: p. 69-77.

39.B. Cai, Q. Wang, S. Yin, H. Gu, H. Wang, H. Zhen, and L. Zhang, *Energy analysis of spray flash evaporation from superheated upward jets.* Applied Thermal Engineering. Vol. 148, 2019: p. 704-713.

40.B. Cai, X. Tuo, Z. Song, Y. Zheng, H. Gu, and H. Wang, *Modeling of spray flash evaporation based on droplet analysis.* Applied Thermal Engineering. Vol. 130, 2018: p. 1044-1051.

41.A.H. Araghi, M. Khiadani, and K. Hooman, *A novel vacuum discharge thermal energy combined desalination and power generation system utilizing R290/R600a.* Energy. Vol. 98, 2016: p. 215-224.

42.X.-S. Wang, B. Chen, R. Wang, H. Xin, and Z.-F. Zhou, *Experimental study on the relation between internal flow and flashing spray characteristics of R134a using straight tube nozzles.* International Journal of Heat and Mass Transfer. Vol. 115, 2017: p. 524-536.

43.J.S. Chin and A.H. Lefebvre, *Some Comments on the Characterization of Drop-Size Distributions in Sprays.* Int. J. Turbo Jet Engines. Vol. 2, 1986: p. p. IVA/1/1-IVA/1/12.

44.A.W. Pacek, C.C. Man, and A.W. Nienow, *On the Sauter mean diameter and size distributions in turbulent liquid/liquid dispersions in a stirred vessel.* Chemical Engineering Science. Vol. 53, 1998: p. 2005-2011.

45.M.D. Protheroe, A. Al-Jumaily, and R.J. Nates, *Prediction of droplet evaporation characteristics of nebuliser based humidification and drug delivery devices.* International Journal of Heat and Mass Transfer. Vol. 60, 2013: p. 772-780.

46.A. Muthunayagam, K. Ramamurthi, and J. Paden, *Low temperature flash vaporization for desalination.* Desalination. Vol. 180, 2005: p. 25-32.

47.F.J. Förster, S. Brack, R. Poser, J. von Wolfersdorf, and B. Weigand, *A novel surface-integrated spray-on thermocouple for heat transfer measurements.* Experimental Thermal and Fluid Science. Vol. 93, 2018: p. 356-365.

48.R.J. Moffat, *Describing the uncertainties in experimental results.* Experimental Thermal and Fluid Science. Vol. 1, 1988: p. 3-17.

49.H.W. Coleman and W.G. Steele, *Experimentation and Uncertainty Analysis for Engineers* Quality and Reliability Engineering International. Vol. 6, 1990: p. 231-231.

50.W.C. Hinds, *Aerosol technology: properties, behavior, and measurement of airborne particles*. 1999: Wiley.

51.C.E. Lapple and C.B. Shepherd, *Calculation of particle trajectories.* Industrial & Engineering Chemistry. Vol. 32, 1940: p. 605-617.

52.H.T. Shin, Y.P. Lee, and J. Jurng, *Spherical-shaped ice particle production by spraying water in a vacuum chamber.* Applied Thermal Engineering. Vol. 20, 2000: p. 439-454.

53.E.L. Cussler, *Diffusion: mass transfer in fluid systems*. 2009: Cambridge university press.

54.D.B. Da Vies, *Evaporation of airborne drolplets.* Reson. Spectrosc. Vol. 12, 1978: p. 135.

55.W.s. J. Tong, *Engineering Thermodynamics.* Higher education press. 2007.

56.H. Witlox, M. Harper, P. Bowen, and V. Cleary, *Flashing liquid jets and two-phase droplet dispersion: II. Comparison and validation of droplet size and rainout formulations.* Journal of Hazardous Materials. Vol. 142, 2007: p. 797-809.

57.K.G. Nayar, M.H. Sharqawy, L.D. Banchik, and J.H. Lienhard V, *Thermophysical properties of seawater: A review and new correlations that include pressure dependence.* Desalination. Vol. 390, 2016: p. 1-24.

58.W. Wagner and H.-J. Kretzschmar, *IAPWS industrial formulation 1997 for the thermodynamic properties of water and steam.* International Steam Tables: Properties of Water and Steam Based on the Industrial Formulation IAPWS-IF97. 2008: p. 7-150.

59.J. Steelant, *High-Speed Shadowgraphy Investigations of Superheated Liquid Jet Atomisation H. Kamoun, G. Lamanna, B. Weigand Institute of Aerospace Thermodynamics Universität Stuttgart, 70569 Stuttgart Germany.*

60.Q. Chen, Y. Li, and K.J. Chua, *On the thermodynamic analysis of a novel low-grade heat driven desalination system.* Energy Conversion and Management. Vol. 128, 2016: p. 145-159.

61.R. Andrade, O. Skurtys, and F. Osorio, *Experimental study of drop impacts and spreading on epicarps: Effect of fluid properties.* Journal of Food Engineering. Vol. 109, 2012: p. 430-437.

62.M.Y. Naz, S.A. Sulaiman, B. Ariwahjoedi, and K.Z. Ku Shaari, *Investigation of Vortex Clouds and Droplet Sizes in Heated Water Spray Patterns Generated by Axisymmetric Full Cone Nozzles.* The Scientific World Journal. Vol. 2013, 2013: p. 9.

63.C. Farnham, M. Nakao, M. Nishioka, M. Nabeshima, and T. Mizuno, *Effect of water temperature on evaporation of mist sprayed from a nozzle.* J Heat Island Inst Int. Vol. 10, 2015: p. 35-44.

64.H. Ikeuchi. *Hydraulic Spray Nozzles (Full Cone Spray Pattern)*. 2018; Available from: https://www.kirinoikeuchi.co.jp/eng/products/spray/03/.

Chapter 4

Performance improvement of spray flash evaporation desalination systems using multiple nozzle arrangement[1]

Abstract

This research aims to improve the performance of the spray flash evaporation as a key component of Discharge Thermal Energy Combined Desalination (DTECD) systems using a multi-nozzle head in various arrangements for the first time. Two novel nozzle arrangements were proposed and compared with the conventional single nozzle. The injection of saline water inside the vacuum chamber was performed under various operating conditions including inlet flow rate, pressure injection, superheat degree, and salinity. Furthermore, the droplet sizes and distribution were observed and analysed using shadowgraph imaging. A similar outcome was reached between the droplets measurement analysis and measured evaporation rate and gain output ratio which implied the most efficient arrangement. The proposed arrangement in which five nozzles are located in the farthest distance totally improved the efficiency of the system under various conditions up to a maximum 28% compared to the conventional single nozzle for the same flow rate. In addition, it was found that the number of nozzles plays a more significant role than their arrangements for a certain pressure injection. Moreover, the optimised maximum superheat degree for the most efficient arrangement was found to be 19˚C. These results provide new fundamental understanding in the area of spray flash evaporation and reveal that increasing the number of nozzles and placing them in the farthest distance apart can improve the efficiency of the system.

---

[1] This chapter has been submitted for publication as a full research paper in:
F. Fathinia, M. Khiadani, Y.M. Al-Abdeli, and A. Shafieian, *Performance improvement of spray flash evaporation desalination systems using multiple nozzle arrangement.* Applied Thermal Engineering. Vol. 163, 2019: p. 114385. https://doi.org/10.1016/j.applthermaleng.2019.114385
Whilst efforts were made to retain original content of the article, minor changes such as number formats, font size and style were implemented in order to maintain consistency in the formatting style of the thesis.

Keywords: Spray flash evaporation, Nozzle arrangement, Evaporation rate, Gain output ratio

4.1 Introduction

Desalination technologies involve separating fresh water from the nearly inexhaustible supply of seawater for different applications, and most of these techniques require large amounts of energy [1]. Using fossil fuels has been considered as a common solution to solving the challenge of supplying energy for water purification. However, statistics show that both world energy consumption and CO_2 emissions from burning fossil fuels have doubled from 1971 to 2010 [2]. It is apparent that this upward trend has a negative impact on the environment and finding solutions using alternative energy resources for thermal desalination is essential. This has motivated researchers to find economically viable but environmentally sustainable desalination systems.

Uehara et al. [3] utilized an integrated hybrid cycle to desalinate seawater based on an Ocean Thermal Energy Conversion (OTEC) process. This process uses the temperature differences between warmer seawater (at the surface) and cooler seawater (at the depth of 1000 m) to drive the desalination plant. It also needs no preheating of the supply seawater and is categorized as Low Temperature Thermal Desalination (LTTD). LTTD process has low energy requirements and is one of the promising methods that has been constructed in different ways with unit concept. Some systems were established based on LTTD for cogenerating power and water desalination [4-8]. One of the newest desalination plants based on this concept is the Discharge Thermal Energy Combined Desalination (DTECD) [4, 9, 10]. This utilizes flash evaporation sprays such as those in the present study as the core mechanism to produce potable water. In this context, studies into the operational and design factors influencing the performance of flash evaporation processes are warranted.

Research into the field of flash evaporation has tackled two main approaches; pool evaporation and spray flash evaporation. In pool evaporation, a specified amount of liquid is kept in a (pressure controlled) sealed chamber connected to a vacuum tank. The liquid becomes superheated by being exposed to an environment at a pressure lower than the liquid's saturation pressure. Temperature variation in fluid occurs due to the latent heat of vaporization. This type of evaporation has a wide range of applications in various industries such as salt disposal systems [11],

cooling systems using a low pressure water [12], cooling grapes during wine production [13], and seawater desalination [14]. Alternatively, in spray flash evaporation, the liquid is injected into a vacuum chamber through a nozzle having an orifice. This approach has gained much attention since Miyatake et al. [15] proved that spray flash evaporation has better evaporation performance compared to pool evaporation. Moreover, Ikegami et al. [16] found that upward spray flash evaporation takes less time for evaporation compared to those injected downwards. Hence, they are also oriented in this manner within the present study. Since then, several studies have been carried out to improve the thermal performance [17, 18], increase the evaporation rate [19, 20], and study the effect of operating parameters and design on spray flash evaporation efficiency [8, 21]. Chen et al. [22] reported that fine droplets (shattering) due to atomization lead to evaporation rate improvements [23]. Cai et al. [24] also found better atomization and evaporation rates using a 3 mm nozzle in the spray flash evaporation under high temperature and high pressure. Whilst Mutair and Ikegami [25] conducted experiments to evaluate the influence of nozzle diameter on evaporation rate and observed that increasing the nozzle diameter decreases evaporation rate due to enhanced nucleation.

With the above in mind, it is evident that most research into spray flash evaporation uses single spray nozzles (smaller orifices) for quicker evaporation rates. However, despite its obvious influence on atomization and the rate of evaporation, the interaction between multiple (adjoining) sprays and arrangements of these spray nozzles has received no attention. Therefore, the aim of this research is to improve the fundamental understanding of the performance of flash evaporation systems if using multiple nozzles (compared to single nozzles). To achieve this goal, the influence of key operating parameters on the evaporation rate and Gain Output Ratio (GOR) are evaluated and discussed.

4.2 Experimental setup and procedure

4.2.1 Vacuum spray flash evaporator

Figure 4.1 shows the hardware and schematic diagram of the system used to study fine droplet flash evaporation. It is a single stage vacuum spray flash evaporator in which saline water is vaporized and condensed. In this setup, the saline water is

firstly preheated in a tank by a heater (OMEGA, Immersion CTS-75, 7.5 kW) until reaching the desired temperature. After that, the saline water is pumped into the chamber using a variable speed pump (Southern Cross, SBI-9T). The injection pressure of the pump is controlled manually by changing the pump speed. The preheated saline water is then injected upward through the nozzle placed inside the chamber. A three-way pipe connector is installed after the variable speed pump and is used to recirculate saline water inside the tank by an adjustable valve. A flow meter (MFS Magmaster) with ±0.2% accuracy (full scale) and a thermocouple (TC Measurement, T- Class1) with the accuracy of ±1(˚C) are installed in the pipeline before the multi-nozzle head to measure flow speed and inlet temperature of injected fluid, respectively. A pressure gauge after the injection pump and before nozzle outlet is used aiming to indicate the amount of pressure that is provided. In addition, eleven similar thermocouples (TC Measurement, T- Class1), same as inlet one, are installed with intervals of 3 mm on a horizontal movable holding bar to measure both the radial and axial temperatures above the multi-nozzle head.

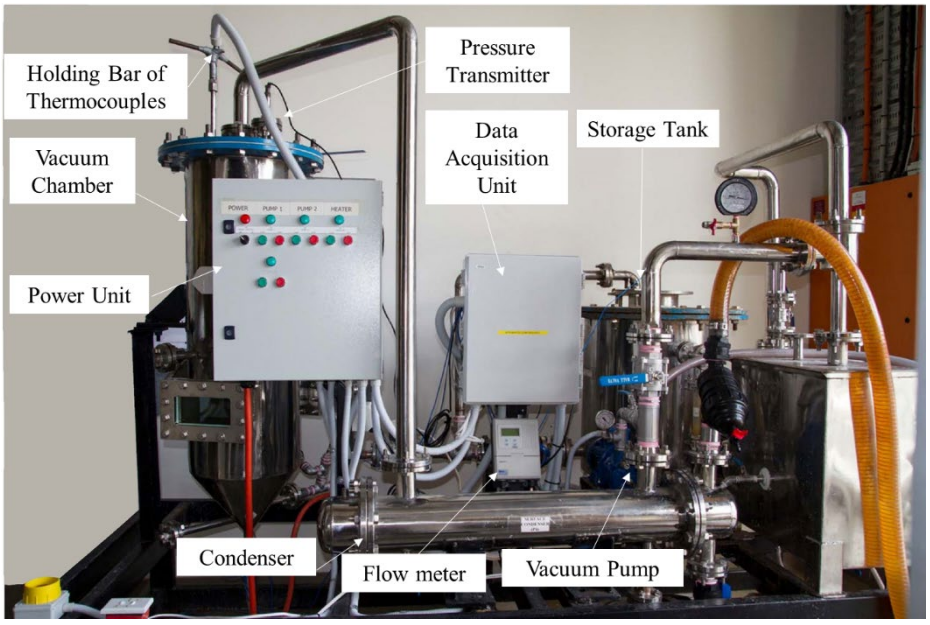

(a)

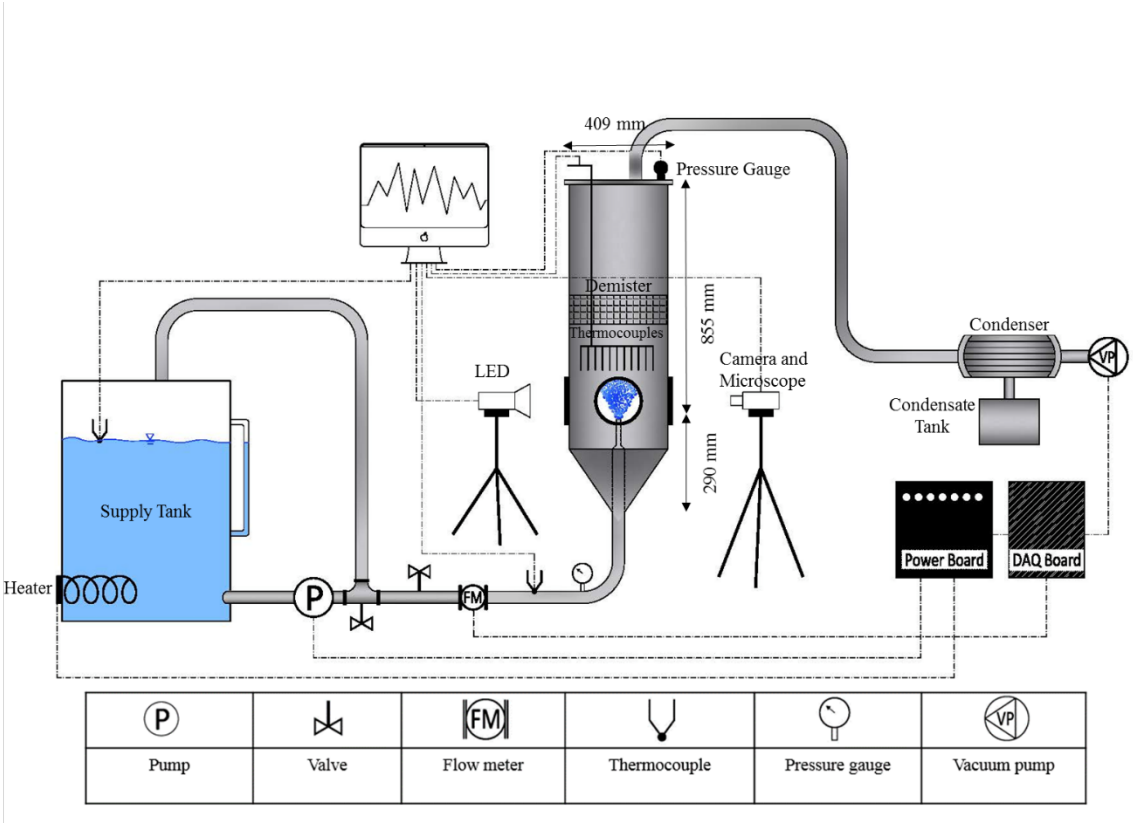

(b)

Figure 4.1 (a) Hardware layout, and (b) schematic diagram of the vacuum spray flash evaporator

A vacuum pump (Speck, V-30-55.0012) equipped with a regulator valve is connected to the chamber after the condenser (full capacity of 0.06 bar) to attain the desired vacuum pressure. In order to measure the pressure, a vacuum pressure transmitter (General electric, UNIK 5000, PTX-5-0-6-2-TA-A3-CA-H0-PE, and range 0 to 6 bar gauge) with ±0.04% accuracy (full scale) is installed at the top side of the chamber. When the heated seawater is injected into the vacuum zone, it is exposed to a sudden pressure drop (below its saturated pressure) and starts to evaporate.

To trap any droplets which are probably entrained into the vapour flow, and ensure they are not routed to the (potable water) condensate tank, a demister (Haver Standard) with 98% voidage is installed 320 mm above the multi-nozzle head. Vapour from the chamber is drawn to the shell and tube condenser where cooling water from another tank is circulated inside the tubes to condense the vapour. The

pure fresh water is later collected and stored in the condensate tank. During the experiments, the flow rates, temperatures, and pressure of the chamber are logged using the National Instrument LabVIEW V.2014.

4.2.2 Multi-nozzle head

Figure 4.2 illustrates the multi-nozzle spray head which was designed and manufactured at school of engineering for this study. This device is used to investigate the effect of nozzle number and arrangement on the evaporation rate and gain output ratio of flash evaporation system. To compare these parameters, three different configurations are considered where nozzles are positioned either along the periphery of the 165 mm pitch diameter (to minimize spray interaction) or closer together as shown in Figure 4.3. This specific diameter is chosen based on the chamber size to avoid any wall effects on the spray flows. A single nozzle arrangement is also included as a benchmark. All the applied nozzles are similar to specifications summarised in Table 4.1.

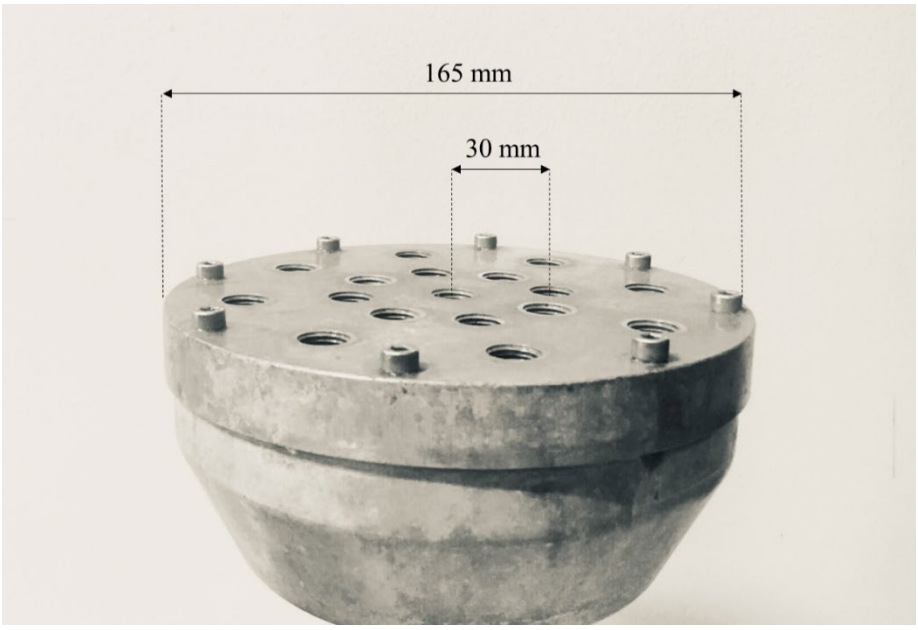

Figure 4.2 Multi-nozzle head

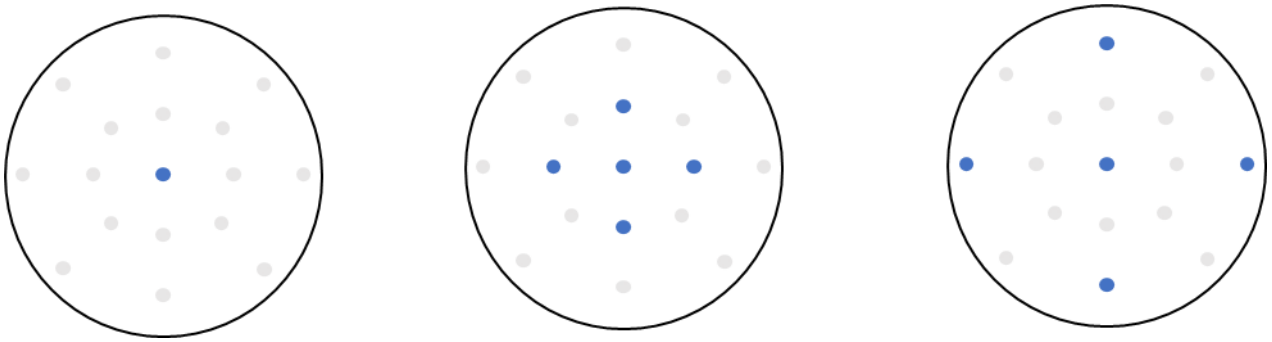

Arrangement No.1 (1 Nozzle) | Arrangement No.2 (5 Compact Nozzles) | Arrangement No.3 (5 Sparse Nozzles)

Figure 4.3 Three different configurations of similar nozzles

Table 4.1 Specifications of full cone spray nozzle (with circular area) at 2 bar pressure [**26**]

Type	Spray angle (˚)	Spray capacity (l/min)	Mean Drop Dia. (µm)	Free pass Dia. (mm)
JJXP-PP	65	2	280~410	1.5

Although the multi-nozzle head is employed in this work, the measurement and analysis are focused on the produced distilled water. This may raise the concern whether the flow through the nozzles are the same or not as any uniformity distribution of the flow may provide misleading results. Hence, the graduated cylinder was used over each nozzle orifice to measure the accumulation of saline water over time. The flow rate was set at 5 l/min to run the injection pump over 10 min for all three configurations under ambient pressure.

According to the test results, the accumulated saline water from arrangement No.1 was nearly 4.99 and 4.97 times more than the amounts of accumulated saline water of each nozzle in arrangements No.2 and No.3, respectively. Considering the fact that there are five nozzles in arrangement No.2 and No.3 (5 times more than arrangement No.1), the amount of collected water is almost same in all arrangements implying minor variation and indicating the reliable uniformity of flow through each nozzle.

4.2.3 Evaporation rate and Gain Output Ratio

In these experiments, Evaporation rate (E) and Gain Output Ratio (GOR) are used as two indicators to describe the performance of spray flash evaporation system. To determine the evaporation rate, a graduated glass beaker with a scaled increment (resolution) of 1 ml was used to measure the condensate water over a specific period of time. The GOR represents the efficiency of energy transformation and is defined as the energy required to evaporate the distillate to the input superheating energy. The GOR expression is defined as [27]:

$$GOR = \frac{\dot{Q}_v}{\dot{Q}_{in}} \tag{4.1}$$

The superheating energy which is stored in the seawater is calculated by [27]:

$$\dot{Q}_{in} = \dot{m}_{in} c_p \Delta T \tag{4.2}$$

where $\dot{m}_{in}$ (kg/s) is the inlet seawater mass flow rate, c_p (kJ/kg˚C) is the heat capacity of liquid, and ΔT (˚C) is the superheat degree which is given by [7]:

$$\Delta T = T_{in} - T_{sat} \tag{4.3}$$

here T_{in} (˚C) is the inlet temperature of saline water and T_{sat} (˚C) is the saturation temperature corresponding to the vacuum pressure.

The energy utilized to evaporate the distillate is estimated by [27]:

$$\dot{Q}_v = \dot{m}_v L \tag{4.4}$$

Where $\dot{m}_v$ (kg/s) is the vapour mass flow rate and L (J/kg) is the latent heat of vaporization.

4.2.4 Measurement of droplet sizes and distributions

Image Method Analysis (IMA) was used based on shadowgraph imaging to discuss the possible reasons for different outcomes of various nozzle configurations. For this purpose, the LED light source was positioned opposite to the microscope (QM 1 long mouth with a resolution of 3 microns at 55.9 cm) as displayed in Figure 4.1b. A high speed camera (SpeedSense1040/CMC-4000) with 100 mm f/2.0 lens was

also coupled with a microscope to image the droplets. ImageJ software was employed to perform all the processing steps including image binarization, enhancement, denoising, illumination correction, elimination of defocused and imperfect droplets, and filling of the holes to acquire droplet sizes and distributions. The droplet measurement and image processing principles, used in the present study, have been described in detail by Zhou et al. [28]. Accordingly, the shadowgraph imaging was applied to perform droplet size measurements and distribution at the inflection height, which is where the highest rate of evaporation occurs along the axial distance from the nozzle exit point. To define this height, it is essential to resolve the height along the spray centreline where the radial temperature distribution remains relatively unchanged and the evaporation is completed. Thus, leading to an equilibrium temperature. A more detailed definition of inflection height and its related equations can be found in [8]. Therefore, eleven thermocouples were employed to resolve the radial temperature distribution over multiple axial distances along the spray and the inflection height for the arrangements No.1, No.2, and No.3 were obtained to be 100 mm, 96 mm, and 93.5 mm, respectively. At these heights, five different points with 30 mm intervals were chosen to measure droplet sizes and distributions based on shadowgraph imaging [28]. Two points were selected on the both boundary lines of spray sheet and the other points were chosen equally between them.

To calculate and compare the droplet sizes of different nozzle configurations measured by the shadowgraph imaging, Chin and Lefebvre [29] suggested that D_{32} (Sauter mean diameter (SMD)) is the best indication for spray atomization. Hence, SMD was determined for the results obtained from the experiments as follows:

$$D_{32} = \frac{\sum n_i d_i^3}{\sum n_i d_i^2} \tag{4.5}$$

Where n_i is the number of droplets with a diameter d_i.

4.3 Uncertainty analysis

Experimental uncertainty is calculated to present the total values of measured uncertainties, whether due to random errors (i.e. unpredictable changes in the

measuring instruments or environmental conditions) or systematic errors (i.e. the accuracy of measurement devices or their calibration), and calculated as [30]:

$$\varepsilon = \pm\sqrt{\varepsilon_s^2 + \varepsilon_r^2} \tag{4.6}$$

where ε is the total uncertainty, ε_s is the systematic error and ε_r is the random error which can be calculated by [30]:

$$\varepsilon_s = \sqrt{\sum_{i=1}^{n} \varepsilon_{s,i}^2} \tag{4.7}$$

$$\varepsilon_r = \sqrt{\sum_{i=1}^{n} \varepsilon_{r,i}^2} \tag{4.8}$$

where *n* is the number of error source and $\varepsilon_{r,i}$ can be calculated from [30]:

$$\varepsilon_{r,i} = \sqrt{\frac{\sum_{i=1}^{n} (\varphi_i - \bar{\varphi})^2}{N(N-1)}} \tag{4.9}$$

where *N* and φ_i are the number of samples of the repeated observation and the average value, respectively. Table 4.2 summarizes the total uncertainty of the measured parameters including temperature, flow rate, and vacuum pressure.

Table 4.2 Uncertainty of measured parameters

Parameter	Systematic uncertainty (± %)	Random uncertainty (± %)	Total uncertainty (± %)
TC1(tank)	0.75	0.21	0.77
TC2(Inlet)	0.75	0.18	0.77
Flow meter	0.20	0.05	0.21
Vacuum pressure transmitter	0.04	0.00	0.04

4.4 Results and discussion

The primary task of this study is to investigate and improve the performance of spray flash evaporation which is why results presented will be based on the evaporation rate and gain output ratio. Various operating and design parameters (three nozzle configurations) will be studied including inlet flow rate (Q), pressure injection (P_{in}), superheat degree (ΔT), and salinity (C).

Although these parameters are related to each other and subject to change over different nozzle configurations in actual conditions, it is assumed that they can be controlled independently due to the fact that mutual influence is not significant [27]. Table 2 contains the investigated parameters and their experimented range.

Table 4.3 Influencing factors and their experimented range.

Parameter	Experimented range
Initial temperature, T_{in} (°C)	70
Superheat, ΔT (°C)	4-36
Injection pressure, P_{in} (bar)	0.25-6
Flow rate, Q (l/min)	1.7-17.8

The primary objective of using different nozzle configuration is to investigate the effects of using densely spaced, versus sparsely related, nozzles on spray flash evaporation. This section first analyses the behaviour of droplets under different arrangements and then investigates improvements associated with changing operating conditions.

4.4.1 Droplet size and distribution

Measurement of the droplet sizes and distributions is important for better recognition of the behaviour of the droplets when different nozzle configurations are used under the same conditions.

Figure 4.4 indicates the full cone saline water film formed by three various arrangements having similar nozzles and the specified inflection height for each arrangement. The operating conditions are the same and considered as follow:

T=70˚C, C=3.5%, Q= 5 l/min, and ΔT=14˚C. Figure 4.5 compares the Sauter mean diameter and distribution of droplets for three different arrangements. Two main conclusions can be made from the obtained results presented in these two figures. Firstly, it is clear that by increasing the number of nozzles, the number of droplets ($Count/Count_{max}$) increases which is expected to lead to more evaporation [31]. The count is the number of droplets which has been counted by ImageJ software at a specific area at a particular time. For instance, the number of droplets for arrangement No.1 (single nozzle) is 37% and 42% lower at points 4 and 5, respectively, than for arrangement No.2 (5 nozzles).

These data suggest that more evaporation rate can be likely achieved through increasing the number of nozzles for the same operating conditions. Secondly, although number of the droplets for arrangement No.2 and arrangement No.3 are closely similar due to using 5 similar nozzles in both configurations, the Sauter mean diameter of arrangement No.3 is lower than No.2 at all points. The average value of Sauter mean diameter for No.3 in points 1-5 is about 307 μm while this value for No.2 is around 344 μm. This is mainly because No.3 produces smaller aggregated droplet sizes which in return increases the surface area and consequently hastens the flash evaporation [22]. Based on the results, one can roughly predict that the most efficient arrangement is No.3 having 5 nozzles, however, this needs further evidence.

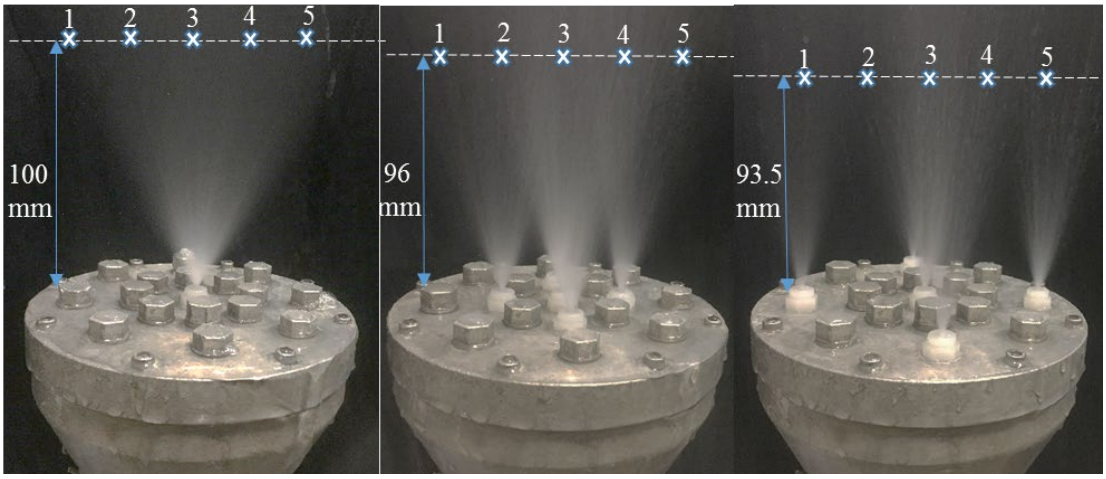

Arrangement No.1 Arrangement No.2 Arrangement No.3

Figure 4.4 Photo of conical shapes of water formed by three various arrangements with their inflection height (T=70˚C, C=3.5%, Q= 5 l/min, and ΔT=14˚C)

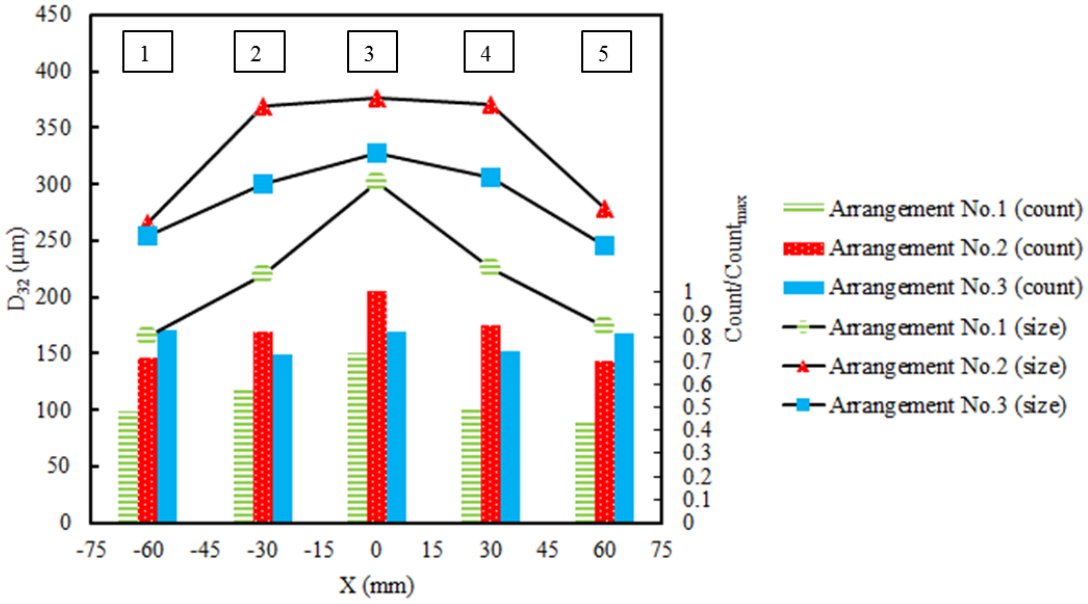

Figure 4.5 Sauter mean diameter and distribution of three different arrangements at 5 nominated points (T=70˚C, C=3.5%, Q= 5 l/min, and ΔT=14˚C)

4.4.2 Inlet flow rate

Figure 4.6 shows the effect of varying inlet flow rate on evaporation rate while other parameters are kept constant. These fixed parameters are T_{in}=70˚C, C=3.5%, and ΔT=26˚C. It is apparent that the evaporation rate is higher for arrangement No.3, while arrangement No.1, consisting of a single nozzle has the lowest evaporation rate at all flow rates. Arrangement No.3 at the flow rate of 4 l/min reached evaporation rate of 0.16 l/min, while the values are 0.15 and 0.14 l/min for arrangements No.2 and No.1, respectively. These different nozzle configurations also affect GOR as illustrated in Figure 4.7, which shows GOR is maximal for arrangement No.3 compared with arrangements No.1 and No.2 for different flow rates. As observed, for arrangement No.3, GOR is calculated to be 0.83 for the maximum flow rate (5 l/min), whereas for arrangements No.1 and No.2 these values are respectively 6% and 3% less than No.3. This can be attributed to the fact that according to the observation of spray characteristics, increasing the number of nozzles has a positive impact on the evaporation rate and consequently increase GOR. In addition, the most efficient configuration shows a minimum of 6% system efficiency (GOR) improvement compared to arrangement No.1 at considered flow rates. As it was predicted before, the nozzles in this arrangement (No.3) produce

finer droplets because they are placed in the farthest point to minimise droplets interaction and coalescence.

Another observation from Figure 4.6 and 7 is the upward trend of evaporation rate and GOR in all nozzle configurations with the increase of flow rate which is mainly attributed to the fact that increasing the flow rate in spray nozzles leads to creation of smaller droplets. In fact when the flow rate increases, it supplies higher kinetic energy and pressure for the atomization process and enhances saline water hydrodynamic instability [23]. As a result, integration of these two factors leads to generation of more vapour and increases GOR. Such an observation in fine orifice sprays, which is used in the current study, differs from previous research regarding single large orifice nozzles [8], which found that higher flow rate decreases the evaporation rate. This is mainly because of increasing inertia of the large orifice nozzle which denotes as a retarding force due to the increase of the static pressure at the nozzle exit. The enhancement of this force keeps the large orifice nozzle unshattered, while there is no unshattered area in the fine nozzle and all liquid is atomized completely.

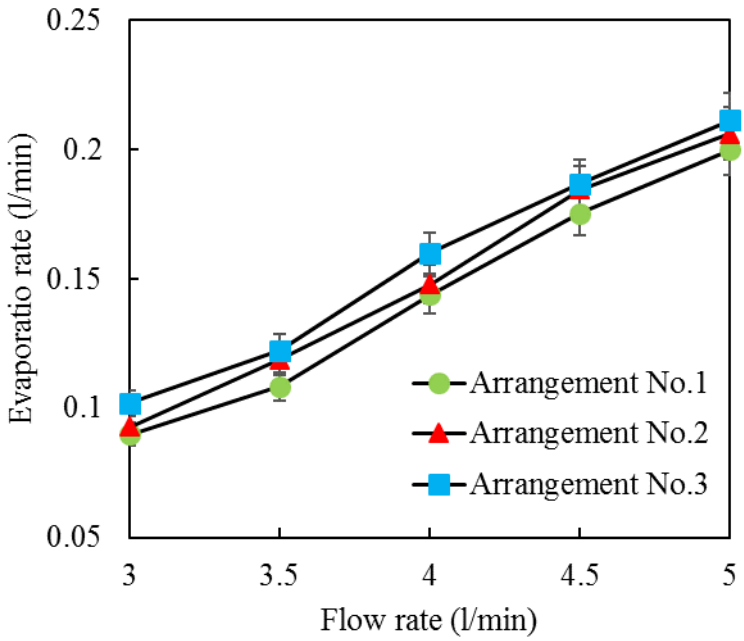

Figure 4.6 Evaporation rate under different flow rate for T_{in}=70˚C, C=3.5%, and ΔT=26˚C

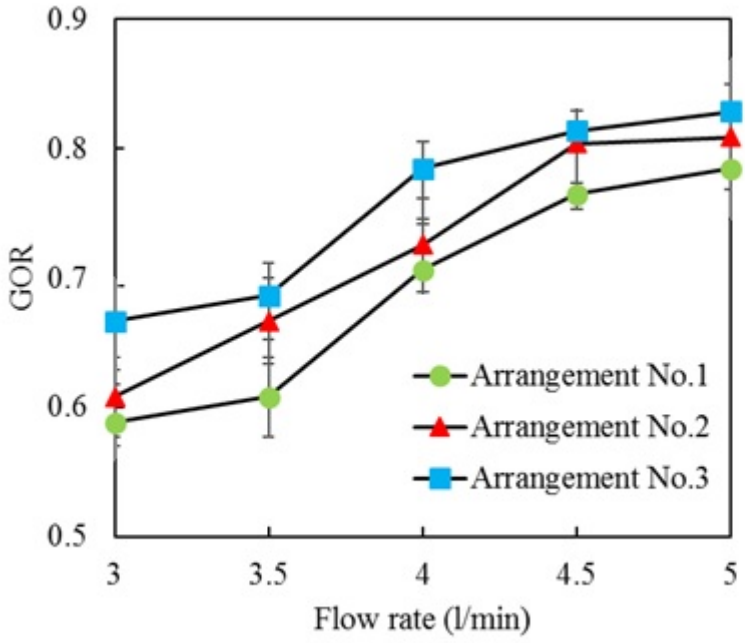

Figure 4.7 GOR under different flow rate for T_{in}=70˚C, C=3.5%, and ΔT=26˚C

4.4.3 Injection pressure

The influence of injection pressure on the evaporation rate is displayed in Figure 4.8. It should be taken into the account that the inlet temperature, superheat degree, and salinity are maintained at 70˚C, 26 ˚C, and 3.5%, respectively. As can be seen, although arrangement No.3 again has higher values of evaporation rate compared with other types, there is a significant difference between using 5 nozzles (arrangement No.2 and 3) and 1 nozzle (arrangement No.1) for the same pressure. For example, the evaporation rate for arrangements No.2 and 3 at the pressures of 2, 4, and 5 bar are approximately five times more than No.1. In other words, one major conclusion is that the number of nozzles plays a more important role than their configuration for a certain pressure injection.

For better understanding and justifying the aforementioned conclusion, Figure 4.9 compares the amounts of collected distilled water for a specific volume of injected water (20 L) under different injection pressures and corresponding flow rates. The solid lines correspond to volume collected and the dotted lines correspond to flow rate. This figure reveals that for the same injection pressure, increasing the flow rate, which is caused by using different arrangements, is the main reason for

hastening the evaporation rate. As a sample, the largest quantity of distilled water is collected for arrangement No.3, and this parameter increases slightly from 0.85 L at 0.25 bar to around 1.05 L at 6 bar. Water collected for arrangement No.1 also increases, but its rate of increase significantly slow down after 2 bar. The corresponding flow rate for arrangement No.3 from 0.25 bar to 6 bar shows a dramatic increase from 7.7 l/min to 17.1 l/min, while this increase has a shallow slope for arrangement No.1 to only 5 l/min. The enhancement of flow rate which is caused by applying more pressure, as observed and discussed earlier, accelerates the evaporation rate for the reason explained before.

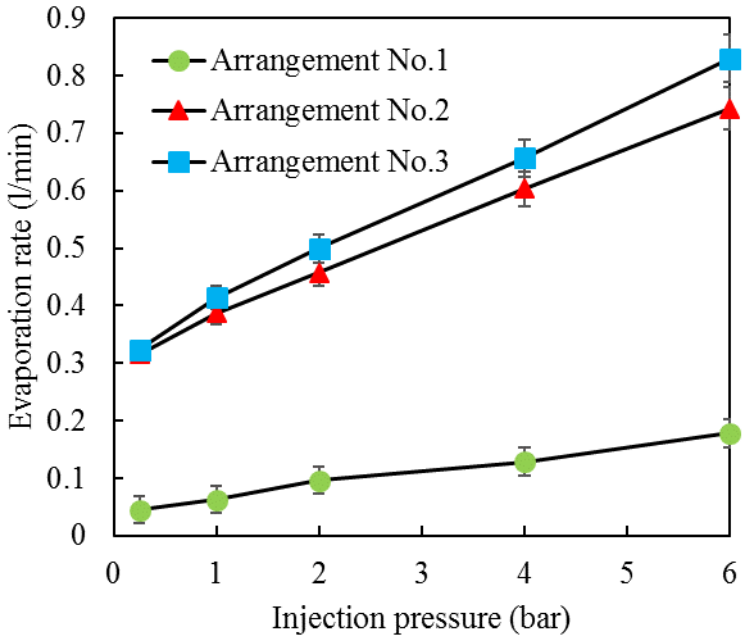

Figure 4.8 Evaporation rate under different injection pressure for T_{in}=70˚C, C=3.5%, and ΔT=26˚C

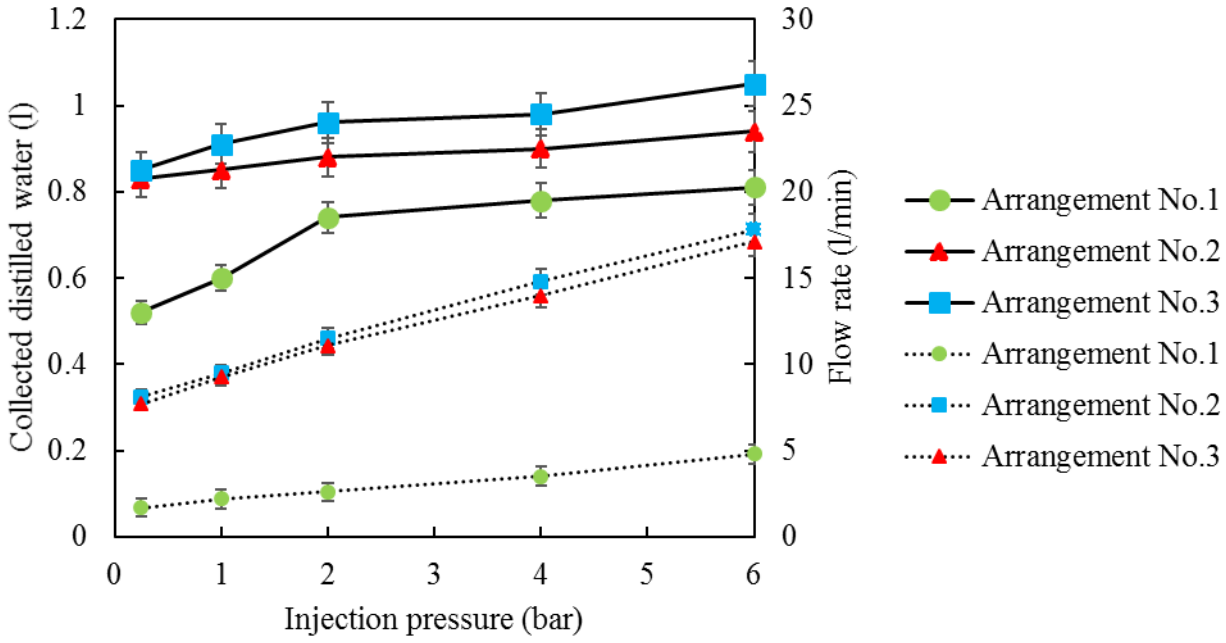

Figure 4.9 Comparison between collected distilled water under different injection pressure and corresponding flow rate for T_{in}=70˚C, C=3.5%, and ΔT=26˚C

Figure 4.10 illustrates the calculated GOR under different injection pressures. One can see that GOR for arrangement No.3 is higher than 0.80 for all corresponding pressures from 0.25 bar to 6 bar, while the maximum value for arrangement No.1 is about 0.76. Moreover, arrangement No.2 including 5 nozzles in the centre also provides better performance compared with the single nozzle. It is also apparent that GOR is an increasing function of the injection pressure so that the maximum efficiency of the system is reached at 6 bar. The quantitative values for arrangements No.1, No.2, No.3 at this pressure are 0.76, 0.88, and 0.98, respectively. According to the earlier discussion, the explanation for the improvement of efficiency by applying more pressure is the enhancement of flow rate which directly affects the evaporation rate.

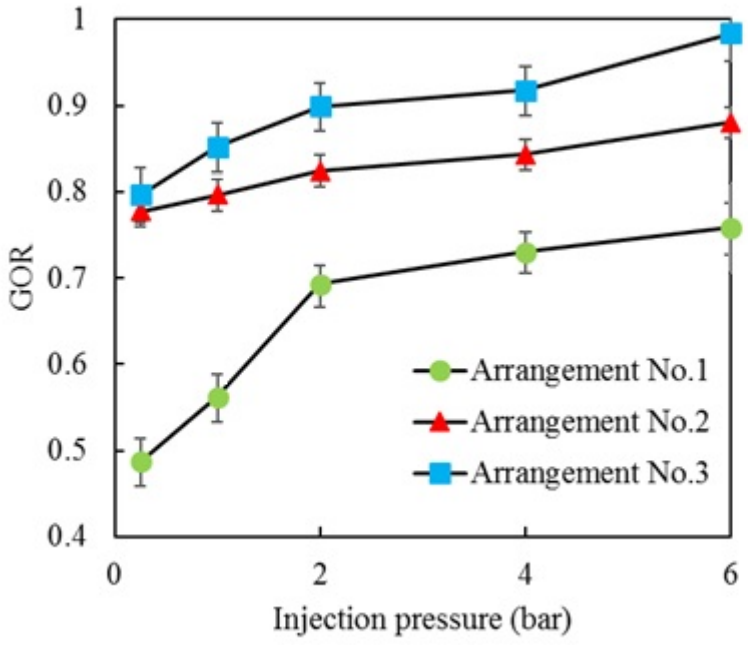

Figure 4.10 GOR under different injection pressure for T_{in}=70˚C, C=3.5%, and ΔT=26˚C

4.4.4 Superheat degree

Figure 4.11 illustrates the influence of superheat degree as a driving force for various configurations of nozzles, whereas the chamber vacuum pressure is varied while the other parameters are kept fixed at T_{in}=70˚C, C=3.5%, and Q=5 l/min. It is clear that although the general trend for evaporation rate in all arrangements is upward at higher superheat degrees, the quantitative values for each arrangement are different. For example, when arrangement No.1 is used, the measured evaporation rate for superheating degrees of 9, 18, and 36˚C are obtained to be 0.05, 0.13, and 0.27 l/min, respectively. These values are 0.06, 0.15, and 0.30 l/min for arrangement No.2 and 0.07, 0.16, and 0.31 l/min for arrangement No. 3. Taken together, these results indicate that firstly higher superheat degree supplies more thermal energy required for evaporation and consequently enhances the vapour density differences between the surface of droplets and the surrounding. The integration of the mentioned impacts results in higher values of evaporation rate [32]. Secondly, arrangement No.3 shows better atomization and distribution which has improved evaporation rate compared with other types.

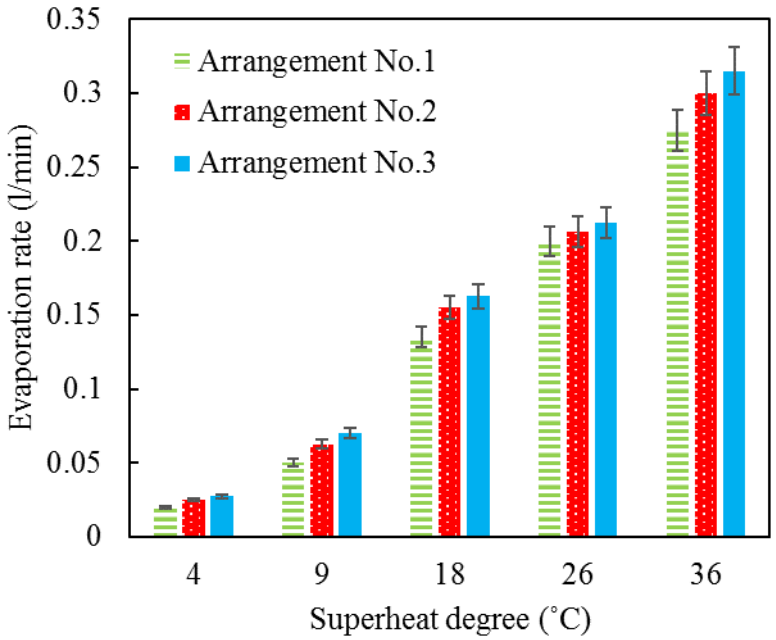

Figure 4.11 Evaporation rate under different superheat degree for T_{in}=70˚C, C=3.5%, and Q=5 l/min

The GOR profile for various nozzle configurations under different superheat degrees is plotted in Figure 4.12a. It can be seen that by reducing T_{sat}, more superheating energy is transferred into the latent heat of generated vapour which finally promotes the efficiency of the system. However, a much steeper variation occurs at lower superheat degrees (ΔT=4-18˚C) than at higher ones. For instance, GOR for arrangement No.2 is about 0.68 at superheat degree of 4˚C, then climbs rapidly to a peak value of 0.9 at superheat degree of 18˚C, and remains relatively unchanged thereafter. This trend is similar for other arrangements but quantitative values are different.

An explanation for this behaviour might be that each spray nozzle has a maximum transverse distribution and beyond this point, the spray scattering remains fairly stable for the system affecting the efficiency of flash evaporation [33]. This point can be extracted from Figure 4.12b, in which P_{in}/P_{sat} is plotted against spray angle based on the experimental data. These data are produced by capturing the photos using high speed camera at T_{in}=70˚C, C=3.5%. The results show that the quantitative value of maximum transverse distribution corresponds to P_{in}/P_{sat} equal to or higher than 26. This value is also determined from Figure 4.12a and obtained to be 27, based on the point after which in GOR becomes relatively constant.

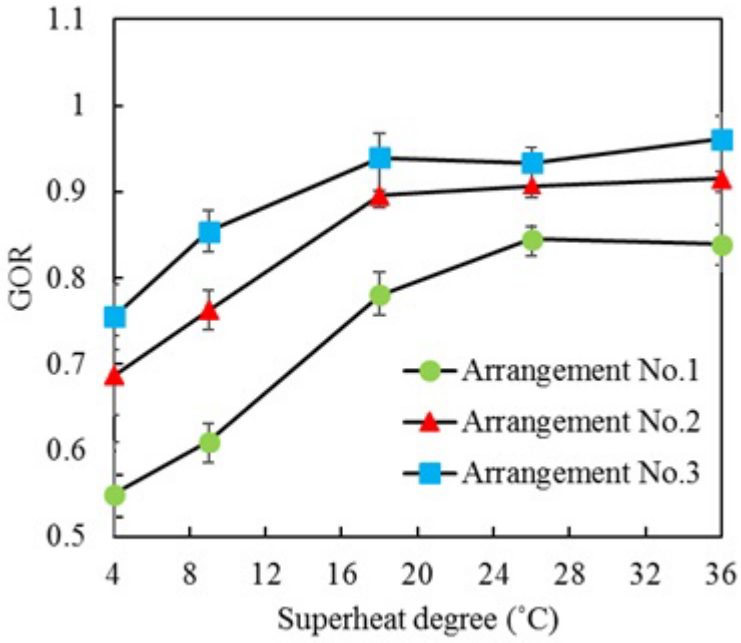

(a)

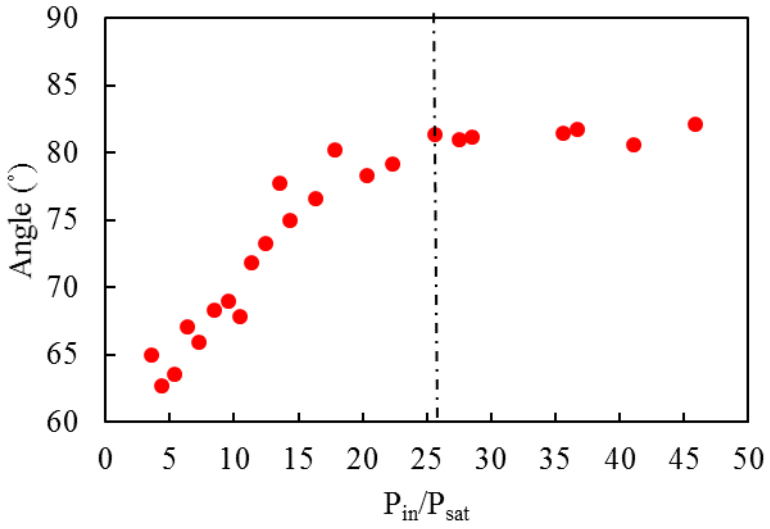

(b)

Figure 4.12 (a) GOR under different superheat degree at T_{in}=70˚C, C=3.5%, and Q=5 l/min (b) spray angle against P_{in}/P_{sat} at T_{in}=70˚C, C=3.5%

It is found that there is good agreement between the values are obtained from Figure 4.12a and 12b. This information would be helpful to find the optimal range of superheat energy in order to prevent energy loss. On the other hand, arrangement No.3 has the highest GOR at all considered superheat degrees with a maximum and

minimum improvement of 28% and 7% compared to arrangement No.1, respectively; and proves the results obtained and presented in Section 4.3.1.

4.4.5 Salinity

The experimental variation of salinity has been carried out in the range of 0 to 20% to evaluate the performance of the system at T_{in}=70˚C, ΔT=26˚C, and Q= 5 l/min by employing the multi-nozzle head as delineated in Figure 4.13. It is obvious that salt and its concentration has an influence on the evaporation rate. In this study, 3.5% salinity is chosen to compare the average seawater salinity to others. This amount of salinity leads to the average reduction of 2% in evaporation rate for all considered arrangements compared to pure water. Although this rate of reduction is not noticeable, comparing the wider ranges of salinity such as 10% and 20% with pure water shows approximately 20% and 50% decline in evaporation rate, respectively. The main feature that can be obtained from these findings is that higher salt solution in the water ensures the lower intensity of flash evaporation. This conclusion is obtained under vacuum condition but well agreed with the results of the research by Al-Shammiri [34] who performed the experimental measurement to determine the evaporation rate of saline water in the range of 0 to 6.5% at ambient condition. The main reason for the reduction of evaporation rate by increasing salt concentration can be attributed to the fact that salt solution in pure water strengthens the interaction force between molecules and consequently increases the surface tension. By adding salt, these effects are intensified which leads to less evaporation rate [34, 35]. Besides the influence of salinity, better atomization capability of arrangement No.3 should be considered. So that, despite the reduction in the evaporation rate of all configurations, this arrangement has the highest evaporation rate among all configurations.

On the other side, the influence of salinity on the efficiency of the system is calculated based on the GOR profile against salinity as portrayed in Figure 4.14. It is clear that the reduction of GOR is an increasing function of salinity. A useful example of this functionality is the decline of GOR from 0.85 for pure water to 0.47 for 20% saline water by using arrangement No.3. But this reduction of efficiency in seawater with 3.5% salinity is about 2.5% and it is not as much as 10% and 20% salinities.

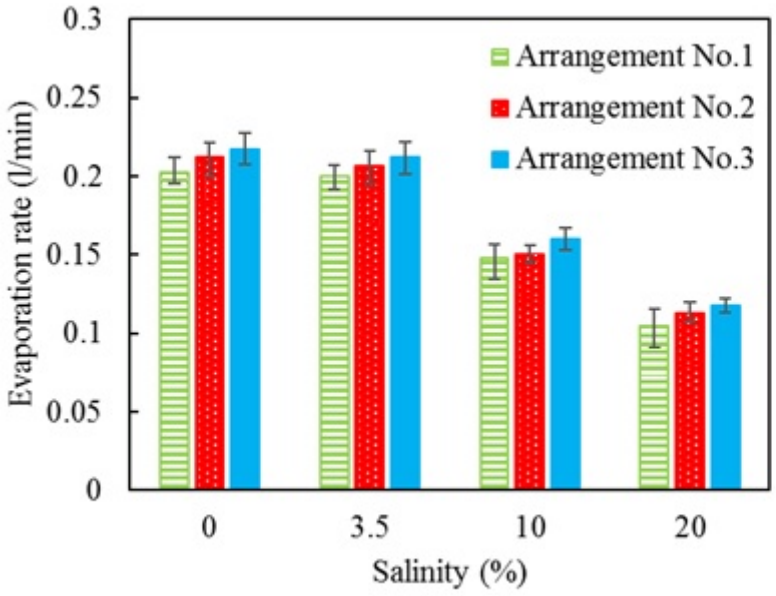

Figure 4.13 Evaporation rate under different salinity for T_{in}=70˚C, ΔT=26˚C, and Q= 5 l/min

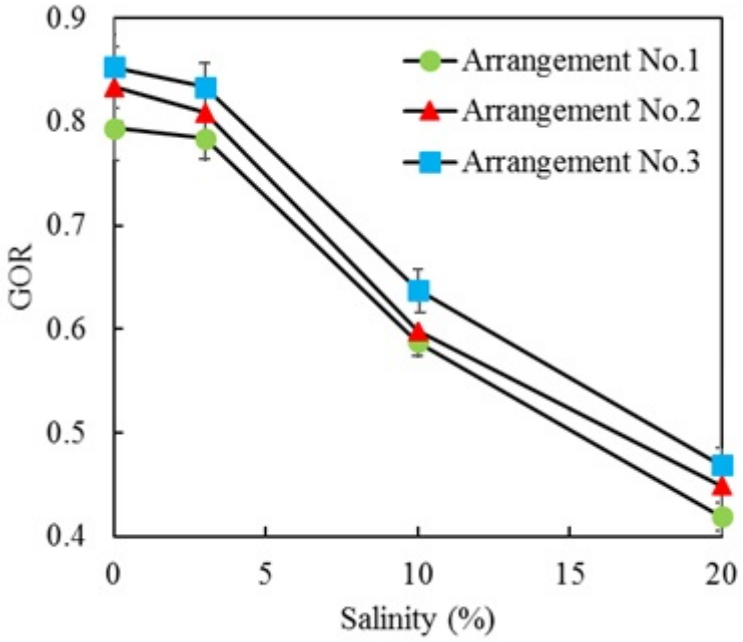

Figure 4.14 GOR under different salinity for T_{in}=70˚C, ΔT=26˚C, and Q=5 l/min

4.5 Conclusions

This study aimed to experimentally improve the performance of spray flash evaporation by using multiple nozzles. To achieve this aim, a multi-nozzle head was designed and built to investigate the impact of key operational parameters on

the evaporation rate and gain output ratio. This experiment was conducted in saline sprays (C=0 to 20%) under a wide range of conditions (T_{in}=70˚C, Q=1.7-17.8 l/min, P_{in}=0.25-6 bar, and ΔT=4-36˚C) and the following points were concluded:

- Overall increasing the number of nozzles in spray flash evaporation system increases the performance of the system considering the flow rate, injection pressure, superheat degree, and salt concentration.
- The most efficient arrangement was found to be 5 nozzles positioned in the farthest distance of each other which improved the efficiency of the system up to 28% when the flow rate was constant.
- The effect of nozzle numbers on the efficiency was more noticeable than the nozzle arrangements when the injection pressure was fixed.
- The optimum superheat degree of the system was determined to be around 19˚C based on GOR profile which helped to avoid energy loss when the superheat degree was constant.
- The salt solution decreased the evaporation rate and efficiency of the system, however, 5 nozzles positioned in the farthest distance of each other, as the most efficient arrangement, showed the best performance under all the operational conditions of the experiments.

Although this study investigated the improvement of spray flash evaporation using multiple nozzles, further research on spray characteristics, droplets velocity, and size changes in all directions is recommended for future studies.

Acknowledgements

This research was supported by the School of Engineering at Edith Cowan University. The first author acknowledges the School of Engineering for awarding scholarship to pursue his PhD.

4.6 References:

1.A.D. Khawaji, I.K. Kutubkhanah, and J.-M. Wie, *Advances in seawater desalination technologies.* Desalination. Vol. 221, 2008: p. 47-69.

2.*Key world energy statistics*. 2016: International Energy Agency.

3.H. Uehara, A. Miyara, Y. Ikegami, and T. Nakaoka, *Performance Analysis of an OTEC Plant and a Desalination Plant Using an Integrated Hybrid Cycle.* Journal of Solar Energy Engineering. Vol. 118, 1996: p. 115-122.

4.A.H. Araghi, M. Khiadani, and K. Hooman, *A novel vacuum discharge thermal energy combined desalination and power generation system utilizing R290/R600a.* Energy. Vol. 98, 2016: p. 215-224.

5.A.H. Araghi, M. Khiadani, K. Hooman, and G. Lucas, *Efficiency of a Combined Desalination and Power System Utilising a Two-Phase Flow Multi-Stream Heat Exchanger.* Heat Transfer Engineering. Vol. 38, 2016: p. 1000-1007.

6.A.H. Araghi, M. Khiadani, M. Sadafi, and K. Hooman, *A numerical model and experimental verification for analysing a new vacuum spray flash desalinator utilising low grade energy.* Desalination. Vol. 413, 2017: p. 109-118.

7.A. Muthunayagam, K. Ramamurthi, and J. Paden, *Low temperature flash vaporization for desalination.* Desalination. Vol. 180, 2005: p. 25-32.

8.S. Mutair and Y. Ikegami, *Experimental investigation on the characteristics of flash evaporation from superheated water jets for desalination.* Desalination. Vol. 251, 2010: p. 103-111.

9.F. Fathinia, M. Khiadani, and Y.M. Al-Abdeli, *Experimental and mathematical investigations of spray angle and droplet sizes of a flash evaporation desalination system.* Powder Technology. Vol. 355, 2019: p. 542-551.

10.F. Fathinia, Y.M. Al-Abdeli, and M. Khiadani, *Evaporation rates and temperature distributions in fine droplet flash evaporation sprays.* International Journal of Thermal Sciences. Vol. 145, 2019: p. 106037.

11.D.H. Kim, *A review of desalting process techniques and economic analysis of the recovery of salts from retentates.* Desalination. Vol. 270, 2011: p. 1-8.

12.I. Aoki, *Water flash evaporation under low pressure conditions.* Previews of Heat and Mass Transfer. Vol. 6, 1995: p. 518.

13.P. Sebastian and J.P. Nadeau, *Experiments and modeling of falling jet flash evaporators for vintage treatment.* International journal of thermal sciences. Vol. 41, 2002: p. 269-280.

14.K. Al-Shayji, S. Al-Wadyei, and A. Elkamel, *Modelling and optimization of a multistage flash desalination process.* Engineering optimization. Vol. 37, 2005: p. 591-607.

15.O. Miyatake, T. Tomimura, Y. Ide, and T. Fujii, *An experimental study of spray flash evaporation.* Desalination. Vol. 36, 1981: p. 113-128.

16.Y. Ikegami, H. Sasaki, T. Gouda, and H. Uehara, *Experimental study on a spray flash desalination (influence of the direction of injection).* Desalination. Vol. 194, 2006: p. 81-89.

17.O. Miyatake, T. Tomimura, Y. Ide, M. Yuda, and T. Fujii, *Effect of liquid temperature on spray flash evaporation.* Desalination. Vol. 37, 1981: p. 351-366.

18.J. Wellmann, K. Neuhäuser, F. Behrendt, and M. Lehmann, *Modeling an innovative low-temperature desalination system with integrated cogeneration in a concentrating solar power plant.* Desalination and Water Treatment. Vol. 55, 2015: p. 3163-3171.

19.O. Miyatake, T. Tomimura, and Y. Ide, *Enhancement of spray flash evaporation by means of the injection of bubble nuclei.* Journal of solar energy engineering. Vol. 107, 1985: p. 177.

20.A. Hosseini Araghi and M. Khiadani, *Experimental investigation and analysis of a new single-stage vacuum spray flash desalinator utilising a gas-liquid ejector.* Journal of Cleaner Production. Vol. 190, 2018: p. 118-127.

21.A.K. El-Fiqi, N.H. Ali, H.T. El-Dessouky, H.S. Fath, and M.A. El-Hefni, *Flash evaporation in a superheated water liquid jet.* Desalination. Vol. 206, 2007: p. 311-321.

22.Q. Chen, Y. Li, and K.J. Chua, *On the thermodynamic analysis of a novel low-grade heat driven desalination system.* Energy Conversion and Management. Vol. 128, 2016: p. 145-159.

23.Q. Chen, K.J. M, Y. Li, and K.J. Chua, *Experimental and mathematical study of the spray flash evaporation phenomena.* Applied Thermal Engineering. Vol. 130, 2018: p. 598-610.

24.B. Cai, Q. Zhang, Y. Jiang, H. Gu, and H. Wang, *Experimental study on spray flash evaporation under high temperature and pressure.* International Journal of Heat and Mass Transfer. Vol. 113, 2017: p. 1106-1115.

25.S. Mutair and Y. Ikegami, *Experimental study on flash evaporation from superheated water jets: Influencing factors and formulation of correlation.* International Journal of Heat and Mass Transfer. Vol. 52, 2009: p. 5643-5651.

26.H. Ikeuchi. *Hydraulic Spray Nozzles (Full Cone Spray Pattern)*. 2018; Available from: https://www.kirinoikeuchi.co.jp/eng/products/spray/03/.

27.B. Cai, Q. Wang, S. Yin, H. Gu, H. Wang, H. Zhen, and L. Zhang, *Energy analysis of spray flash evaporation from superheated upward jets.* Applied Thermal Engineering. Vol. 148, 2019: p. 704-713.

28.W. Zhou, J. Hu, M. Feng, B. Yang, and X. Cai, *Study on imaging method for measuring droplet size in large sprays.* Particuology. Vol. 22, 2015: p. 100-106.

29.J.S. Chin and A.H. Lefebvre, *Some Comments on the Characterization of Drop-Size Distributions in Sprays.* Int. J. Turbo Jet Engines. Vol. 2, 1986: p. p. IVA/1/1-IVA/1/12.

30.A. Shafieian, M. Khiadani, and A. Nosrati, *Thermal performance of an evacuated tube heat pipe solar water heating system in cold season.* Applied Thermal Engineering. Vol. 149, 2019: p. 644-657.

31.B. Cai, X. Tuo, Z. Song, Y. Zheng, H. Gu, and H. Wang, *Modeling of spray flash evaporation based on droplet analysis.* Applied Thermal Engineering. Vol. 130, 2018: p. 1044-1051.

32.Q. Chen, K. Thu, T. Bui, Y. Li, K.C. Ng, and K. Chua, *Development of a model for spray evaporation based on droplet analysis.* Desalination. Vol. 399, 2016: p. 69-77.

33.X.-S. Wang, B. Chen, R. Wang, H. Xin, and Z.-F. Zhou, *Experimental study on the relation between internal flow and flashing spray characteristics of R134a using straight tube nozzles.* International Journal of Heat and Mass Transfer. Vol. 115, 2017: p. 524-536.

34.M. Al-Shammiri, *Evaporation rate as a function of water salinity.* Desalination. Vol. 150, 2002: p. 189-203.

35.L. Liu, Q.c. Bi, and H.x. Li, *Experimental investigation on flash evaporation of saltwater droplets released into vacuum.* Microgravity Science and Technology. Vol. 21, 2009: p. 255-260.

Chapter 5

A comparative study of scalable jet and spray flash evaporation desalination[1]

Abstract

Despite various investigations into the characteristics of upward and downward flowing flash evaporation sprays, there remains ambiguity on the efficiency (evaporation) gains achieved when upscaling from single nozzle atomisation, to that involving multiple nozzles. Moreover, the performance of these types of water desalination methods has not been assessed between spray and jet generating orifices. In this study, an experimental analysis of a flash evaporation desalination has been carried out to explore the efficiency gains between jet and spray nozzle atomisation, under configurations of both single and multiple nozzle arrangements (5 nozzles). A wide array of conditions (Tin=70-80 ˚C, ΔT=4-36 ˚C, Q=3-5 l/min) are tested for the saline (C=3.5%) water evaporated and then condensed under low pressure (Pvac=0.06-0.4 bar).

Results based on the centreline temperature distribution indicate evaporation rate in spray nozzles is higher than the one in the jet nozzles. Moreover, utilizing multiple nozzles in flash evaporation both jets and sprays is more efficient than single nozzle with efficiency improvements of 32 and 40%, respectively.

Keywords: Flash evaporation, Spray, Jet, Temperature distribution, Evaporation rate, Gain output ratio

[1] This chapter has been published as a full research paper:
F. Fathinia, M. Khiadani, Y.M. Al-Abdeli, 2020. *A comparative study of jet and spray flash evaporation desalination systems*. Experimental Thermal and Fluid Science (In review). Whilst efforts were made to retain original content of the article, minor changes such as number formats, font size and style were implemented in order to maintain consistency in the formatting style of the thesis.

5.1 Introduction

Water is an essential part of mankind's life and demand for this valuable resource never drops due to the growing population and increasing droughts in different regions around the world. Although 98% of the earth is covered with seas, lakes, and reservoirs as well as groundwater [1, 2], supplying fresh water remains challenging and provides motivation for developing alternative resources and methods to derive portable water. Desalination technology, which involves removing salt from saline and brackish water, can be classified into the three main approaches including membrane based, thermal based, and electrochemical methods [3].

High running costs and energy consumption are two major challenges which motivate researchers to push the boundaries of previous methods [4-6]. Thermal desalination as one of the most widely installed technologies, which has received more attention to develop and improve performance due to its high efficiency [7]. Therefore, researchers are proposing various techniques to control and manage the intensity of the energy is required in a thermal desalination system. These techniques have been classified as alternative processes within the thermal branch which modify prior processes in regard to energy, cost, and availability.

Low temperature flash evaporation is a promising method with a low energy requirement. This system seperates liquid and its components when encountering a sudden reduction in its pressure. In other words, the low heated liquid starts to evaporate when it is injected into the vacuum zone, where the pressure is far below its saturation pressure (corresponding to the inlet temperature). As a result, part of the liquid turns to vapor to regain its equilibrium condition and other constituents (i.e. salt, sulphur …), remain stable without phase change due to the extra energy required for breaking their bonds. The vapour generated is then condensed through the heat exchanger and distilled water is produced [8].

It is now well established that flash evaporation is a term referring to the process which involves rapidly vaporizing (saturated liquid) water in a vacuum chamber that the deep understanding of this phenomena is vital for achieving optimal performance. Miyatake et al. [9] conducted several experiments to find the most efficient way of liquid vaporization inside the vacuum chamber for flash

evaporation. Ultimately, they found that the injection of the liquid has much more intense heat transfer. This result provides more insight for other researchers to focus on this type of flash evaporation, but a lack of investigation on the other types of injection was the motivation of this study to complete their investigations.

One of the challenges for an efficient operation of a vacuum flash evaporation system is the way that the flow is introduced inside the vacuum environment, with the realities of scalable production requiring significant process gains. Generally, nozzles are widely used to inject the liquid and control the inlet flow, speed, direction and many related parameters. In the case of flash evaporation, the most common nozzles are spray and jet that liquid is injected through a different diameter into the vacuum environment. Jet nozzles inject liquid in a solid cone-shaped pattern which consists of medium droplets size. These types of nozzles have a round impact area and uniform pattern. A wide variety of jet nozzles are available based on their configuration, capacity, and droplet sizes. Spray nozzles atomize liquid in very fine droplets, with its pattern depending on the type of spray. Many types of sprays are available but three of the most common types are flat fan, cone spray, and solid stream nozzles which are shown in Figure 5.1 [10, 11].

The primary experiments with jet flash evaporation system were conducted by Miyatake et al. [12]. They studied the effect of jet inlet temperature which ranged from 40-80˚C and developed comprehensive equations to predict the variation of centreline temperature along a jet. It was also found that the performance of flash evaporation in jets was not affected by reducing the temperature compared to pool

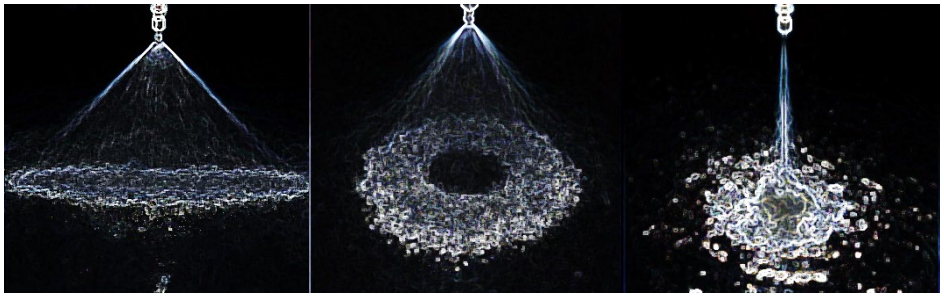

(a) (b) (c)

Figure 5.1 The most common types of spray nozzles include (a) flat fan (b) core, and (c) solid stream nozzles

flash evaporation system, however the behaviour of spray flash evaporation remained unclear which has been analysed in this study. Ikegami et al. [13] used a 20 mm jet temperature compared to pool flash evaporation system. Ikegami et al. [13] used a 20 mm jet nozzle diameter to compare the effect of injection direction on the system performance. As a result, they observed that flash evaporation in upward flowing jets took less time for completion than downward flow jets. Therefore, upward injection was recommended to improve the performance of flash evaporation systems. In the case of jet flash evaporation, several other experiments were studied in relation to nozzle size and geometry [14-16], the effect of operating conditions on the performance of the system [16-18], and numerical and mathematical analysis [19-22]. However, in all these studies only jet nozzle was studied and compared.

Some researchers have compared flash evaporation in jet nozzles with spray nozzles on the basis that smaller droplets with increased surface area, also improve the evaporation [23]. Araghi et al. [24] used an upward spiral spray nozzle with a 1.2 mm orifice diameter to spray superheated saline water inside a vacuum chamber and found that this spray nozzle affected the evaporation rate positively compared to the jet nozzle and recommended that further research is needed in this area. Fathinia et al. [25] also utilized 0.8 mm full cone spray nozzle to establish a correlation between temperature distribution and the evaporation rate. They also found an exponentially decaying curve matches temperature distribution in both spray and jet nozzles. In a follow up work, the spray injection was visualised by shadowgraph technique to estimate the variation of droplet sizes along the spray centreline for three different types of spray with 0.8-1.5 mm orifice diameters and concluded that the spray capacity significantly influenced the droplets' lifetime. [26]. Inspite of this, earlier stuidies have not included a quantitiative comparisons between spray and jet nozzles under various operating conditions in flash evaporation system, and particularly when the sprays and jets atomised are done between single and multiple nozzle arrangements.

Therefore, the present work is aimed at making a comparative study by considering spray and jet nozzles in both single and multiple arrangements. It analyses the effect of inlet flow rate, inlet pressure and superheat degree on evaporation rate and flash evaporation efficiency of the spray and jet nozzles. To the best of the authors'

knowledge, this is the first quantitative comparative study between the performance of flash evaporation jets and sprays, with results providing valuable set of experimental data.

5.2 Methodology

5.2.1 Experimental setup

Figure 5.2 displays the flash evaporation desalination setup which works on the discharge thermal energy combined desalination (DTECD) principle [27]. This single stage lab-scale process consists of a supply tank, chamber, vacuum and injection pump, data acquisition system (recording temperatures), shell and tube condenser, a condensate tank, and a condenser supplied by a cooling water tank to distill evaporated water. In this setup, saline water is warmed up by a heater (OMEGA, Immersion CTS-75, 7.5 kW) until reaching the desired inlet temperature for the flash evaporation process. After that, the heated saline water is injected by a variable speed pump (Southern Cross, SBI-9T) upward in the depressurised chamber through a nozzle placed at its base. A vacuum pump (Speck, V-30-55.0012), connected to the flash evaporation chamber, is capabale of attaining 0.06 bar pressure (absolute pressure) at full capacity. A thermocouple (TC Measurement, T- Class1) with an accuracy of ±1˚C as well as a flow meter (MFS Magmaster) with ±0.2% full scale accuracy are both assembled into the brine solution supply pipe (before the injection) to measure the inlet temperature and flow rate, respectively. In order to measure both the radial and axial temperatures above the multi nozzle head, eleven thermocouples, same as the one at the inlet, are fixed on a horizontal movable holding, and spaced radially bar at 3 mm intervals. Furthermore, to monitor chamber pressure, a vacuum pressure transmitter (General electric, UNIK 5000, PTX-5-0-6-2-TA-A3-CA-H0-PE, and range 0 to 6 bar gauge) with ±0.04% full scale accuracy is installed at the upper side (collection port for evaporated water) of the chamber. More details for the experimental set-up are available in the literature [25-28].

Flash evaporation phenomenon caused by a sudden pressure drop below the saturated temperature of injected heated saline water. To trap any droplets whose trajectory may entrain into the flow of vapour, a demister (Haver Standard) with 98% voidage is attached 320 mm above the nozzle injection point (535 mm below

the upper side of the chamber that is 1145 mm high). Flash evaporated vapour, but not any droplets captured by the demister, is then withdrawn by virue of the negative pressure and transferred to the shell and tube condenser and collected (as distillate) in the condensate tank. In this experiment, the flow rates, temperatures, and the chamber pressure are recorded simultaneously utilizing a National Instrument LabVIEW V.2014 interface.

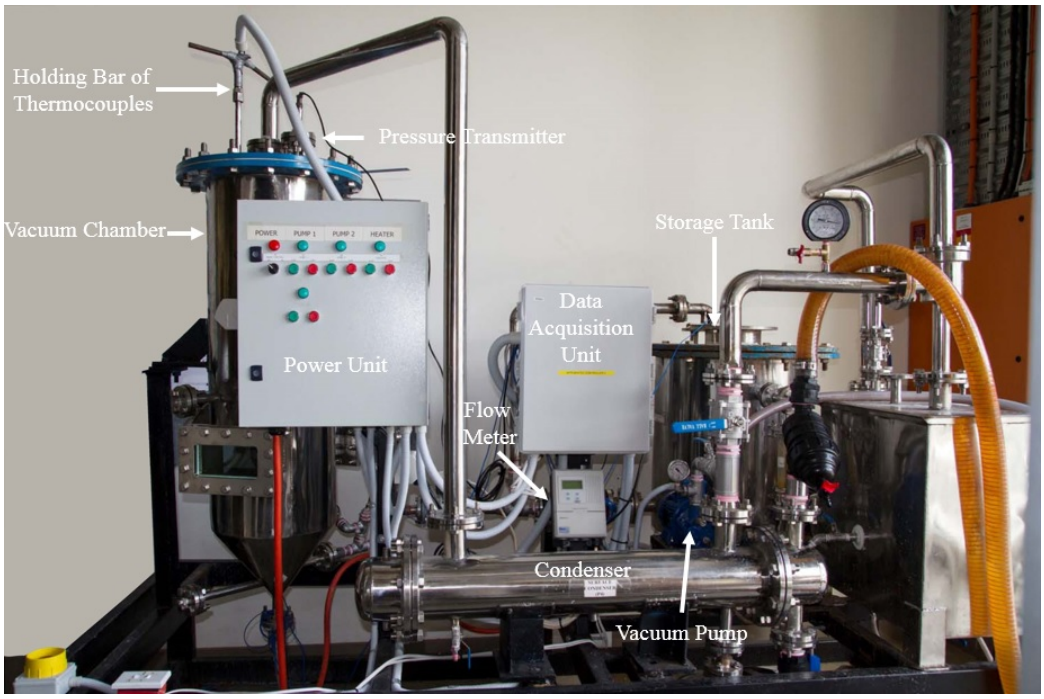

Figure 5.2 A pilot scale flash evaporation desalination system

Figure 5.3 shows the multi-nozzle head which was designed and fabricated in the School of Engineering at Edith Cowan University for the purpose of this study. This device is utilized inside the chamber to establish a single and multiple nozzle arrangements for both spray and jet nozzles. Therefore, for single arrangement, jet and spray nozzles with 1.5 mm orifice are positioned at the centre (Figure 5.4a) and for multiple nozzle arrangements, five jet and five spray nozzles of similar specifications are installed in the farthest point of each other (Figure 5.4b). The nozzles in multiple arrangements are placed along the periphery of the 165 mm pitch diameter nozzle head to minimize droplets interaction. This specific diameter is chosen based on the chamber size to avoid any wall effects on the spray flows [25]. This diameter is to limit wall effects on the spray flows arising from the 409 mm diameter chamber [28].

Based on uncertainty analysis, the total uncertainty for thermocouples, flow meter, and vacuum pressure transmitter are about 0.77± %, 0.21± %, 0.04± %, repectively. Further details are available in earlier studies [25-28].

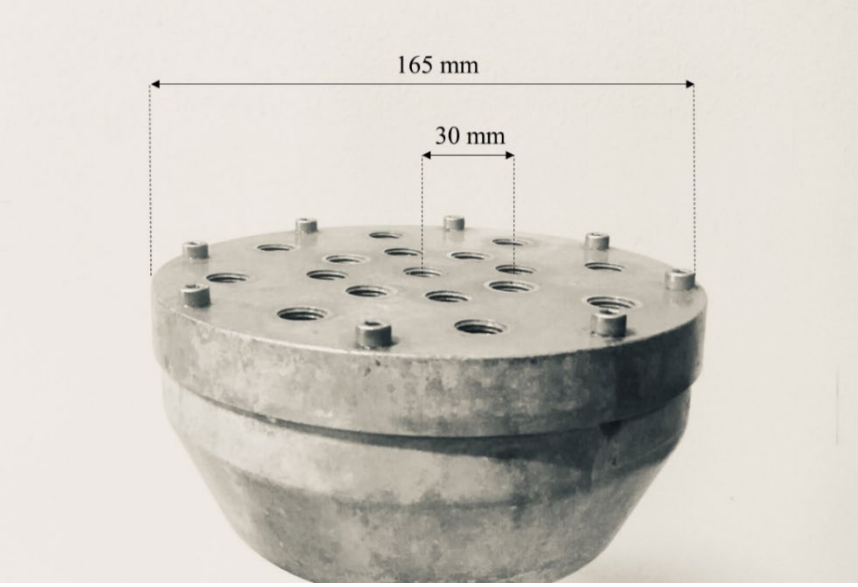

Figure 5.3 Multi-nozzle head

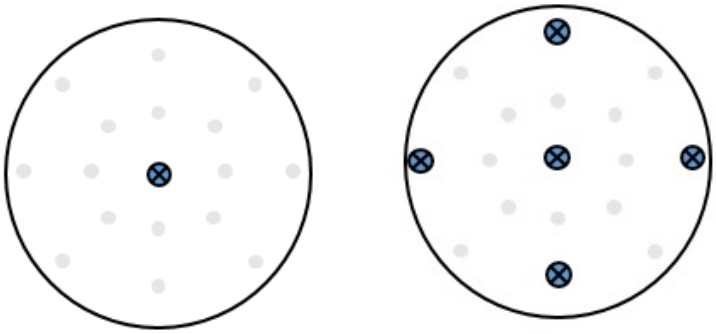

Figure 5.4 Two different configurations for jet and spray nozzles within (a) single arrangement (b) multiple arrangements

5.2.2 Evaporation rate and Gain Output Ratio

In this study, two indicators of Evaporation rate (E) and Gain Output Ratio (GOR) are used for evaluating flash evaporation performance [25]. The GOR indicates the

energy utilization efficiency based on the first law of thermodynamic which is calculated by [19]:

$$GOR = \frac{\dot{Q}_v}{\dot{Q}_{in}} \tag{5.1}$$

This equation is expressed as the energy required to evaporate the distillate over the input superheating energy. The superheating energy which is stored in the saline water is defined as [19]:

$$\dot{Q}_{in} = \dot{m}_{in} c_p \Delta T \tag{5.2}$$

where $\dot{m}_{in}$ (kg/s) and c_p (kJ/kg˚C) represent the inlet saline water mass flow rate and the liquid heat capacity, respectively. ΔT (˚C) also presents the superheat degree which is estimated by [15]:

$$\Delta T = T_{in} - T_{sat} \tag{5.3}$$

where T_{in} (˚C) and T_{sat} (˚C) are the saline water inlet temperature and the saturation temperature corresponding to the vacuum pressure, respectively.

The energy utilized to evaporate the distillate is determined by [19]:

$$\dot{Q}_v = \dot{m}_v L \tag{5.4}$$

where $\dot{m}_v$ (kg/s) and L (J/kg) represent the vapour mass flow rate and the latent heat of vaporization, respectively.

5.3 Results and discussion

The results and discussion section consist of three parts. The first part reports on the centreline temperature distribution under different conditions for the single jet and spray nozzles. The second- and third-part focus on the evaporation rate and GOR, respectively, and include both jet and spray nozzles for single and multiple arrangements under various operational conditions.

5.3.1 Centreline temperature profiles

In order to quantify the influence of various parameters on the centreline temperature profiles of jet and spray nozzles, it is essential to introduce a dimensionless parameter (Θ) for temperature expressed by [22]:

$$\theta = \frac{T(r,z) - T_{equ}}{T_{in} - T_{equ}} \tag{5.10}$$

where T(r,z) is the axial and radial temperature inside the chamber, T_{in} is the inlet temperature of saline water and T_{equ} is the equilibrium temperature. Fathinia et al. [22] also established an equation that the centreline temperature profiles of jet and spray nozzle draw a similar shape at all examined conditions and represented by:

$$\theta_{emp} = \frac{0.9(T(0,0) - T_{equ})}{T_{in} - T_{equ}} e^{-kz} \tag{5.11}$$

Figure 5.5 shows the centreline variation of dimensionless temperature (Θ) and its exponential fit (Θ_{emp}) over the axial distance (z) from 0 to 200 mm for single nozzle. The inlet temperature of 70˚C, the salinity of 3.5%, superheat degree of 9˚C, and inlet flow rate of 1.5 l/min is considered to measure and illustrate the centreline temperature profile of single jet and spray nozzle in Fig. 5.5a. It is apparent that the temperature gradient for sprays is higher than the jets. By increasing the inlet temperature from 70 to 80˚C and keeping the other conditions constant, Fig. 5.5b shows that measurement of temperatures from exit point of nozzles (both jet and spray) to the equilibrium point results in an increase of the slope of Θ_{emp}, while this growth for the spray nozzle, especially at the begining, is steeper. Fig. 5.5c demonstrate the effect of increasing the superheat degree on temperature variation at the centreline of the jet and spray nozzle at T_{in}=80˚C, C=3.5%, ΔT=18˚C, Q=1.5l/min. With the knowledge that the slope of the curve at any location is indicator for the evaporation rate and steeper profile represents more flash evaporation [7], the results in Fig. 5.5 illustrates that the spray nozzle hastens flash evaporation more compared with the jet nozzle. A similar outcome is reached while the flow rate is increased from 1.5l/min to 2l/min in Fig. 5.5d. The profiles are seen to have steep inclinations between 0 to 200 mm while the slope reduction of spray nozzle is again faster. Another observation from comparing Fig. 5.5c with Fig. 5.5d

is the slope reduction and enhancement of jet and spray nozzles, respectively. In fact when the flow rate increases, due to the increase in the inertia of the jet and making more unshattered region after the injection, the flash evaporation is reduced, while the spray nozzle experiences more evaporation as there is no unshattered zone after the nozzle exit and saline water is completely atomized. According to the abovementioned results and analysing the centreline dimensionless profiles, it can be concluded that more flash evaporation has occurred for spray than jet nozzle under similar conditions.

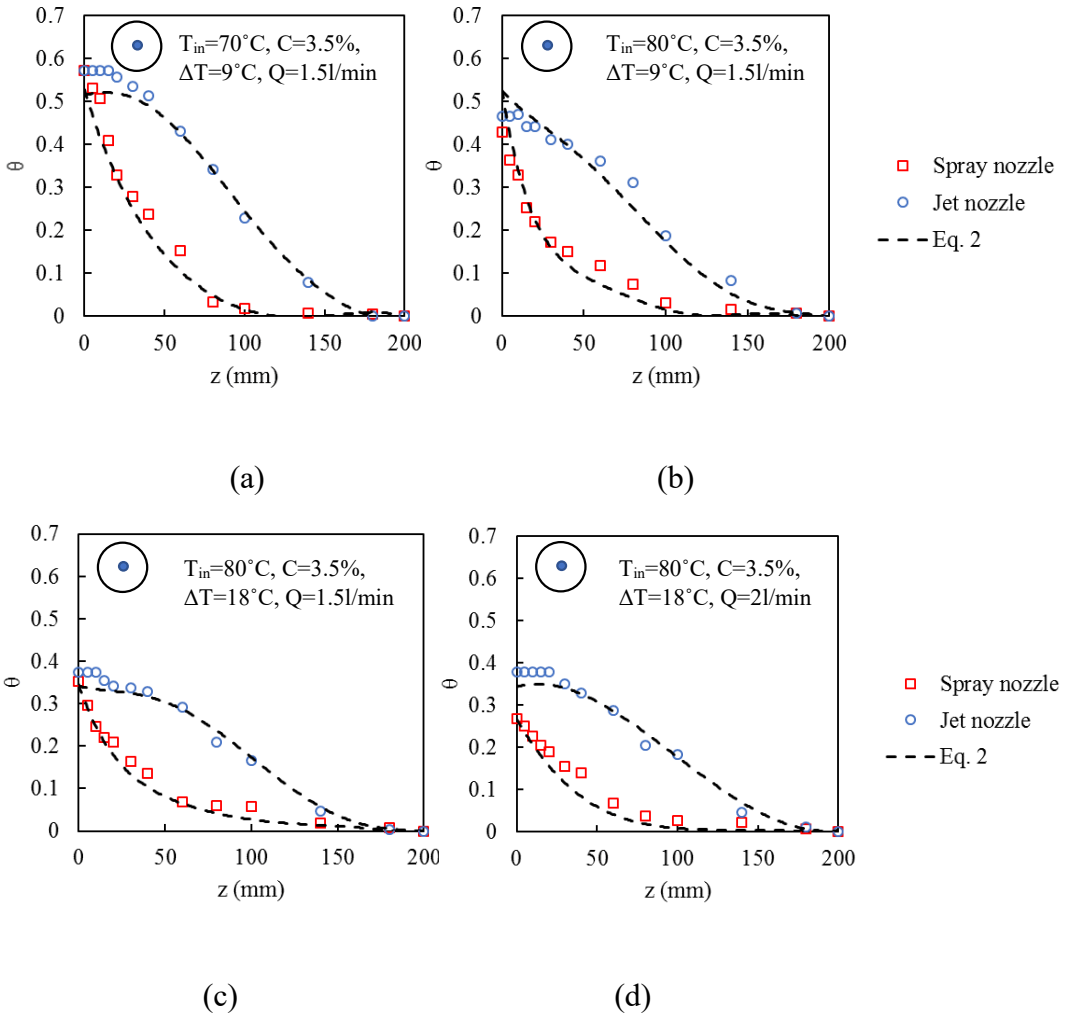

Figure 5.5 Centreline variation of dimensionless temperature (Θ) and its exponential fit (Θ_{emp}) for single jet and spray nozzle at various conditions

5.3.2 Evaporation rate (E)

In this section, the evaporation rates of single and multiple jets and spray nozzle are compared considering the influence of inlet flow rate, pressure injection, and

superheat degree while the other parameters are maintained constant. Figure 5.6 shows the effect of inlet flow rate for 3, 4, and 5 l/min when the inlet temperature, superheat degree, and salinity are kept at 70˚C, 3.5%, and 26˚C, respectively. As can be seen, although the evaporation rates of the spray nozzle in both single (Figure 5.6a) and multiple arrangements (Figure 5.6b) is more than the jet nozzles (at each flow rate), the increase of evaporation rate with increasing the flow rate in all type of nozzle configurations is noticeable. The jet nozzle at the flow rate of 3 l/min reached evaporation rate of 0.066 l/min, while this value is 0.090 for the single spray nozzle. On the other hand, the evaporation rates increase to 0.097 and 0.20 l/min, respectively, as the flow rate increases to 5 l/min. For multiple arrangments, the highest difference between the evaporation rate of the jet and spray nozzle is observed at 5 l/min with around 40%. This can be attributed to the fact that increasing the flow rate provides more potential saturated saline water to be evaporated.

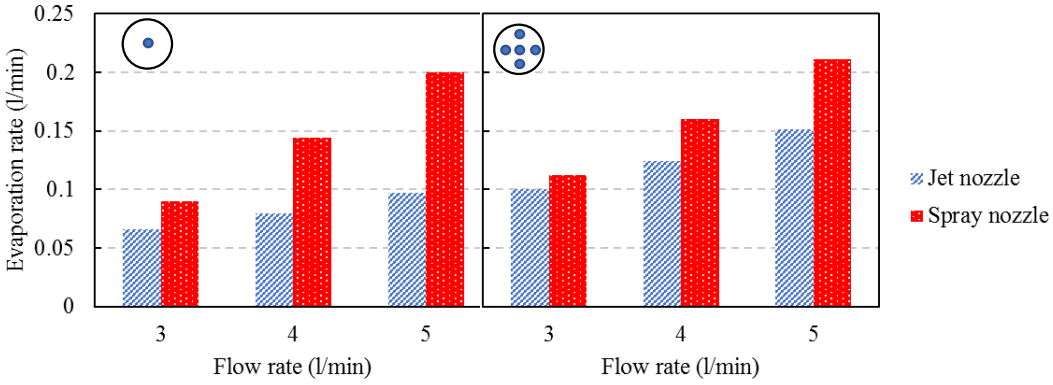

(a) (b)

Figure 5.6 The evaporation rate of jet and spray nozzles at T_{in}=70˚C, C=3.5%, and ΔT=26˚C for (a) single (b) multiple arrangements

The effect of injection pressure on the evaporation rate of the single jet and spray nozzles are shown in Figure 5.7a, whereas the inlet temperature, superheat degree, and salinity are fixed at 70˚C, 3.5%, and 26˚C, respectively. One can see that the evaporation rate for the spray nozzle again is higher compared with the jet nozzle for the same pressure. For example, the evaporation rate for the spray nozzle at a pressure of 2bar is approximately two times more than the jet nozzle. This difference is even larger for multiple nozzle arrangement, as shown in Figure 5.7b. For instance, the evaporation rate difference between multiple jets and spray

nozzles at again 2bar pressure is more than two times. According to the corresponding flow rate of each pressure in this figure, the enhancement of the flow rate, which is caused by applying more pressure, hasten the evaporation rate for both nozzles. It is also worth noting that increasing the flow rate results in the formation of smaller droplets in spray nozzle than jet and this is the main advantage of this nozzle type.

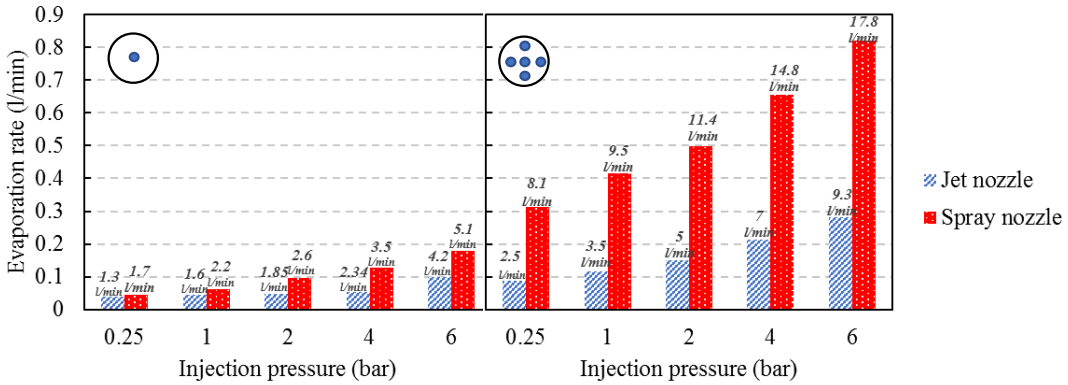

(a) (b)

Figure 5.7 The evaporation rate of jet and spray nozzles at T_{in}=70˚C, C=3.5%, and ΔT=26˚C for (a) single (b) multiple arrangements

An observation from Figure 5.8 shows an upward trend of evaporation rate for both single and multiple nozzles at various superheat degree from 4 to 36˚C. The fixed parameters are inlet temperature of 70˚C, the salinity of 3.5%, and flow rate of 5 l/min. As reported by Fathinia et al. [22], increasing vacuum pressure (higher superheat degree) causes a greater difference in the vapour density between droplet surface and the surrounding vapour. Furthermore, a quicker drop in the pressure in the surrounding environment and more intensive air movement around the droplets is another result of increasing superheat degree. So, the integration of these influences leads to a higher evaporation rate in both single and multiple nozzle arrangements. For example, in the range of 4 to 36˚C superheat degree, the evaporation rate of multiple spray nozzle jumps from 0.027 to 0.315 l/min, and for the jet nozzle jumps from 0.025 to 0.205 l/min. It is apparent that the behaviour of the spray nozzle differs from the jet nozzle, due to production of finer droplets for the tested range of superheat degrees.

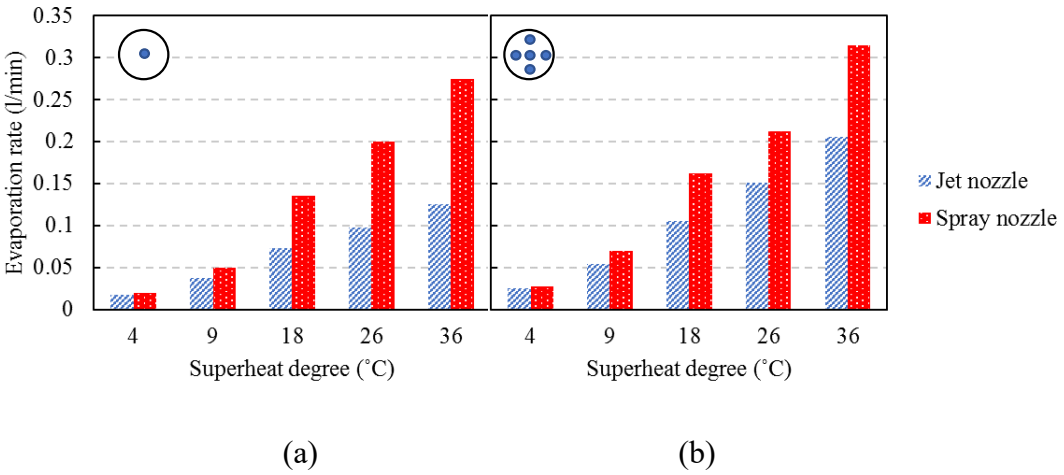

Figure 5.8 The evaporation rate of jet and spray nozzles at T_{in}=70˚C, C=3.5%, and Q=5 l/min for (a) single (b) multiple arrangements

5.3.3 Gain Output Ratio

Gain Output Ratio (GOR) is an indicator in flash evaporation system to evaluate the energy utilization efficiency so that a greater GOR represents more superheat degree is transferred into the latent heat of vapour and reached higher energy utilization efficiency.

The GOR versus flow rate of jet and spray nozzle for single and multiple arrangements is plotted in Figure 5.9a and b, respectively. Results suggest that GOR decreases with the increase of flow rate for the jet nozzle in both single and multiple configurations. Conversely, the higher GOR can be likely achieved through increasing the flow rate of single and multiple spray nozzles. As observed, for single jet nozzle, GOR is calculated to be 0.43 for 3 l/min and 0.38 for 5 l/min, whereas for single spray nozzle these values are 0.58 for 3 l/min and 0.78 for 5 l/min. In addition, comparing between single and multiple arrangements reveal that GOR is maximal in each flow rate for multiple configurations of both nozzle types. This can be attributed to the fact that increasing the number of nozzles has a positive impact on GOR as smaller and more uniform droplets are injected. Figure 5.10a and b show the estimated GOR under various injection pressure for different nozzle types and arrangements. It should be taken into account that the inlet temperature, superheat degree, and salinity is kept at 70˚C, 26 ˚C, and 3.5%, respectively. It can be seen that the highest GOR for the single spray nozzle is 0.84 at maximum

pressure (6 bar), while GOR for single jet nozzle is minimum (0.39) at this point. These findings propose that there is a direct relationship between GOR and increasing pressure for spray nozzle and indirect relationship between those for jet nozzle. This trend can be also seen in Figure 5.10b which shows the influence of injection pressure on GOR for multiple nozzles. Increasing the injection pressure from 0.25 to 6 bar increases the GOR for multiple spray nozzles by 0.81 and 0.98, respectively. It is worth mentioning that GOR decreases 13% for multiple jet nozzles with increases of injection pressure until 2bar and then GOR become stable. By comparing single with multiple nozzles it is concluded that the overall performance of the system is dependent on the number of nozzles.

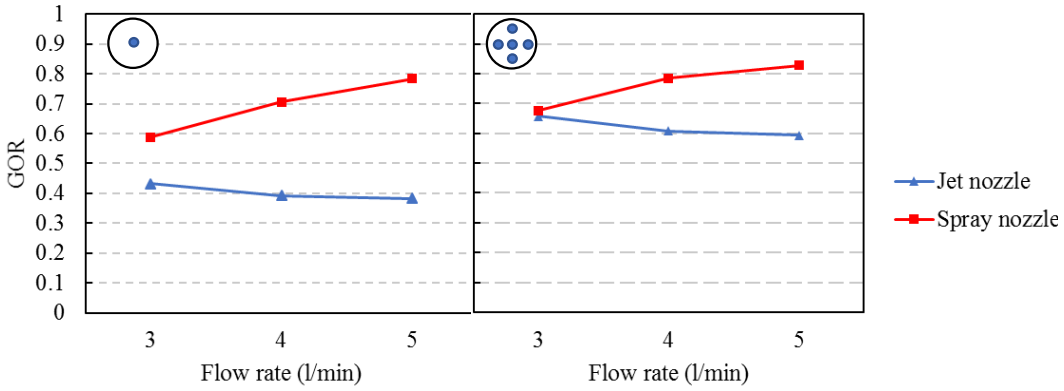

(a) (b)

Figure 5.9 The GOR of jet and spray nozzle at Tin=70˚C, C=3.5%, and ΔT=26˚C for (a) single (b) multiple arrangements

Based on the calculated flow rate for each pressure, the explanation for the improvement of efficiency for the spray nozzle is the enhancement of flow rate. As discussed earlier, increasing flow rate leads to the formation of smaller droplet sizes in the spray nozzle than jet which positively affects the GOR for the spray nozzle and negatively influences the GOR for the jet nozzle.

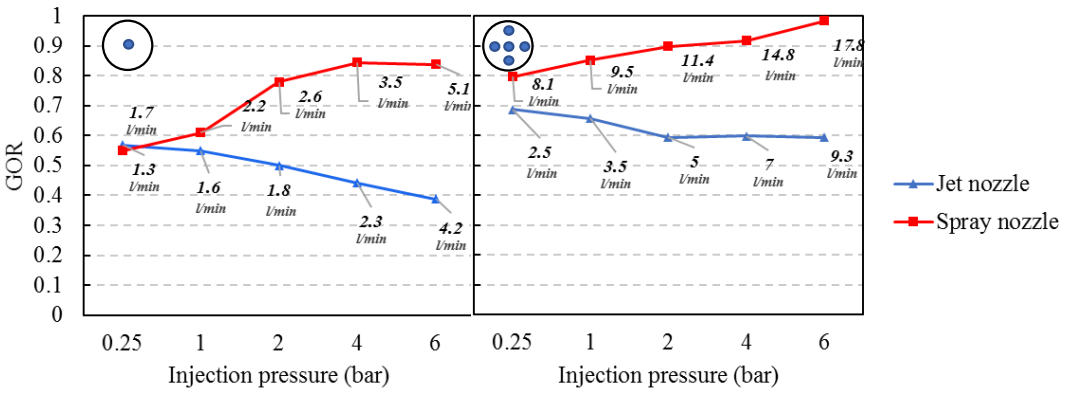

Figure 5.10 The GOR of jet and spray nozzle at Tin=70˚C, C=3.5%, and ΔT=26˚C for (a) single (b) multiple arrangements

The effect of superheat degree as a driving force on the performance of single and multiple jets and spray nozzles while the chamber pressure is changed and the other conditions are maintained constant at T_{in}=70˚C, C=3.5%, and Q=5 l/min is illustrated in Figure 5.11a and b. By looking at both graphs, it is obvious that the general trend of GOR for spray nozzle at higher superheat degrees in both configurations is upward whereas it is downward for the jet nozzle. Despite this difference, there is a common behaviour between those nozzles which can be revealed by a point by point comparison between these two graphs. They indicate that by increasing vacuum pressure inside the chamber (rising superheat degree), multiple nozzles enhance the efficiency of the system regardless of the nozzle type. For instance, at superheat degree of 18˚C, the GOR for single jet and spray nozzle is determined to be 0.44 and 0.78, respectively, while these values are jumped to 0.64 for multiple jets and 0.94 for multiple spray arrangements. This comparison between single and multiple nozzles can be performed for all superheat degrees with similar result. Based on the abovementioned conditions, the range of GOR improvement for spray multiple arrangements is between 3 to 65%. This finding reveals better atomization capability of multiple compared with single arrangements under similar conditions.

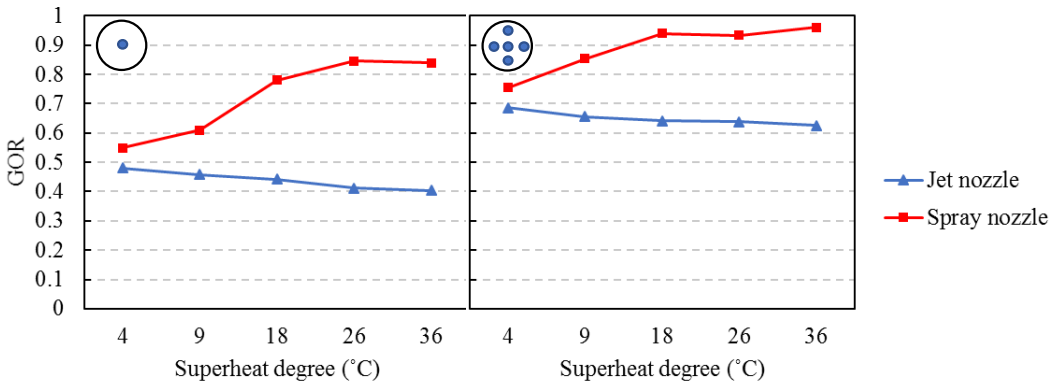

(a) (b)

Figure 5.11 The GOR of jet and spray nozzle at T_{in}=70˚C, C=3.5%, and Q=5 l/min for (a) single (b) multiple arrangements

5.4 Conclusions

An experimental study of two different nozzles (jet and spray), at both single and multiple orifice configurations, has been undertaken at various flash evaporation conditions (3.5% saline water, water inlet temperature 70-80˚C, flow rate 3-5 l/min, injection pressure 0.25-6 bar (absolute), and superheat degree 4-36˚C). The main findings of this study are:

- Based on the centreline temperature profiles, the axial temperature of the spray nozzle declines faster in comparison with the jet nozzle which hastens more flash evaporation under the same operational conditions.
- The evaporation rate is directly affected by the increase of flow rate, injection pressure, and superheat degree regardless of nozzle type or arrangement, but spray nozzle within multiple arrangements play a more dominant role than the others.
- The evaporation rate of the spray nozzle could reach approximately two times more than the jet nozzle for the range of operational conditions.
- The effect of nozzle type and configuration on the efficiency of the system was noticeable so that using the spray nozzle with multiple arrangements has higher GOR with 3 to 65% improvement.

- The evaporation rate in the flash evaporation desalination system is dependent on the number of nozzles whether it is a jet nozzle or a spray. Using multiple jet and spray nozzles increases the evaporation rate up to 32% and 40%, respectively, compared with a single jet and spray nozzle.

Acknowledgements

The first author acknowledges the financial support received by School of Engineering at Edith Cowan University to pursue his PhD.

5.5 References:

1. A.E. Kabeel and E.M.S. El-Said, *A hybrid solar desalination system of air humidification, dehumidification and water flashing evaporation: Part II. Experimental investigation.* Desalination. Vol. 341, 2014: p. 50-60.
2. W. Graves, *Water: The Power, Promise, and Turmoil of North America's Fresh Water*. 1993: National Geographic Society.
3. M. Ghahari, S. Rashid-Nadimi, and H. Bemana, *Metal-air desalination battery: Concurrent energy generation and water desalination.* Journal of Power Sources. Vol. 412, 2019: p. 197-203.
4. J.R. Werber, C.O. Osuji, and M. Elimelech, *Materials for next-generation desalination and water purification membranes.* Nature Reviews Materials. Vol. 1, 2016: p. 16018.
5. R. Semiat, *Energy Issues in Desalination Processes.* Environmental Science & Technology. Vol. 42, 2008: p. 8193-8201.
6. R. Daghigh and A. Shafieian, *Energy and exergy evaluation of an integrated solar heat pipe wall system for space heating.* Sādhanā. Vol. 41, 2016: p. 877-886.
7. S. Mutair and Y. Ikegami, *Experimental investigation on the characteristics of flash evaporation from superheated water jets for desalination.* Desalination. Vol. 251, 2010: p. 103-111.
8. A. Hosseini Araghi and M. Khiadani, *Experimental investigation and analysis of a new single-stage vacuum spray flash desalinator utilising a gas-liquid ejector.* Journal of Cleaner Production. Vol. 190, 2018: p. 118-127.
9. O. Miyatake, T. Tomimura, Y. Ide, and T. Fujii, *An experimental study of spray flash evaporation.* Desalination. Vol. 36, 1981: p. 113-128.
10. H. Ikeuchi. *Hydraulic Spray Nozzles (Full Cone Spray Pattern)*. 2018; Available from: https://www.kirinoikeuchi.co.jp/eng/products/spray/03/.
11. J.J. Nijdam, S.H. Stårner, and T.A.G. Langrish, *An experimental investigation of droplet evaporation and coalescence in a simple jet flow.* Experiments in Fluids. Vol. 37, 2004: p. 504-517.

12. O. Miyatake, T. Tomimura, Y. Ide, M. Yuda, and T. Fujii, *Effect of liquid temperature on spray flash evaporation.* Desalination. Vol. 37, 1981: p. 351-366.
13. Y. Ikegami, H. Sasaki, T. Gouda, and H. Uehara, *Experimental study on a spray flash desalination (influence of the direction of injection).* Desalination. Vol. 194, 2006: p. 81-89.
14. D. Balaji, *Experimental study on the effect of feed water nozzles on non-equilibrium temperature difference and flash evaporation in a single-stage evaporator and an investigation of effect of process parameters on the liquid flashing in a LTTD desalination process.* Desalination and Water Treatment. Vol. 57, 2016: p. 27152-27168.
15. Cai, B., Yin, Y., Zheng, Y., Wang, W., Gu, H., Yao, J., & Wang, H, *Mathematical study of spray flash evaporation in a spray-assisted seawater desalination chamber.* Desalination. Vol 465, 2019: p. 25-37.
16. A. Muthunayagam, K. Ramamurthi, and J. Paden, *Low temperature flash vaporization for desalination.* Desalination. Vol. 180, 2005: p. 25-32.
17. A.K. El-Fiqi, N.H. Ali, H.T. El-Dessouky, H.S. Fath, and M.A. El-Hefni, *Flash evaporation in a superheated water liquid jet.* Desalination. Vol. 206, 2007: p. 311-321.
18. S. Mutair and Y. Ikegami, *On the evaporation of superheated water drops formed by flashing of liquid jets.* International Journal of Thermal Sciences. Vol. 57, 2012: p. 37-44.
19. K.G. Lyras, S. Dembele, and J.X. Wen, *Numerical simulation of flashing jets atomisation using a unified approach.* International Journal of Multiphase Flow. Vol. 113, 2019: p. 45-58.
20. Wang, C., Xu, R., Chen, X., Jiang, P., & Liu, B., *Study on water flash evaporation under reduced pressure.* International Journal of Heat and Mass Transfer. Vol 131, 2019: p. 31-40.
21. Chen, Q., M, K. J., Li, Y., & Chua, K. J., *Experimental and mathematical study of the spray flash evaporation phenomena.* Applied Thermal Engineering. Vol 130, 2018: p. 598-610.

22. B. Cai, Q. Wang, S. Yin, H. Gu, H. Wang, H. Zhen, and L. Zhang, *Energy analysis of spray flash evaporation from superheated upward jets.* Applied Thermal Engineering. Vol. 148, 2019: p. 704-713.
23. Q. Chen, Y. Li, and K.J. Chua, *On the thermodynamic analysis of a novel low-grade heat driven desalination system.* Energy Conversion and Management. Vol. 128, 2016: p. 145-159.
24. A.H. Araghi, M. Khiadani, M. Sadafi, and K. Hooman, *A numerical model and experimental verification for analysing a new vacuum spray flash desalinator utilising low grade energy.* Desalination. Vol. 413, 2017: p. 109-118.
25. F. Fathinia, Y.M. Al-Abdeli, and M. Khiadani, *Evaporation rates and temperature distributions in fine droplet flash evaporation sprays.* International Journal of Thermal Sciences. Vol. 145, 2019: p. 106037.
26. F. Fathinia, M. Khiadani, and Y.M. Al-Abdeli, *Experimental and mathematical investigations of spray angle and droplet sizes of a flash evaporation desalination system.* Powder Technology. Vol. 355, 2019: p. 542-551.
27. A.H. Araghi, M. Khiadani, and K. Hooman, *A novel vacuum discharge thermal energy combined desalination and power generation system utilizing R290/R600a.* Energy. Vol. 98, 2016: p. 215-224.
28. F. Fathinia, M. Khiadani, Y.M. Al-Abdeli, and A. Shafieian, *Performance improvement of spray flash evaporation desalination systems using multiple nozzle arrangement.* Applied Thermal Engineering. Vol. 163, 2019: p. 114385.
29. Y. Wang, Q. He, Q. Yang, D. Zhang, M. Liu, J. Yan, *Energy and exergy analyses of circulatory flash evaporation of aqueous NaCl solution.* Desalination. Vol. 436, 2018: p. 81-90.

Chapter 6

General discussion

The experimental and numerical study of the flash evaporation desalination system using spray nozzle revealed that the proposed system is practical and reliable to produce more pure water than the other common type of nozzles efficiently (specifically jet). Although an earlier study on flash evaporation desalination system has been conducted, little or no information is available in the published literature on suitable nozzle type. Moreover, the study also investigates the influences of various influential parameters including inlet temperature, flow rate, injection pressure, superheat degree, and salinity on performance of the system while using a spray nozzle, which is unnoticed in a number of studies in a literature review. The main objective of this study is the understanding and comparing the evaporation process through fine droplets of spray and jet nozzle to improve the system performance.

The specific outcomes of each chapter have already been discussed. This chapter is focused on the general discussion of fundamental results from this study and their integration. In this regard, the key research questions presented in Chapter 1 are also addressed in the subsequent sections.

6.1 Experimental analysis of spray and jet nozzle

When using thermocouples holding bar to measure the temperature distribution of spray nozzle and estimate evaporation rate, the study first investigates the effect of operating parameters such as inlet temperature, flow rate, superheat degree, and salinity (Chapter 2). The study also includes the effect of those parameters on the jet nozzle (Chapter 5) under similar conditions. In the following discussion, the issues related to research questions RQ 1 have been addressed.

- The results of this study show in **Chapters 2** and **5** that the type of nozzle has a noticeable effect on the centreline temperature profiles and evaporation rate. The performance of spray nozzle in the flash evaporation

desalination system is comparable with the jet nozzle regardless of using single or multiple nozzles; so that spray nozzle reduces droplets temperature and hastens flash evaporation more than the jet nozzle under similar conditions.

- The study presented above is established as an empirical equation in **Chapter 2** to predict an exponential decay in dimensionless centreline temperature as a common pattern in both spray and jet nozzle. This equation is derived using data analysis based on various range of conditions tested. The significance of this equation is that it serves as an indirect indicator of the evaporation rate within the conditions tested.

- Based on a variety of experiments using both nozzles, it is found in **Chapters 2** and **5** that some of the operational parameters do not notably affect the evaporation rate of spray and jet nozzle as long as other conditions are maintained constant. However, by changing the parameters' range in **Chapter 5**, it is realized that considering a wide range of analysis for some parameters is crucial. On the other hand, despite the fact some of the influential parameters affect similarly the system performance of both spray and jet nozzle, the flow rate has a different effect on the evaporation rate depending on whether spray or jet flash evaporation is taking place.

- The effect of nozzle type on the efficiency of the system is considerable so that using the spray nozzle increases evaporation rate and gain output ratio as discussed in **Chapter 5**. This outcome supports our primary hypothesis for replacing the jet nozzle, which utilizing spray nozzle leads to the creation of smaller droplets and enhances the evaporation rate due to increased surface area.

6.2 Spray nozzle characteristics

Analysis of the spray characteristics and mechanism of flashing are very significant for a better understanding of the droplet's atomization inside the vacuum chamber and providing a clear direction on the design of relevant spray applications. Therefore, the project considered spray angle and droplet size to observe and investigate the behaviour of them under different conditions in **Chapter 3.** By using

high-speed camera for observation of spray angel and shadowgraph technique within mathematical modelling for calculating the droplet size, an empirical correlation between droplet size changes and evaporation rate was explored. The analysis presented in the subsequent sections is addressed the research question **RQ 2**.

- Three different spray nozzles with a similar spray angle under ambient conditions are employed to find that all of the angles' profile over injection pressure, approximately fall into almost a single curve which can be used to calculate the spray angle regardless of nozzle type. The way of finding this equation is presented in Chapter 3 and the following figure is shown a schematic illustration of spray angle based on saturation and injection pressure.

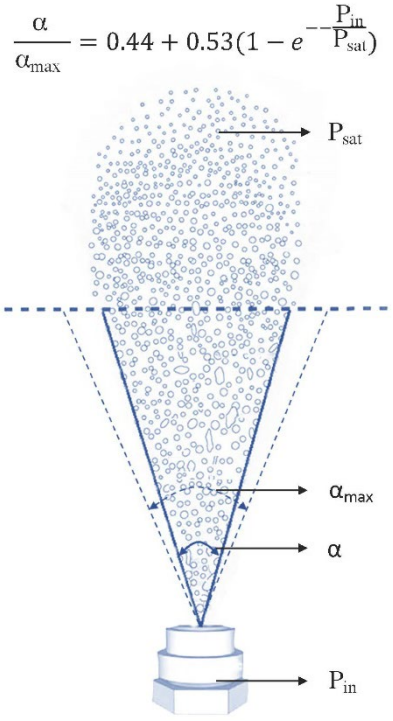

Fig. 6.1 The schematic illustration of spray angle based on pressure

- The interesting result evident from this study (**Chapter 3**) is that droplet size changes (along the centreline of the upward spray flash evaporation) can be calculated by a proposed mathematical model. Good agreement was observed between the model's data with the results obtained through the

shadowgraph technique. For both mathematical and experimental results, increasing the superheat degree leads to the reduction of the droplets' lifetimes, and it is also found that the increase in humidity of the vacuum area delays the completion of evaporation.

6.3 Multiple nozzle arrangement

The results discussed above largely based on a single spray or jet nozzle in the flash evaporation desalination system while the outcomes reported in **Chapter 4** and **5** study the effect of using multiple nozzles in different configurations. A multi-nozzle head was fabricated to examine the influence of multiple nozzles and then measure droplet sizes and distribution of those arrangements for further clarifications. The evaporation rate and gain output ratio are used to describe the performance of the system while similar spray nozzles in different configurations are discussed in **Chapter 4** or multiple sprays and jet nozzles are compared in **Chapter 5**. In this section, **RQ 3** has been identified.

- The number of nozzles plays a significant role in the performance of the system regardless of nozzle type. This outcome is more articulated in **Chapter 5** to clarify the optimum design.

- Placing nozzles at the farthest point of each other in order to minimise droplets interaction and coalescence is the main result of **Chapter 4** which has been achieved. The calculation of optimised maximum superheat degree and estimation of performance improvement of the system for the most efficient arrangement are the other valuable consequences of this chapter.

In summary, this PhD project has studied many parameters that affected the flash evaporation desalination performance using very fine spray nozzle. This system has barely investigated in the current literature where detailed spray nozzle characters and influential factors are investigated and experimental and mathematical results are reported. The proposed system could be benefited to the remote, arid, and coastal areas by improving the overall system performance by replacing nozzles with multiple spray nozzles. In this way, the spray flash evaporation desalination system could reliably produce more pure water cost effectively and environment-friendly compared to a typical type of flash evaporation desalination.

Chapter 7

Conclusion and future work recommendations

7.1 Concluding remarks

This chapter reviews the main findings and results of all research and studies and finally offers suggestions and recommendations for possible future works in this area.

This research mainly focused on using very fine spray nozzle instead of other types in the flash evaporation desalination systems in order to improve the performance of the system. An overall summary of the results is highlighted below:

- Flash evaporation of saline sprays is intensely dependent on the localised and chamber pressure.
- Based on the analysis of temperature distribution and measuring distilled water, it is found that a dimensionless temperature is well correlated to the evaporation rate in the saline sprays.
- The empirical equation is established for the prediction of temperature distribution in both spray and jet nozzles to act as an indirect indicator of the evaporation rate within the conditions tested.
- By conducting sensitivity analysis and parametric optimisation it is concluded that inlet temperature and salinity of the water in the range of 0 to 3.5% do not affect the evaporation rate as long as other conditions are maintained constant.
- In the flash evaporation system, increasing the superheat degree and flow rate leads to an increase in the evaporation rate.
- It is observed that the flow rate has a different effect on the evaporation rate depending on whether spray or jet flash evaporation is taking place.

Increasing the flow rate in sprays leads to higher flash evaporation but lowers the evaporation rate in jets.

- The empirical equation is proposed to correlate the spray angle with injection and chamber pressure under vacuum conditions.
- The mathematical model for the droplet size changes along the centreline of the spray flash evaporation is in good agreement with experimental results.
- Based on the mathematical model, humidity and superheat degree have a contrary effect on the droplet size of spray flash evaporation.
- The spray capacity is largely influenced by the droplets' lifetime and the spray angle is affected by the superheat degrees regardless of the nozzle types.
- Placing spray nozzles at the farthest point of each other and increasing the number of spray nozzles lead to an increase in the performance of the system.
- Utilizing 5 spray nozzles in the farthest place of each other results to increase the efficiency of the system up to 28% while the optimum superheat degree is calculated 19 °C.
- A higher salinity in the water ensures the lower intensity of flash evaporation so that 10% and 20% salinity showed 20% and 50% decline in evaporation rate.
- The effect of nozzle type and configuration on the efficiency of the system was noticeable so that using the spray nozzle with multiple arrangements has higher GOR by 3 to 65% improvement.
- The evaporation rate of the spray nozzle is approximately two times more than the jet nozzle at above standard pressure.
- The performance of the flash evaporation desalination system is dependent of number of the nozzles regardless of nozzle type.

7.2 Future recommendations

This PhD project has considered a number of parameters that are influential on the performance of the flash evaporation desalination system. However, there are still several areas where further study is recommended and include:

- Feasibility studies of coupling heat pipe solar collectors to DTECD process and comparing the economic analysis with the previous model.
- Detailed performance analysis of heat exchanger and obtaining the optimum operating condition.
- CFD analysis of using other types of nozzles to compare their results with the jet and spray nozzle and avoid repeating experimental tests.
- The effect of utilizing different models and configurations of demister inside the vacuum chamber on the performance of the system.
- The optimum design of the vacuum chamber to achieve higher performance and comparing with alternative vacuum systems.
- Analysis and measurement of spray characteristics with other techniques like phase doppler anemometry and compare the accuracy of the results with this study.
- Comparing the performance and efficiency of the vacuum pump with its alternative (i.e. eductor) which was used in previous research.
- Comparing the theoretical calculations on the power consumption of injection and vacuum pumps with experimental results.